European Journal of Medicinal Chemistry 276 (2024) 116672

Contents lists available at ScienceDirect

European Journal of Medicinal Chemistry

journal homepage: www.elsevier.com/locate/ejmech

Research paper

Synthesis and evaluation of chemical linchpins for highly selective CK2α targeting

Francesco A. Greco [a,b], Andreas Krämer [a,b,c], Laurenz Wahl [a,b], Lewis Elson [a,b], Theresa A.L. Ehret [a,b], Joshua Gerninghaus [a,b], Janina Möckel [a,b], Susanne Müller [a,b], Thomas Hanke [a,b,*], Stefan Knapp [a,b,c,**]

[a] Institute of Pharmaceutical Chemistry, Goethe University Frankfurt, Max-von-Laue-Str. 9, 60438 Frankfurt Am Main, Germany
[b] Structural Genomics Consortium, Buchmann Institute for Molecular Life Sciences, Goethe-University Frankfurt, Max-von-Laue-Str. 15, 60438 Frankfurt Am Main, Germany
[c] German Cancer Consortium (DKTK), German Cancer Research Center (DKFZ), DKTK Site Frankfurt-Mainz, 69120 Heidelberg, Germany

ARTICLE INFO

Keywords:
Casein kinase 2
Allosteric inhibitor
Inhibitor binding mode
Rational inhibitor design
Kinase inhibitor selectivity

ABSTRACT

Casein kinase-2 (CK2) are serine/threonine kinases with dual co-factor (ATP and GTP) specificity, that are involved in the regulation of a wide variety of cellular functions. Small molecules targeting CK2 have been described in the literature targeting different binding pockets of the kinase with a focus on type I inhibitors such as the recently published chemical probe SGC-CK2-1. In this study, we investigated whether known allosteric inhibitors binding to a pocket adjacent to helix αD could be combined with ATP mimetic moieties defining a novel class of ATP competitive compounds with a unique binding mode. Linking both binding sites requires a chemical linking moiety that would introduce a 90-degree angle between the ATP mimetic ring system and the αD targeting moiety, which was realized using a sulfonamide. The synthesized inhibitors were highly selective for CK2 with binding constants in the nM range and low micromolar activity. While these inhibitors need to be further improved, the present work provides a structure-based design strategy for highly selective CK2 inhibitors.

1. Introduction

Protein phosphorylation is a crucial regulatory mechanism, playing a key role in signal transduction [1]. This post-translational modification triggers a change in the activation state of various proteins, leading to a plethora of different effects ranging from regulation of the cell cycle [2], apoptosis [3], cell growth [4] as well as regulatory events in mRNA splicing [5]. The enzymes that catalyse this reaction, protein kinases (PK), are a large family of regulatory proteins that have been associated with many different diseases including oncological malignancies, inflammation and neurologic disorders [6–8]. Casein Kinase 2 (CK2) is a PK with probably one of the most extensive interactomes, affecting hundreds of cellular proteins [9,10]. This suggests that CK2 plays an important role in various cellular processes and that an aberrant function of this key regulator can ultimately lead to the development of various disease phenotypes. CK2 associated diseases range from cancer [11,12] and neurodegenerative diseases [13–15] to viral [16–19] and parasitic infections [20,21], making CK2 an attractive potential target for the development of small molecule based therapies (Fig. 1) [22–28].

The most frequently used inhibitor in the literature is CX-4945 (Silmitasertib) [29]. CX-4945 is a benzonaphtyridine analogue with the classic features of a type I kinase inhibitor that reached phase-II clinical trials on cholangiocarcinoma [30]. Apart from its potential as an anti-cancer drug candidate, CX-4945 is not a useful tool compound due to its significant off-target profile that includes potent inhibition of CDK1, CLK1–CLK3, DAPK3, DYRK1A/B, DYRK3, FLT3, HIPK3, PIM1, and TBK1 (IC_{50}s < 100 nM) [31–33]. Indeed, the recent development of highly selective inhibitors of CK2, so called chemical probes, such as SGC-CK2-1 revealed that targeting of CK2 across different cancer cell lines generally does not lead to antiproliferative effects that have been prominently associated with CX-4945, emphasizing the importance of selective chemical probes linking phenotypic responses to targets [34]. SGC-CK2-1 is a pyrazolopyrimidine-based type I kinase inhibitor and, like CX-4945, shares critical interactions in the hinge region and the

* Corresponding author. Institute of Pharmaceutical Chemistry, Goethe University Frankfurt, Max-von-Laue-Str. 9, 60438 Frankfurt am Main, Germany.
** Corresponding author. Institute of Pharmaceutical Chemistry, Goethe University Frankfurt, Max-von-Laue-Str. 9, 60438 Frankfurt am Main, Germany.
E-mail addresses: hanke@pharmchem.uni-frankfurt.de (T. Hanke), knapp@pharmchem.uni-frankfurt.de (S. Knapp).

https://doi.org/10.1016/j.ejmech.2024.116672
Received 27 May 2024; Received in revised form 8 July 2024; Accepted 9 July 2024
Available online 14 July 2024

back pocket of CK2. In an SAR study of the pyrazolopyrimidine scaffold leading to the discovery of SGC-CK2-1, it has been shown that even minor structural modifications can lead to a significant loss of selectivity and/or potency. This can be an issue if physicochemical-, or pharmacokinetic properties such as metabolic stability are altered without seriously affecting the overall pharmacodynamic features of the compound. Another important driver for chemical modifications at the compound level is the occurrence of mutations in the catalytic domain of kinases [35,36]. These point mutations can occur throughout the catalytic domain, typically at the gatekeeper position, located deep in the ATP-binding pocket, which negatively affects the affinity of ATP-competitive compounds [37].

The divergent phenotypes observed in studies comparing the promiscuous inhibitor CX-4945 with selective compounds such as SGC-CK2-1 challenge the role of CK2 in many disease processes discovered with CX-4945, including its role in regulation cell proliferation and cancer [38]. However, inhibitors with different binding modes, such as allosteric and orthosteric inhibitors, have been associated with different phenotypes. Such observations may be based on the regulation of CK2 by protein interactions and its quaternary structure consisting of two catalytic (α and α`) and two regulatory (β) subunits [39]. The discovery of allosteric inhibitors targeting a unique pocket adjacent to αD and the ATP binding site provides an opportunity for the design of selective CK2 inhibitors [40,41]. However, while the αD pocket provides an interesting anchor point, targeting the pocket alone is unlikely to lead to potent inhibitors. Indeed, the combination of fragments binding to the αD pocket with moieties targeting the CK2 ATP site back pocket led to potent compounds, exemplified by the bivalent inhibitor CAM4066 (K_D: 320 nM), which was highly selective and, in contrast to SGC-CK2-1, showed anti-proliferative effects at 10–20 μM concentration [26]. More recently, the inhibitor AB668 demonstrated that bivalent compounds targeting the ATP site back pocket and the αD pocket simultaneously can have excellent selectivity and potency and induce apoptotic cell death in several cancer cell lines [42].

Although AB668 targets the ATP site, it does not form the canonical hinge hydrogen bonds usually required for high potency of ATP-competitive orthosteric inhibitors while still showing high affinity to the target ($K_D = 86$ nM). In this study, we aim to investigate if αD pocket targeting moieties could be linked to ATP mimetic scaffolds. This combination poses a challenge in linker design between the two moieties, as the linker needs to introduce a 90-degree kink, which we achieved by introducing a sulfonamide moiety directly attached to the hinge binding ring system. Testing diverse hinge binding moieties and linkers, we succeeded developing bivalent inhibitors with nM K_D assessed by ITC (Isothermal titration calorimetry) and excellent selectivity.

2. Results

The catalytic subunits of CK2 have unique structural features that render this kinase constitutively active and facilitate the design of selective CK2 inhibitors. Firstly, the N-terminal segment of CK2 is tightly bound to the activation loop, stabilizing an active conformation. Secondly, the DFG motif in CK2 is changed to DWG, allowing the formation of an additional hydrogen bond between the W176 and the backbone of L173 which is also contributing to the stability of the active state [43]. Third, the αD helix has been shown to be flexible even in the apo forms

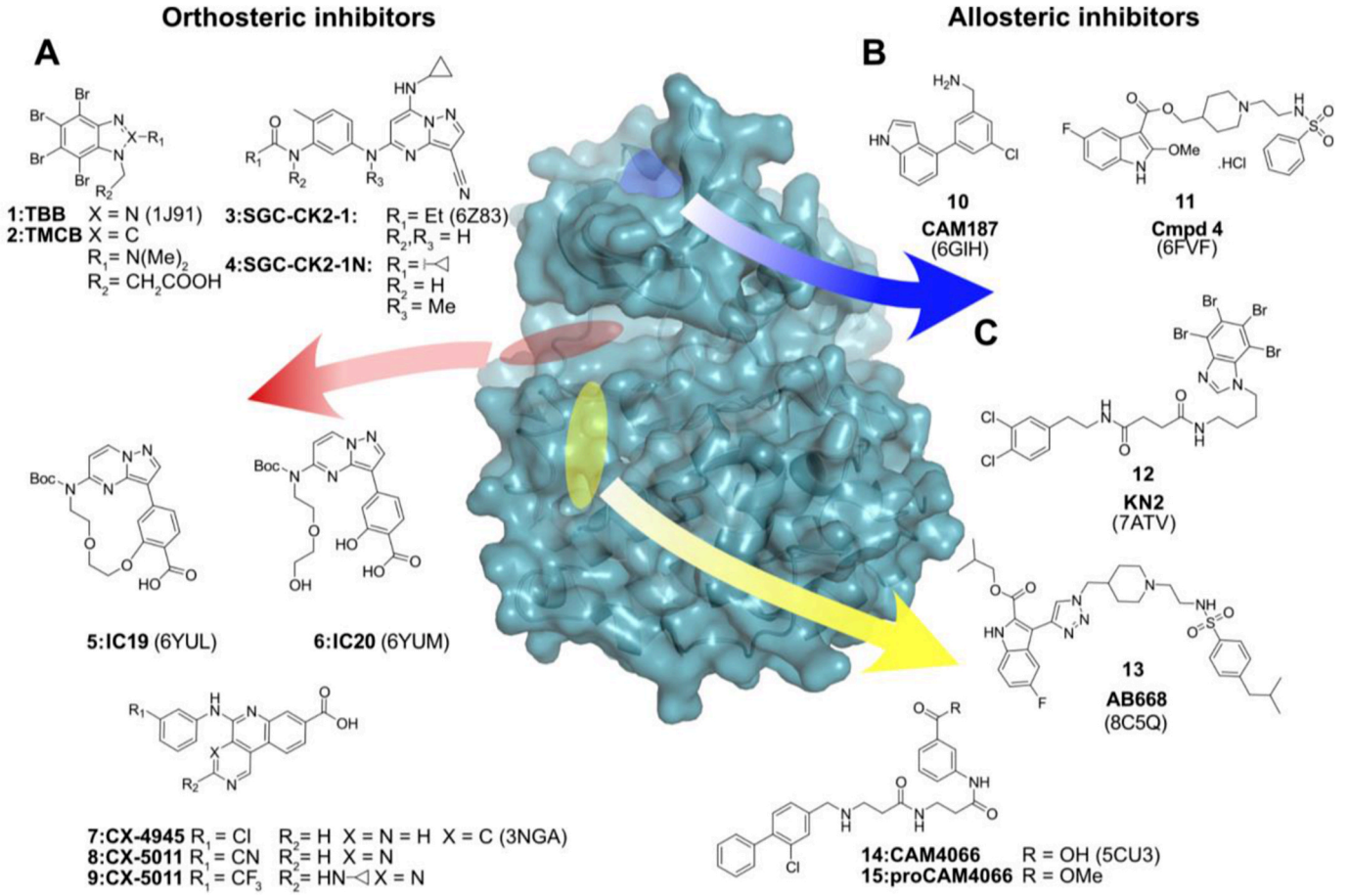

Fig. 1. Overview of small molecules targeting CK2α sorted by binding pockets: (A) Orthosteric inhibitors targeting the ATP binding site of CK2α sharing classical hinge binding motifs like pyrazolo[1.5-a]pyrimidines and 2,6-naphtyridines. The PDB code of the corresponding crystal structure is shown in brackets. (B) Allosteric binders targeting the interface between CK2α/CK2β. (C) Ligands targeting the αD out conformation of CK2.

of the enzyme [44]. Brear et al. have used high-throughput crystallography to show that a binding site created by an outward movement of αD can be targeted by small molecular fragments and can therefore be used for the development of allosteric CK2 inhibitors [41].

In our study, we pursued three main strategic considerations for our compound design.

1) The biphenyl-methanamine moiety served as a linchpin molecule that targets the αD out conformation (Fig. 2A).
2) An appropriate linker length of at least 8–9 Å was employed to connect the αD ligand to an ATP site binding moiety (Fig. 2A, ellipse).
3) An angle of approximately 90° between the ATP binding site moiety and the linker region was introduced to position the ATP mimetic moiety of the molecule towards the hinge region (Fig. 2B).

Compounds **26**–**58** were synthesized using a 5-step synthetic route as outlined in Scheme 1. The αD ligand was assembled by DMAP catalyzed functionalization of commercially available 3-chloro-4-hydroxybenzaldehyde **16** with triflate anhydride yielding the corresponding triflated product **17** in 86 % yield on a 12 g scale [45]. **17** underwent LiCl accelerated Suzuki Miyaura cross coupling with commercial benzene boronic acid in yields of **18** from 60 to 70 % [45]. Di-amino linkers of varying complexities were combined with **18** via reductive amination with yields ranging from 57 to 80 % (**19**–**24**). Deprotection of the Boc group protected amines proceeded with TFA in DCM yielding the corresponding TFA salts that were used without further purification. These compounds were reacted in high dilution with different commercially available sulfonyl chlorides in THF and excess of base at ambient temperature with yields from 71 to 92 % (**26**–**58**).

Due to the paucity of commercially available sulfonyl chlorides directly attached to fused heterocyclic cores, we tried different reactions conditions for the *de novo* synthesis of this moiety to further expand the chemical space. Unfortunately, various attempts ranging from direct chlorosulfonylation and Li-halogen exchange to Grignard type mediated sulfinate syntheses failed on a range of heterocyclic compounds. Willis *et al.* published a milder palladium-catalyzed method for the *in situ* generation of sulfinate salts starting from brominated aromatic compounds and the SO_2 surrogate DABSO (DABCO-Bis(sulfur dioxide)) [46]. The sulfinate salt can be reacted directly with an electrophilic F^+ reagent such as NFSI to yield sulfonyl fluorides, which are suitable for chromatographic purification due to their higher chemical stability [47]. Thus we applied this chemistry and synthesized sulfonyl fluoride **60** by reacting 6-bromo-3-methyl-3*H*-imidazo[4,5-*b*]pyridine (**59**) with DABSO, $Pd(amphos)_2Cl_2$, *N,N*-dicyclohexylmethylamine and isopropanol serving both as solvent and reducing agent under microwave irradiation (46 % isolated yield) [47]. **60** was then coupled with deprotected compound **19** that was synthesized according to Scheme 1 yielding the final product **61** in 72 % overall yield (Scheme 2). However, it must be noted that this approach still has a limited substrate scope in terms of heterocyclic scaffolds, which restricts the synthesis of further sulfonyl fluorides.

The first generation of compounds contained a simple alkyl chain with 4–5 carbon atoms, flanked by the αD-binding moiety and the fused heterocycle (henceforth referred to as the 'head group', H), which was designed to reach the ATP binding site. The binding of **26** (pentyl linker) to both CK2 isoforms was verified by differential scanning fluorimetry (DSF) and the proposed binding mode was confirmed by X-ray crystallography (Fig. 3, left panel). Remarkably only the compounds carrying a linker motif and a hinge binding moiety showed significant shifts in the DSF assay, in contrast to the allosteric biphenyl fragment (**S1**) alone (Table S3).

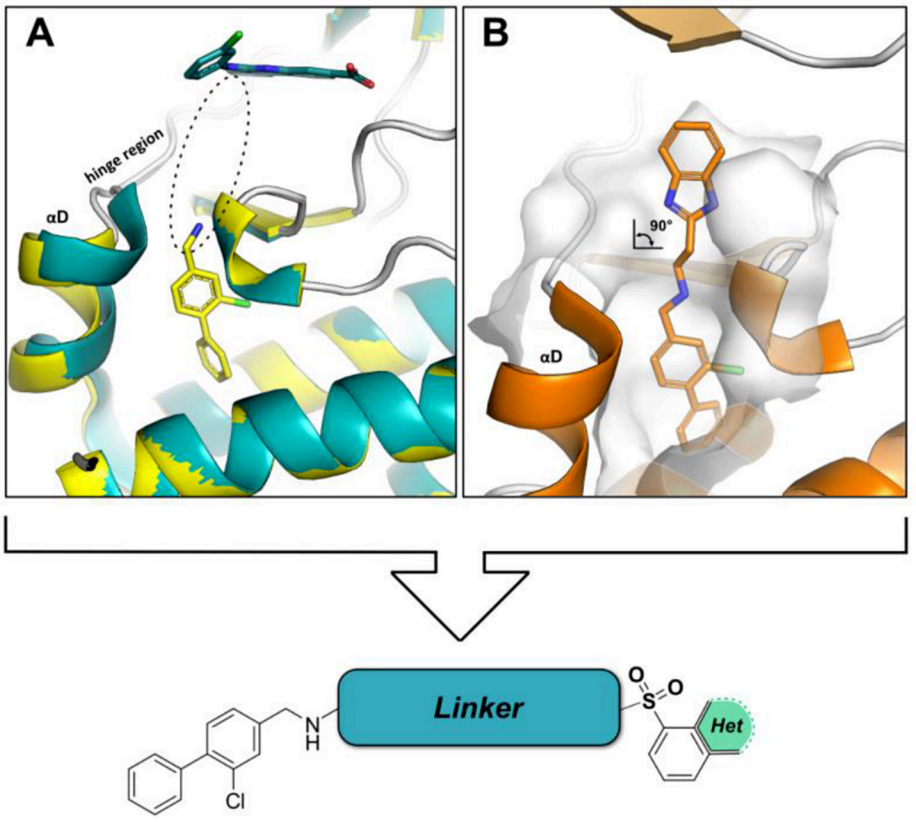

Fig. 2. Design strategy: (A) Overlay of CK2α bound to the type-I inhibitor CX-4945 (teal, PDB 3NGA) and the αD targeting biphenyl (yellow, PDB 5CSH). Dotted ellipse indicates the position for linker design. (B) Benzimidazole motif (orange, PDB 5OUU) protruding from the αD pocket emphasizing the need of an orthogonality inducing functional group like sulfonamides or sulfones.

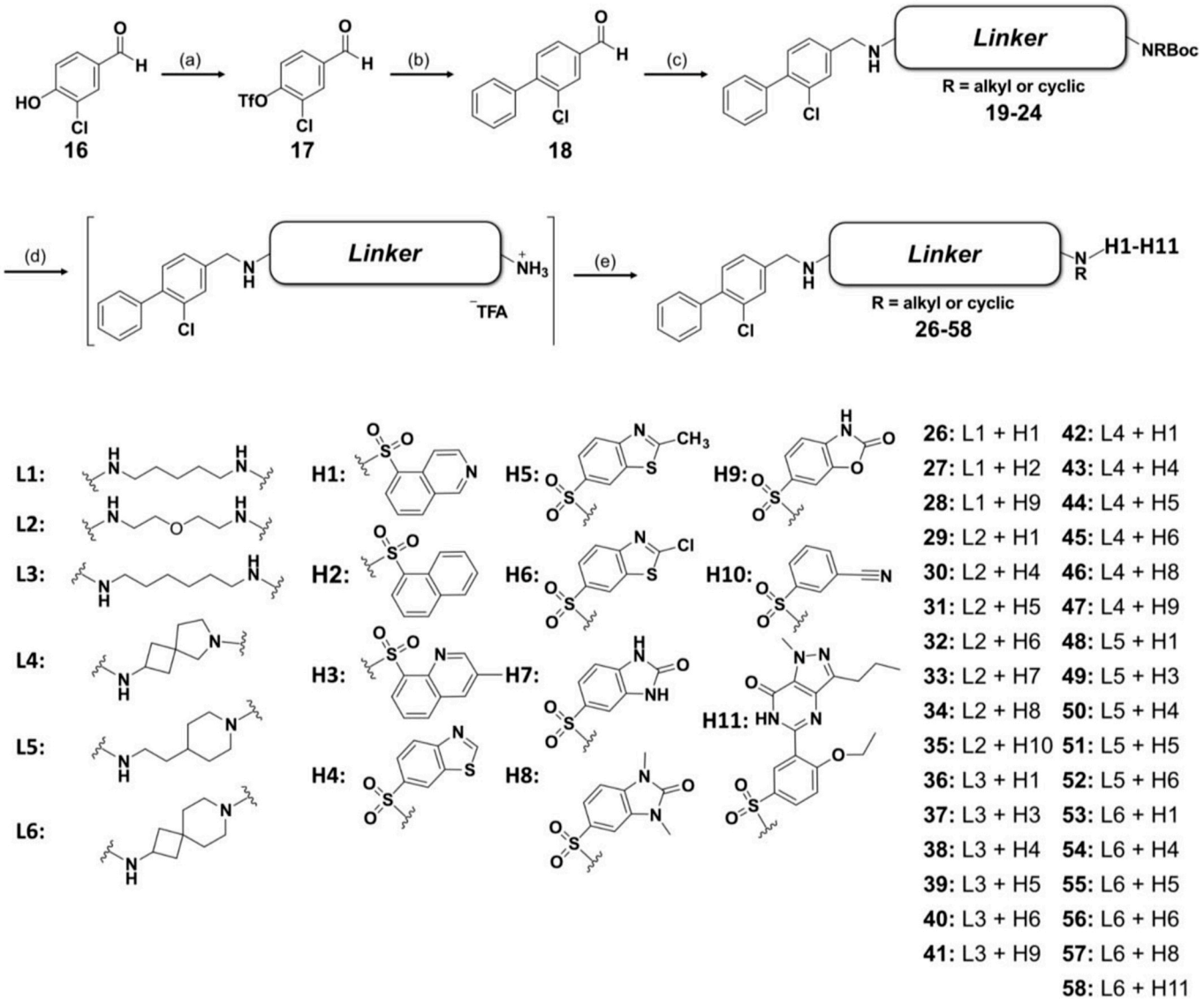

Scheme 1. Synthesis of **26**–**58**[a] [a] Reagents and conditions: (a) Tf_2O (1 M DCM), pyridine, cat. DMAP, DCM, rt, overnight, 86 %; (b) Phenyl boronic acid, $Pd(PPh_3)_4$, LiCl, DME, μW, 80 °C, 3 h, 60–70 %; (c) $Na[(CH_3COO)_3BH]$, $MgSO_4$, DCM, overnight, rt, 57–80 %; (d) TFA, DCM, 0 °C-rt, 1 h, quant.; (e) Sulfonyl chloride, $N(Et)_3$, THF, overnight, rt; 71–92 %. L = linker and H = head group.

The co-crystal structure analysis of **26** and CK2α shows that the combination of a pentyl linker connected to both the biphenyl and a quinoline successfully induces the desired binding mode (Fig. 3, left side).

Based on the first DSF results, we considered the linker to be the key component of our inhibitor design. A more detailed analysis of the conformation of the aliphatic linker inspired us to use both a rigidification strategy to stabilize this conformation and to test whether the sulfonamide H-donor interferes with binding, leading to compounds **48** and **53**. **48** contains a piperidine-4-ethanamine ring, which rigidizes the linker in the upper part of the molecule and simultaneously masks the N–H of the sulfonamide. The main feature of compound **53** is a 7-azaspiro[3.5]-nonane linker designed so that the linker is pre-organized at both ends. Derivatives of **48** and **53** were co-crystallized on CK2α to additionally test whether the modifications may still address the ATP binding site (Fig. 3, right side showing **50** and **55**). Both DSF and X-Ray structural analysis demonstrated that the new linking strategy and the introduction of different binding moieties at the ATP pocket were promising and that there was no apparent loss of binding (Table 1). ITC data of **26** and **48** supported the DSF results revealing K_D values of and 316 nM and 263 nM, respectively (Fig. 5). Based on these results, we extended our SAR with different linkers in combination with several ATP binding site moieties and tested them using DSF as an initial assay system (Table 1). Aliphatic linkers of varying complexity were used to investigate different conformations of this moiety, replacing the more labile linear amide linkers that has been used in previous reports [26, 45]. All aliphatic linkers were tolerated with linkers bearing more carbon atoms performing better than short ones. Hexyl linkers, used in compounds **36**–**41**, boosted ΔTm shifts by 1–4 °C compared to butyl- (**25**) or pentyl linker (**26**–**28, 61, 72**). Cmpd **26** (**Fig. 4A)** and 25 (**Fig. 4B)** differed in terms of linker length (pentyl vs butyl) and in the orientation of the isoquinoline ring in the ATP binding site. In conjunction with longer linkers, the isoquinoline ring was more aligned with the hinge region, while the shorter butyl linker was more aligned towards the back pocket of the kinase. Additionally, the quinoline moiety of **25** was tilted out of the plane of both **26** and **CX-4945** (Figure S2) which might explain the overall lower affinity of this compound since a surface complemental, coplanar orientation of the ATP site binding moiety was detrimental to be perfectly sandwiched between the N and C lobe of the kinase. Surprisingly the substitution of the C3 to

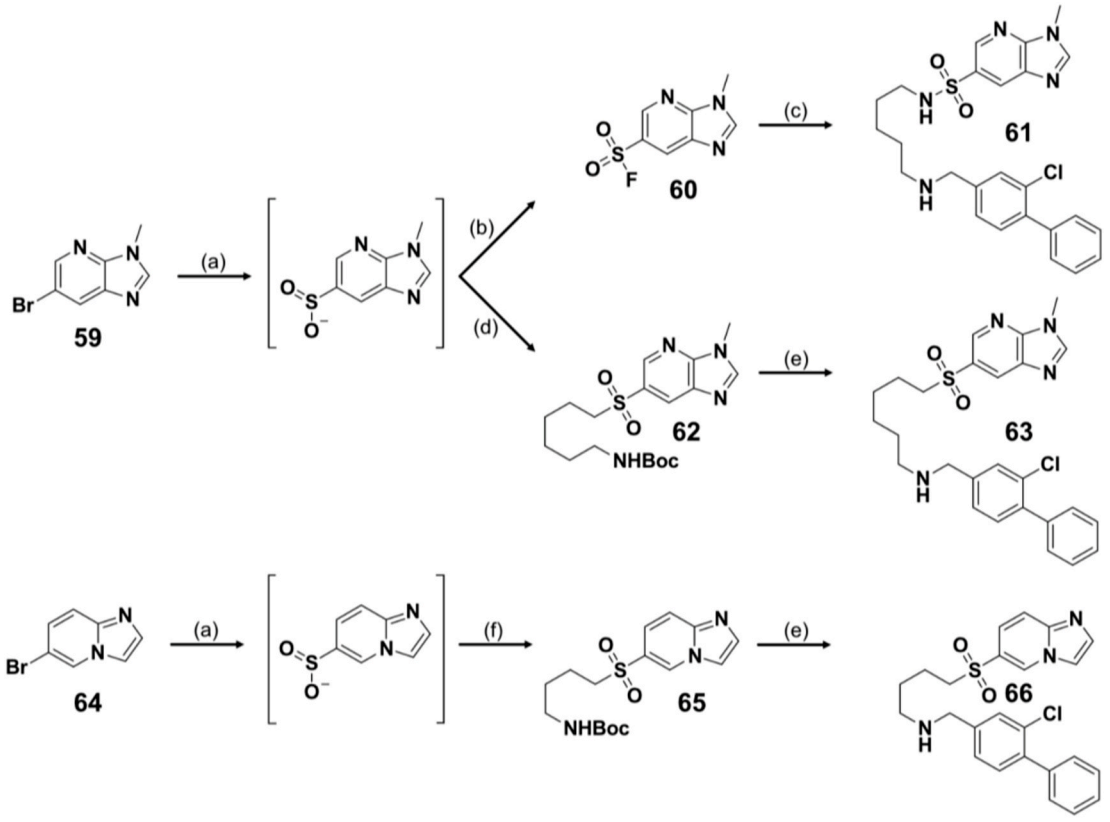

Scheme 2. Synthesis of 61, 63 and 66[a] [a]Reagents and conditions: (a) DABSO, $Pd(amphos)_2Cl_2$, Cy_2NME, *i*-PrOH, 110 °C, 1 h, μW; (b.1) NFSI, 3 h, rt, 46 %; (c) **19** (deprotected), DMSO, 18 h, 110 °C, μW, 72 %; (d) *tert*-butyl (6-bromohexyl)carbamate, DMF, 2 h 100 °C, μW, 40 %; (e) TFA, DCM, 0 °C-rt, 1 h, quant.; **18**, Na $[(CH_3COO)_3BH]$, $MgSO_4$, DCM, overnight, rt, 25 % (**63**) and 23 % (**66**); (f) *tert*-butyl (4-bromobutyl)carbamate DMF, 2 h 100 °C, μW, 14 %.

an oxygen atom in the pentyl linker series rendered molecules largely inactive (**29**–**35**). Polyethyleneglycol (PEG) linkers are known to adopt twisted, meander-like conformations [48], possibly resulting in the αD ligand and/or head group being pushed out of their corresponding pocket.

The spectrum of more rigid linkers included the aforementioned piperidine-4-ethanamine (**48**–**52**), 7-azaspiro[3.5]nonane (**53**–**58**) as well as a 6-azaspiro[3.4]octane-2-amine (**42**–**47**) linker designed to evaluate different ring strains and to optimize the length of the original pentyl linker. The 6-azaspiro[3.4]octane-2-amine linker was chosen to leave the linear architecture of the molecules and thus conveying a certain degree of directionality of the head group. These linkers were tolerated in all head groups examined, with values similar to those of the pentyl linker series.

In addition to masking the N–H donor moiety of the sulfonamide group by making it tertiary, we also wanted to formally remove the nitrogen. This was done by replacing the nitrogen of the sulfonamide group with a carbon atom, thus converting it into a sulfone group. To achieve this transformation, we used the protocol of Willis et al. but instead of using F^+ as the electrophile, we took *N*-Boc protected bromo alkyl linkers and reacted them with the corresponding sulfinate salt, resulting in compounds **63** and **66** (Scheme 2, bottom). Direct comparison of compounds **61** and **63** shows that simple deletion of the nitrogen atom unexpectedly boosts the ΔTm shift from 2,7 to 6,7 °C rendering the 3-methyl-imidazopyridine head group interesting for future studies. The shorter butyl linker (**66**) with the imidazo[1,2-*a*] pyridine moiety showed significantly smaller ΔTm shifts than compound (**63**).

Numerous head groups were investigated, and the binding mode was analyzed by X-Ray crystallography (Fig. 4). All compounds share a bicyclic 6-6 (Fig. 4 A–C) or a 5–6 (**D–G**) annulated heterocyclic ring system, which was linked to a corresponding linker moiety via an orthogonality enforcing sulfone group (not shown) or a sulfonamide group. All head groups extend into the ATP binding site assuming different orientations of the annulated ring systems. **49** (Fig. 4D) bears a 3-methylquinoline head group, suggesting that the orientation of the quinoline nitrogen atom was not important for binding (ΔTm shift of 7.0 and 6.9 °C respectively, Table 1). 5–6 fused heterocyclic ring systems of the benzothiazole type (Fig. 4 D–F) showed a similar binding mode to **26** and **49.** Due to the contracted 5 ring unit, functional groups attached to the 2-position of the benzothiazole ring were preferentially oriented towards the gatekeeper residue of the kinase (Fig. 4E and F). **56** bears a chlorine residue that gives the opportunity for organometallic coupling reactions that can be used to explore the back pocket of the kinase (Fig. 4F). In addition to the aromatic rings, we also investigated fused 5–6 heterocycles with saturated 5-membered rings. **57** contained a 1,3-dimethyl-benzimidazolone moiety gave rise to a similar DSF shift compared to the aromatic counterparts and a similar binding mode compared to the aforementioned ATP mimetic groups (Fig. 4G). The transition from traditional aromatic heterocyclic systems that have been almost exclusively used in the development of kinase inhibitors [49,50] to saturated ring systems could not only yield more favorable selectivity profiles, but may also improve physicochemical and pharmacokinetic properties of inhibitors [51,52].

Motivated by this finding, we expanded the spectrum of saturated ring systems (**28, 33, 34, 41, 46, 47, 57**). Interestingly, the benzoxazolone scaffold exhibited higher DSF shifts in combination with several linker combinations that matched or even exceeded the ΔTm shift of the reference compound **CAM4066 (15)** (see entries **28, 41, 47** in Table 1).

To correlate the ΔTm shifts of the compounds with binding constants in solution, we examined the binding of individual compounds using ITC (Fig. 5). Comparison of binding constants of **26** with **48** showed that the

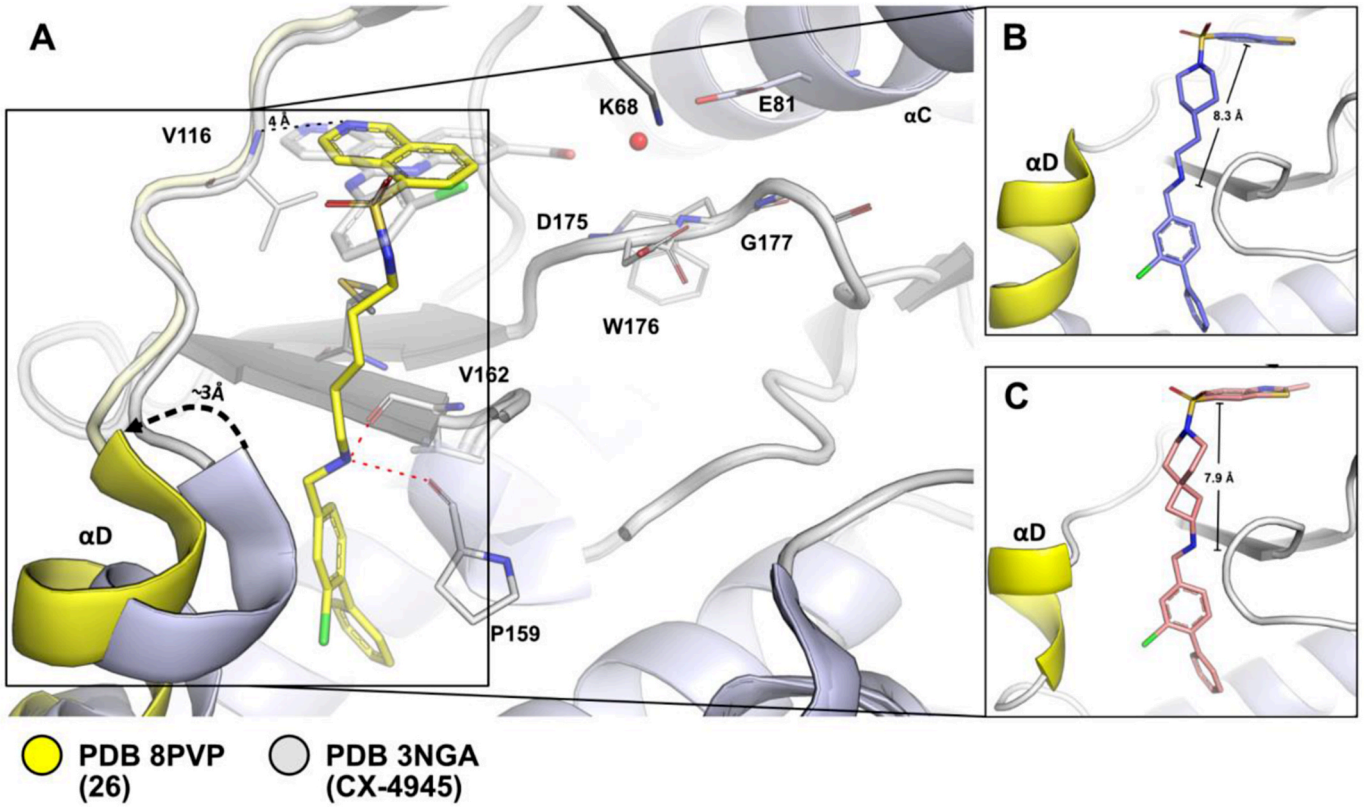

Fig. 3. Proof of principle and comparison of linkers: (A) **26** crystallized with CK2α (yellow) overlayed with CX-4945 (grey). Interactions of **26** between P159 and V162 are shown in red. The basic nitrogen of **26** is in ca. 4 Å distance to V116 which hinders the formation of a hydrogen bond. The black arrow indicates the shift of the αD helix from the *in* to the *out* conformation. (B) **50** bearing a piperidine-4-ethanamine moiety. (C) **55** showing that further rigidification to a 7-azaspiro[3.5] nonane is tolerated.

rigid piperidine-4-ethanamine performed similarly to the more flexible analogue (K_D values of 263 ± 89 nM and 316 ± 71 respectively) with a slightly higher contribution of entropy to overall binding for **48**. These values correlated well with the DSF data that showed comparable shifts for both compounds. We were interested in the overall contribution of the nitrogen atom in isoquinoline derivative **26** to the binding and therefore replaced it with a carbon atom in compound **27**. **27** was synthesized according to Scheme 1 and evaluated in DSF and ITC. **27** performed similarly in DSF to **26** (6.0 vs 6.1 °C for CK2α) demonstrating again that the nitrogen was not involved in direct polar interaction with the kinase. This can be confirmed based on the crystal structure of **26** with CK2α that shows a distance of ≈4 Å between the basic nitrogen and V116, which is too far away for a hydrogen bonding interaction (Fig. 3A). ITC revealed a binding constant of 515 ± 181 nM which was comparable to the nitrogen containing counterpart **26.**

Next, we evaluate the selectivity of the synthesized inhibitors. We chose **48**, **51**, **55** and **57**, harbouring different head groups and linkers and evaluated them in a DSF screen with an in-house panel of 101 protein kinases. All compounds showed excellent selectivity irrespective of the chosen hinge binding moiety or linker. **48** was chosen as an example and the obtained ΔTm shifts were mapped onto the kinome. We also evaluated non-selective compounds as positive controls (Fig. 6A). To test against a wider panel of kinases, **26** and **50** bearing a benzothiazole ring were profiled in an orthogonal tracer displacement assay [53]. Values are shown as % inhibition again highlighting the tolerance of different ATP site binding moieties while preserving high selectivity (Fig. 6B). Additional selectivity data for compounds **51, 55, 57** (DSF data) and **26** (tracer displacement assay) are summarized in the supplemental data file (Table S1, S2 and Figure S1). To illustrate the broad range of kinase coverage used in this study we overlayed the different panels of selectivity assays in a Venn diagram. A total of 177 different kinases were screened with 23 kinases overlapping in the assays used (Fig. 6C). ΔTm data, NanoBRET IC_{50} in permeabilized cells and *in vitro* activity values were compared for a few selected compounds and these data showed good correlation between these orthogonal assays (Fig. 6D) [33,54].

The sulfonamide moiety not only ensured the correct angle between the linker and ATP binding function, but it also offered a possibility for additional derivatization by introducing tertiary sulfonamides. Derivatization at this position allowed extending the inhibitors towards the solvent region, and it can serve as a position for physicochemical optimization or as an attachment point for degrader development such as PROTACs (PROteolysis Targeting Chimeras). The accessibility of this position was confirmed by X-ray structures of **25** and **26**, in which the N–H of the sulfonamide was as expected pointing out of the orthosteric binding pocket. We decided for S_N2 alkylation using methyl bromoacetate to generate the proof-of-concept compound **73**. In contrast to Scheme 1, the synthetic route to this target molecule was changed to avoid a loss of chemoselectivity in the alkylation step (Scheme 3).

The binding of **73** to CK2α and α′ was assessed using the DSF assay, resulting however in smaller thermal shifts comparable to that of compound **72** (6.0/3.2 °C and 8.6/4 °C for α/α' respectively). In addition, the structure of **73** in complex with CK2α was solved to elucidate the binding mode of the molecule (Fig. 7). Encouragingly, we found that the expected orientation of the methyl ester pointed towards the triphosphate region of the kinase, while it did not significantly affect the binding mode of the biphenyl and the benzothiazole moiety in comparison to **50** (overlay of PDB 8PVO and PDB 9EQ1, not shown). In addition, the binding mode indicated that around the tertiary sulfonamide was sufficient space to extend this linker further to solvent exposed moieties and thus enable chemical modifications which can be achieved as suggested in Scheme 3 using different haloalkanes or by

Table 1
Overview of synthesized molecules 25–58, 61, 63, 65, 69 and 70 compounds sorted by linkers: corresponding ΔTm values against CK2α/α' in °C. 14 and 15 are used as reference compounds. Measurements were performed in technical triplicates. H1–H13 represent the employed head groups.

Cpd ID	Linker	Het	ΔTm [° C]		Cpd ID	Linker	Het	ΔTm [° C]	
			CK2α	CK2α'				CK2α	CK2α'
25	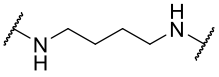	H1	5.1	3.0	42	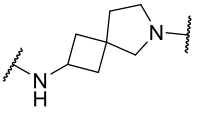	H1	7.0	3.9
26	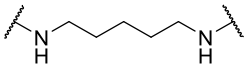	H1	6.1	2.7	43		H4	7.9	4.0
27		H2	6.0	3.2	44		H5	8.0	3.9
72		H4	8.6	4.0	45		H6	6.9	3.5
61		H13	2.7	1.2	46		H8	6.0	3.0
28		H9	8.1	4.2	47		H9	8.9	3.8
29	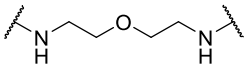	H1	2.2	1.1	48	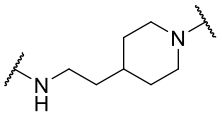	H1	7.0	5.0
30		H4	4.0	1.3	49		H3	6.9	3.6
31		H5	2.6	0.6	50		H4	6.2	5.0
32		H6	3.6	1.4	51		H5	6.0	3.0
33		H7	1.0	0.5	52		H6	8.2	4.2
34		H8	1.8	0.5	53	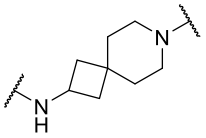	H1	6.4	4.7
35		H10	1.2	1.0	54		H4	5.8	5.2
36	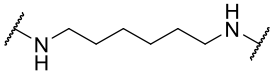	H1	10.0	8.7	55		H5	4.8	3.9
37		H3	7.1	3.0	56		H6	5.4	3.7
38		H4	9.0	5.1	57		H8	6.7	4.1
39		H5	8.6	3.9	58		H11	2.0	0.5
40		H6	8.7	4.3	73	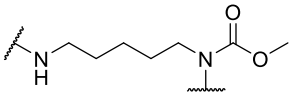	H4	6.0	3.2
41		H9	9.9	6.3					
66	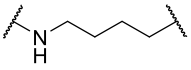	H12	4.3	0.8	Pro CAM 4066 (14) R = Me	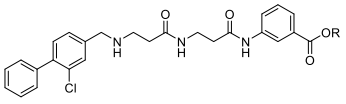	4.5	0.8	
63	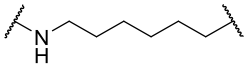	H13	6.7	2.8	CAM 4066 (15) R═H		8.6	4.2	

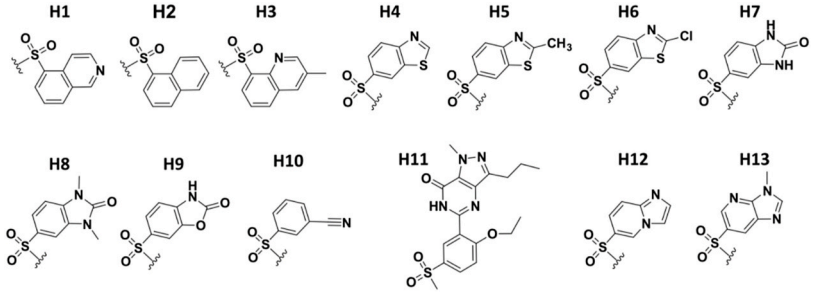

using the methyl ester of **73.** This functional group can undergo further reactions such as amide couplings after hydrolysis providing a roadmap for modification of this scaffold in the future.

3. Conclusion/discussion

In this study we outlined a strategy for CK2 inhibitor design combining known allosteric inhibitors with ATP mimetic moieties. We chose both a sulfonamide and sulfone group as a hinge element for the construction of a series of bivalent molecules. SAR of different combinations of the linker region and the head group demonstrated that 30 of the 39 compounds showed significant binding affinity to CK2 (6–10 °C in DSF assay and ITC values of 263 nM for **26** and 316 nM for **48**). Binding to the kinase was achieved despite the lack of a classical hydrogen bond to backbone amino acids of the hinge region. A structural alignment between **50** and AB668 (Figure S3A) as well as **26** and CAM4066 (Figure S3B) was performed that highlights the key differences between the bivalent inhibitors and the common lack of a polar interaction to the hinge region. This is also in agreement with the binding mode of some natural products such as Emodin, first synthetic molecules including TBB and potent inhibitors of CK2 like GO289 [55–57]. While omitting the hinge region can be a valid strategy to increase selectivity, as this segment is highly conserved throughout the kinome, it usually comes at the cost of potency. In future optimization efforts, both an elongation to said region and growing towards the back pocket of the kinase might be pursued to increase the affinity of the compounds. In fact, the molecules synthesized in this study offer a comprehensive set of starting points that can be derivatized by simple transformation reactions towards different areas of the kinase. Firstly, all hinge binding moieties (except for **H11**) show high selectivity and

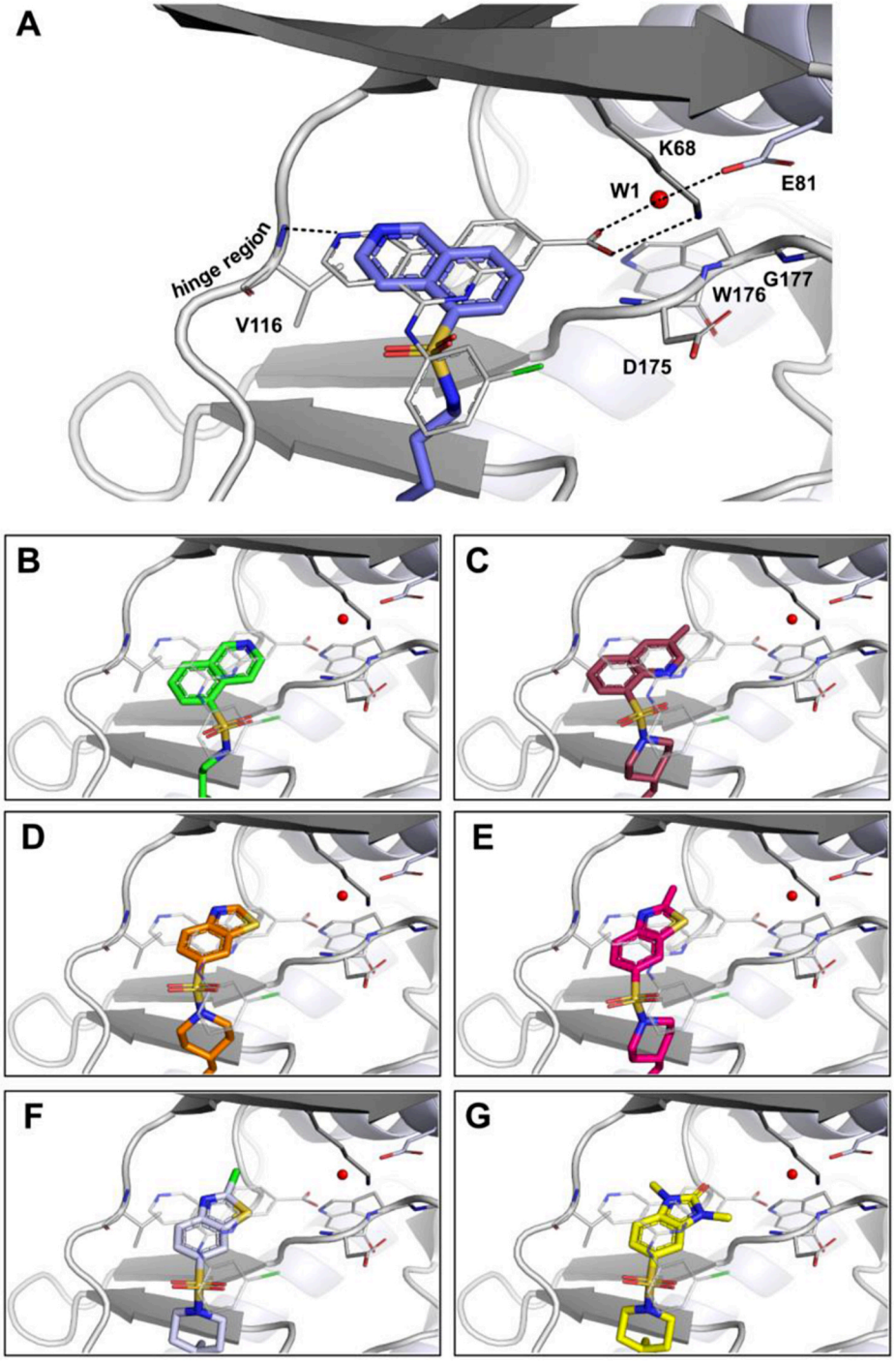

Fig. 4. Overview of different ATP site binding moieties: (A) Overlay of **26** (PDB 8PVP) and CX-4945 (PDB 3NGA) as a reference compound for ATP site targeting scaffolds. Polar interactions of CX-4945 are shown as dotted lines. (B, C) Annulated 6 membered rings of the quinoline type bound to CK2α (**25** PDB 9EQ0, **49** PDB 9EPW). A pentyl linker attached to the quinoline orients the basic nitrogen towards the hinge region (A) as opposed to (B) bearing a butyl linker. 3- methylquinoline pointing towards the back of the kinase (C). (D–F) Benzothiazole derivatives bound to CK2α (**50** PDB 8PVO, **51** PDB 9EPZ, **56** PDB 9EPX). The chlorine moiety in (F) can be used as a chemical handle for further derivatization. (G) The dimethylbenzimidazolone scaffold showcases the tolerance of saturated ring systems in the ATP binding region of the kinase (**57** PDB 9EPV).

can be extended either towards the back pocket or to the hinge region. Secondly, derivatization at the tertiary sulfonamide enables targeting of less addressed regions by inhibitors like the triphosphate binding site. Shorter butyl linkers (**25** and **65**) and the incorporation of a PEG moiety were less well tolerated (**29–35**). Crystal structure analysis showed that these linkers induce an unfavorable conformation of the hinge binding moieties that weakens hydrophobic interactions in the active site cleft and thus should be avoided in future studies. NanoBRET data in intact cells (Table S4) show no measurable activity for most of the bivalent inhibitors, including the reference compounds proCAM4066/CAM4066. **36** was the only compound showing displacement of the tracer with a EC50 of 19 ± 5 μM. Thus, cellular potency of the series is still low, and it needs to be optimized further to allow cellular studies at low compound concentrations [58]. This limitation might be overcome combining the different targeting strategies mentioned above that can result in compounds that can effectively inhibit the kinase *in cellulo*. The biological

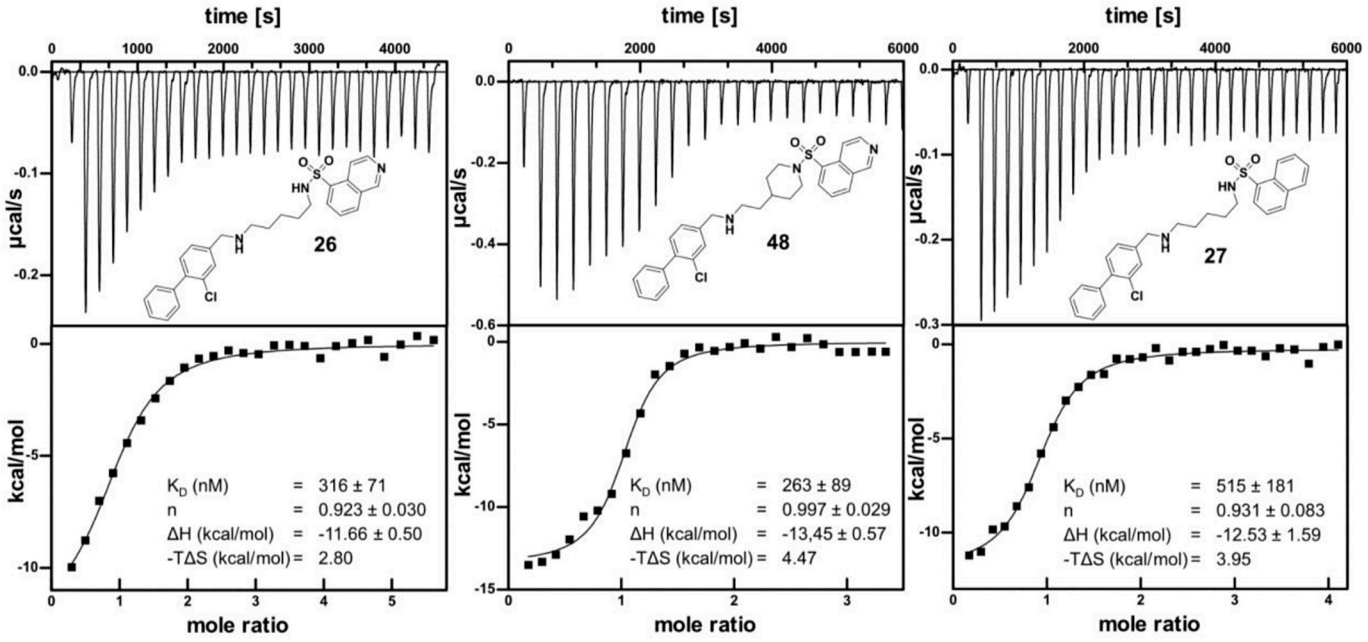

Fig. 5. ITC measurement of **26, 27** and **48**. Rigidization and *N*-deletion strategies (**48, 27**) are investigated in ITC in comparison to proof-of-principle molecule **26**.

effects of CK2 *in vivo* are not exclusively linked to the catalytic activity of the protein [38]. Indeed, it has been shown, that subunits of the holoenzyme can independently serve as scaffolding proteins [59]. **73** was designed to extend into the solvent region of CK2 with the methyl ester serving as an exit vector. This position can be linked to an E3 ligase and harnessed for PROTAC development. Such an approach can conceivably circumvent the problem of low potency and low activity of the compounds which are both parameters that do not necessarily correlate with the pharmacological modality of protein degradation. Additionally, this might allow to further push the biological exploration of kinase-independent functions of CK2.

4. Experimental procedures

4.1. Differential scanning fluorimetry assay

Recombinant protein kinase domains with a concentration of 2 µM were mixed with a 10 µM compound solution in DMSO, using a final buffer consisting of 20 mM HEPES, pH 7.5, and 500 mM NaCl. SYPRO Orange (5000× , Invitrogen) was added as a fluorescence probe (1 µl per mL). Subsequently, temperature-dependent protein unfolding profiles were measured, using the QuantStudio™ 5 realtime PCR machine (Thermo Fisher). Excitation and emission filters were set to 465 nm and 590 nm. The temperature was raised with a step rate of 3 °C per minute. Data points were analyzed with the internal software (Thermal Shift SoftwareTM Version 1.4, Thermo Fisher) using the Boltzmann equation to determine the inflection point of the transition curve. Differences in melting temperature are given as ΔTm values in °C. Measurements were performed in duplicates.

4.2. Isothermal titration calorimetry (ITC)

The dissociation constants (K_D) of the compounds were assessed using isothermal calorimetry. Both the sample cell and injection syringe were pre-equilibrated with gel filtration buffer (25 mM HEPES at pH 7.5, 500 mM NaCl, and 0.5 mM TCEP). The sample cell was loaded with a solution of the compound (at concentrations ranging from 10 to 20 µM in gel filtration buffer), while the injection syringe contained the protein solution (ranging from 80 to 120 µM in gel filtration buffer). Following device equilibration (Nano ITC, TA Instruments), protein was incrementally injected over 30 injections, each comprising 8 µL (except a first injection of 4 µL). Analysis of the resulting data involved defining baseline and integration points to ascertain binding heats. Subsequently, data fitting to the Boltzmann equation enabled the determination of thermodynamic parameters.

4.3. Kinome-wide selectivity profile (tracer displacement assay)

Compounds **26** and **30** was tested at a concentration of 5 µM against a panel of 104 kinases in an *in vitro* tracer displacement assay as described previously (Fig. 6) [53].

4.4. Kinome-wide selectivity profile (Tm panel)

Recombinant protein kinase domains with a concentration of 2 µM were mixed with a 10 µM compound solution in DMSO, 20 mM HEPES, pH 7.5, and 500 mM NaCl. SYPRO Orange (5000 × , Invitrogen) was added as a fluorescence probe (1 µl per mL). Subsequently, temperature-dependent protein unfolding profiles were measured, using the QuantStudio™ 5 realtime PCR machine (Thermo Fisher, Waltham, MA, USA). Excitation and emission filters were set to 465 and 590 nm. The temperature was raised with a step rate of 3 °C per minute. Data points were analyzed with the internal software (Thermal Shift SoftwareTM Version 1.4, Thermo Fisher) using the Boltzmann equation to determine the inflection point of the transition curve. Differences in melting temperature are given as ΔTm values in °C. Measurements were performed in duplicates.

4.5. ADP glo assay

The ADP Glo assay was carried out in concordance with the ADP-GloTM Kinase Assay Protocol (Promega). Recombinant protein kinase domain CK2 was seeded in a 384 well plate at a concentration of 200 nM with addition as 1 µM casein (Merck, C8654-500G) as substrate in Kinase Reaction Buffer (50 mM TRIS pH 7.5, 20 mM $MgCl_2$, 0.1 % Glycerin, 0.01 % Triton X100). Inhibitors of interest were titrated in wells between a range of 7.5 nM and 200 µM, respective negative and positive controls were also included. 20 µM of Ultra-Pure ATP (Promega) was added to the wells to initiate the kinase reaction. All reactions were performed in a 5 µl volume at 37 °C and incubated for 3 h. After

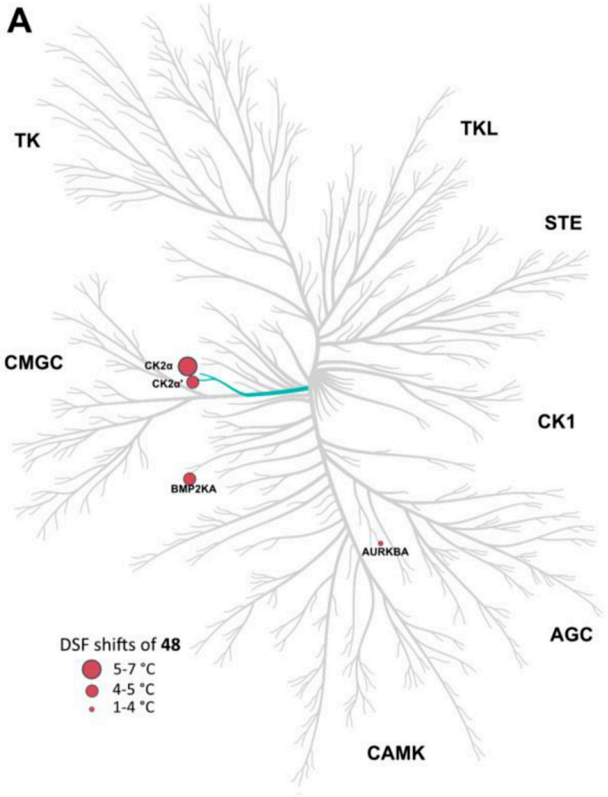

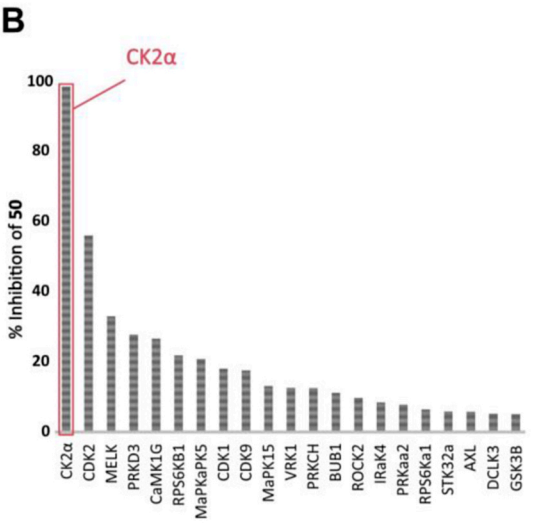

Kinase	% inhibition of 50
CK2α	98.4
CDK2	56.0
MELK	33.0
PRKD3	27.7

Kinase	ΔTm [°C]	% of reference	KD of reference [nM]
CK2α	7.7	57*	9.25*
CK2α'	5.1	45*	9*
BMP2KA	5.0	27	5.6
AURKBA	4.2	30	19

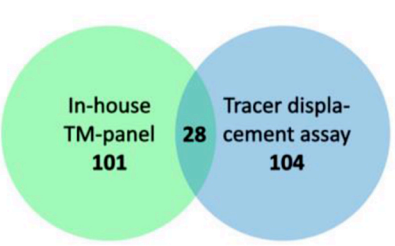

D

	ΔTm [°C]		NanoBRET IC_{50} (lysed) [μM]	ADP glo IC_{50} [μM]
	CK2α	CK2α'	CK2α	CK2α
29	2.2 ± 1.9	1.1 ± 0.4	49 ± 5.0	90
33	1.0 ± 1.3	0.5 ± 0.6	>100	>200
50	6.2 ± 1.7	5.0 ± 0.7	6.0 ± 0.4	3.4 ± 2.3
48	7.0 ± 0.6	5.0 ± 0.9	7.0 ± 0.1	4.3 ± 0.4
26	6.3 ± 1.1	2.7 ± 1.2	31 ± 3.0	28.5 ± 1.4
27	6.0 ± 0.7	3.2 ± 0.9	17 ± 1.0	20.9 ± 5.8
36	10.0 ± 0.2	8.7 ± 0.1	2.0 ± 0.2	0.9 ± 0.3
40	8.7 ± 0.2	4.3 ± 0.3	20 ± 1.0	14.4 ± 0.2
42	7.0 ± 0.9	3.9 ± 0.4	13 ± 0.3	24.4 ± 6.2
53	6.4 ± 0.1	4.7 ± 0.9	25 ± 4.0	13.1 ± 8.2
ProCAM4066 (14)	4.5 ± 1.4	1.0 ± 0.3	>100	>200
CAM4066 (15)	8.6 ± 0.6	4.2 ± 0.4	3.0 ± 0.1	3.4 ± 2.3

Fig. 6. Selectivity profiling and on target evaluation: (A) Kinome tree representation of Tm shifts of **48** tested in an in-house panel of 101 protein kinases. Values are shown in °C. ΔTm values of top hits of DSF screen of **48** as absolute values and in relation to the reference compound Staurosporine. *CX-4945 was used as reference compound. (B) Structurally related cmpd **50** profiled in a panel of 104 kinases using a tracer displacement assay. Values are shown as % inhibition. Compound conc. 5 μM. (C) Venn diagram representation of the two kinase panels used in this study. A total of 177 different kinases were screened with an overlap of 28 kinases. (D) Summary of tm shifts of compounds across different scaffolds in °C. Corresponding enzyme kinetic IC_{50} values for CK2α. The values were determined using a NanoBRET assay in permeabilized cells and ADP glo (*in vitro*). The ADP-Glo assay was measured with biological and technical duplicates. NanoBRET Assay measurements were performed in biological and technical duplicates (N = 2).

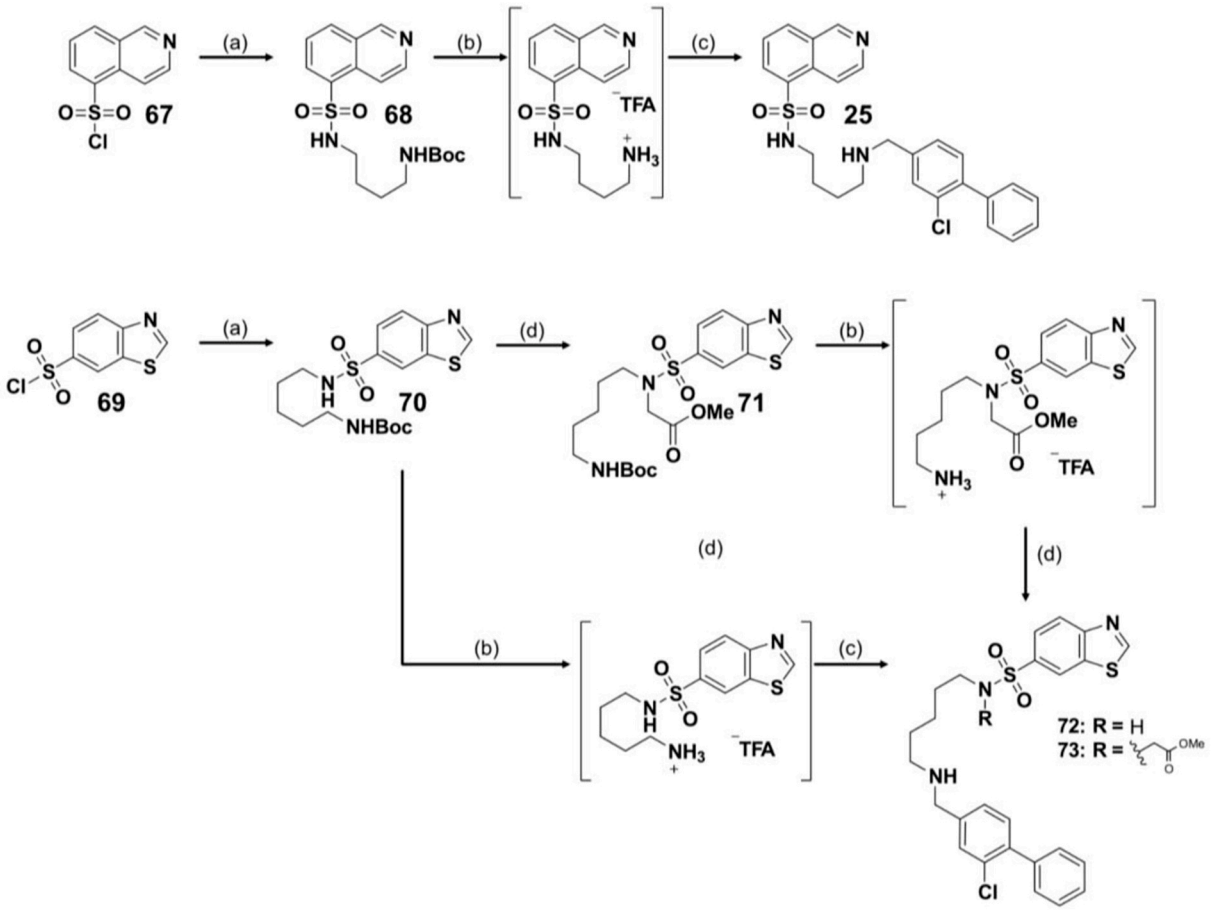

Scheme 3. Synthesis of **25**, **72** and **73** starting from the hinge binder.[a] [a] Reagents and conditions: (a) *tert*-butyl (5-aminopentyl)carbamate, $N(Et)_3$, THF, overnight, rt, 58 % (**68**) 70 % (**70**); (b) TFA, DCM, 0 °C-rt, 1 h, quant.; (c) **18**, $Na[(CH_3COO)_3BH]$, $MgSO_4$, DCM, overnight, rt, 46 % (**25**), 87 % (**72**) and 42 % (**73**); (d) Methyl bromoacetate, K_2CO_3, ACN, 16 h 0–60 °C, quant.

incubation, 5 μl of ADP-GloTM Reagent (Promega) was added to each well and incubated at room temperature for 40 min to stop the kinase reaction and deplete unconsumed ATP. 10 μl of Kinase Detection Reagent (Promega) was added to each well and incubated at room temperature for 45 min to convert ADP to ATP and introduce luciferase and luciferin to detect ATP. Luminescence of each well was recorded using the PHERAstar plate reader (BMG Labtech, Ortenberg, Germany). Data were analyzed using Graphpad Prism 9 software with a normalized response vs log(inhibitor) model with the following equation: Y = 100/(1 + 10^((X-LogIC50))) to determine IC_{50}s of the tested compounds.

4.6. NanoBRET™ assay

The NanoBRET Assay was conducted following the methodology described in the literature [33,54,60]. Briefly, HEK293T cells were transfected with the CSNK2A1-NanoLuc Fusion Vector (Promega, NV2981). This vector is used to express full-length CSNK2A1 kinase fused C-terminal to NanoLuc Luciferase. After trypsinization and resuspension in Opti-MEM without phenol red (Life Technologies), cells were seeded into white 384-well plates (Greiner 784075) at a density of 2 × 10^5 cells/mL. They were then transfected using FuGENE HD (Promega, E2312). Proteins were allowed to express for 20 h at 37 °C/5 % CO2. Using an ECHO acoustic dispenser (Labcyte), the protein-transfected cells were exposed to increasing compound concentrations and NanoBRET K10 Tracer (Promega, TracerDB ID: T000008) at the Tracer KD concentration taken from TracerDB (tracerdb.org). To establish equilibrium, the system was incubated for 2 h at 37 °C/5 % CO2. In accordance with the manufacturer's protocol, NanoBRET NanoGlo Substrate (Promega, N1573) was added, and filtered luminescence was measured using the PHERAstar plate reader (BMG Labtech) equipped with a luminescence filter pair (450 nm BP filter for the donor and 610 nm LP filter for the acceptor). Subsequently, competitive displacement data were analyzed and graphed using GraphPad Prism 10, employing a normalized 3-parameter curve fit with the following equation: $Y = 100/(1 + 10^{(X - \log IC)}_{50})$. For the generation of the permeabilized data, the transfected cells were permeabilized using digitonin (0.05 μg/μL). After an equilibration period of 10 min, luminescence measurements were taken, and the displacement data were analyzed as described previously.

4.7. Protein expression and purification

Expression and purification were performed as described previously [25,34,61]. Briefly, transformed BL21(DE3) cells were grown in Terrific Broth medium containing 50 mg/mL kanamycin. Protein expression was induced at an OD_{600} of 3 by using 0.5 mM isopropyl-thio-galactopyranoside (IPTG) at 18 °C for 12 h. Cells expressing His_6-tagged CK2α were lysed in lysis buffer containing 50 mM HEPES pH 7.5, 500 mM NaCl, 25 mM imidazole, 5 % glycerol, and 0.5 mM Tris(2 carboxyethyl)phosphine (TCEP) by sonication. After centrifugation, the supernatant was loaded onto a Nickel-Sepharose column equilibrated with 30 mL lysis buffer. The column was washed with 60 mL lysis buffer. Proteins were eluted by an imidazole step gradient using 50, 100, 200, 300 mM imidazole concentrations. Fractions containing protein were pooled together and dialyzed overnight using 1L of final buffer (25 mM HEPES pH 7.5, 500 mM NaCl, 0.5 mM

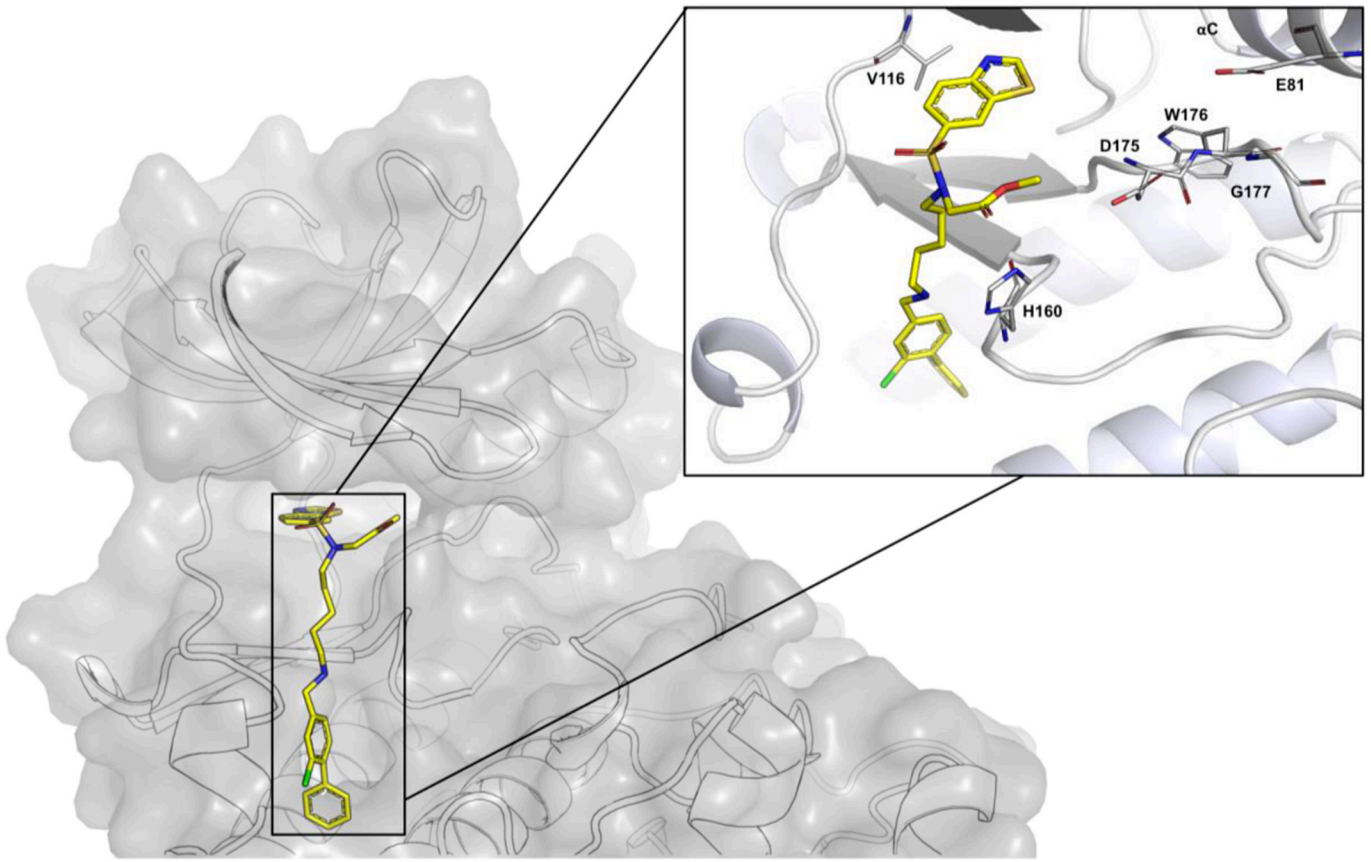

Fig. 7. Co-crystal structure of **73** in CK2α, showcasing the third derivatization direction harnessing the sulfonamide moiety. The methyl ester chemical handle can be further extended both in the direction of the triphosphate pocket and out to the solvent region.

TCEP) at 4 °C. Additionally, TEV protease was added (protein:TEV 1:20 M ratio) to remove the tag. The following day the protein solution was loaded onto Nickel-Sepharose column beads again to remove the TEV protease and cleaved tag. The combined flow through fraction and the wash fraction (25 mM imidazole) containing the protein were combined and concentrated to approximately 4–5 mL and loaded onto Superdex 75 16/60 Hi-Load gel filtration column equilibrated with final buffer. The protein was concentrated to approximately 9 mg/mL.

4.8. Crystallization

CK2α was crystallized using the sitting-drop vapor diffusion method by mixing protein (9 mg/mL) and well solutions in 2:1, 1:1, and 1:2 ratios. The reservoir solution contained 0.2 M ammonia sulfate, 0.1 M bis-tris pH 5.5 and between 23 and 26 % (v/v) PEG 3350. The reservoir solution supplemented with 20 % ethylene glycol was used as cryo-protectant for crystals. Crystals were stored in liquid nitrogen until measurement.

4.9. Data collection, structure solution and refinement

Diffraction data were collected either at beamline X06SA and X06DA (Villigen, CH) or Diamond Light Source I03 (Didcot, UK) at a wavelength of 1.0 Å at 100 K. Data were processed using XDS [62] and scaled with aimless [63]. The PDB structure with the accession code 6Z83 [34] was used as an initial search MR model using the program MOLREP [64]. The dictionary files for the ligands were generated by the Grade Web Server (https://grade.globalphasing.org). The final model was built manually using Coot [65] and refined with REFMAC5 [66], which is a part of the CCP4 suite [65]. Data collection and refinement statistics are summarized on pages S180–S181.

4.10. Chemistry

The synthetic routes of compounds will be outlined in the following and the analytical data can be found on pages S6–S180. All commercial chemicals were purchased from BLD Pharm, TCI, Merck, Enamine and Activate Scientific, with a purity ≥95 % and were used without further purification. Commercial sulfonylchlorides used in this study alongside the corresponding suppliers and catalogue numbers are listed in Supporting Table S4. The solvents with an analytical grade were obtained from VWR Chemicals, Honeywell and Merck and all dry solvents Acros Organics and Thermofischer. All reactions were carried out under an argon atmosphere. The thin layer chromatography was done with silica gel on aluminium foils (60 Å pore diameter) obtained from Macherey-Nagel and visualized with ultraviolet light (λ = 254 and 365 nm). The purification of the compounds was performed by flash chromatography using puriFlash XS 420 device with a UV-VIS multiwave detector (200−400 nm) from Interchim. Pre-packed normal-phase PF-SIHP and pre-packed PF-C18HP reverse phase columns with particle sizes of 15 and 30 μm (Interchim) were used for purification. DMSO was evaporated using a SpeedVac Concentrator (ThermoFischer Scientific, Model#: SPD121P-230) coupled to a Savant RVT5105 Refrigerated Vapor Trap (ThermoFischer Scientific) and a VLP80 vacuum pump (ThermoScientific). Nuclear magnetic resonance spectroscopy (NMR) was performed with DPX250, AV300, AV400, AV500, AV600 MHz spectrometers from Bruker. Chemical shifts (δ) are reported in parts per million (ppm). DMSO-d_6 and methylene chloride-d_2 were used as a solvent, and the spectra were calibrated to the solvent signal: 2.50 ppm (^{1}H NMR) or 39.52 ppm (^{13}C NMR) for DMSO-d_6, 7.26 ppm (^{1}H NMR) or 54.00 ppm (^{13}C NMR) for methylene chloride-d_2. Coupling constants (J) were reported in hertz (Hz) and multiplicities were designated as followed: s (singlet), d (doublet), dd (doublet of doublet), t (triplet), dt

(doublet of triplets), td (triplet of doublets), ddd (doublet of doublet of doublet), q (quartet), m (multiplet). Mass spectra were measured on a Surveyor MSQ device from ThermoFisher measuring in the positive- or negative-ion mode. Final compounds were additionally characterized by HRMS using a MALDI LTQ Orbitrap XL from ThermoScientific and a microOTOF-Q ESI source. The purity of the final compounds was determined by HPLC using an Agilent 1260 Infinity II device with a 1260 DAD HS detector (G7117C; 254 nm, 280 nm, 310 nm) and a LC/MSD device (G6125B, ESI pos. 100–1000). The compounds were analyzed on a Poroshell 120 EC-C18 (Agilent, 3 × 150 mm, 2.7 μm) reversed phase column using 0.1 % formic acid in water (A) and 0.1 % formic acid in acetonitrile (B) as a mobile phase. The following gradient was used: 0 min 5 % B - 2 min 5 % B - 8 min 98 % B - 10 min 98 % B (flow rate of 0.5 mL/min). UV-detection was performed at 254, 280 and 310 nm and all compounds used for further biological characterization showed a purity ≥95 %.

Synthesis of 2-chloro-4-formylphenyltrifluoromethanesulfonate (17). 3-chloro-4-hydroxy-benzaldehyde (**16**) (12.0 g, 76.64 mmol, 1 eq.) and DMAP (911 mg, 6.86 mmol, 0,09 eq.) were charged into a round bottom flask. 250 mL of dry DCM were added through a septum. The mixture was cooled to 0 °C in an ice bath and dry pyridine (18.5 mL, 230 mmol, 3 eq.) were added. The flask was cooled in an ice bath and 1 M trifluoroacetic anhydride (TFAA) solution in DCM (154 mL, 154 mmol, 2 eq.) were added dropwise through a dropping funnel. The solution was warmed to ambient temperature and stirred over 16 h under argon atmosphere. The solvent was evaporated in vacuo. The residue was solved in EtOAc, 1 M aq. HCl were added to the flask and stirred vigorously for 5 min. After transfer into a funnel the organic phase was washed with 1 × 1 M aq. HCl, 3x sat. $NaHCO_3$-solution and 2x with brine. The EtOAc-phase was dried over $MgSO_4$, filtrated and evaporated in vacuo. The crude product was purified by silica column chromatography (*n*-hexanes/EtOAc 4:1). The product was dried overnight using a high vacuum pump to obtain a pale yellow, oily substance that can be stored for up to one year in - 20 °C (19,0 g, 86 %). ^{1}H NMR (250 MHz, DMSO-d_6) δ 10.03 (s, 1H), 8.29 (d, 1H), 8.06 (dd, 1H), 7.91 (d, 12H). ^{13}C NMR (126 MHz, DMSO-d_6) δ 190.93, 148.21, 137.07, 132.16, 130.10, 126.97, 124.53, 116.78. MS-ESI *m/z* $[M+H]^+$: calcd 288.2, found 288.91.

Note: After addition of pyridine the mixture becomes clear.

Synthesis of 2-chloro-[1,1′-biphenyl]-4-carbaldehyde (18). 2-chloro-4-formylphenyltrifluor-methansulfonate (**17**) (500 mg, 1.73 mmol, 1 eq), phenylboronic acid (316 mg, 2.6 mmol, 1.5 eq.), lithium chloride (132 mg, 3.12 mmol, 1.8 eq.), potassium phosphate (1.1 g, 5.2 mmol, 3 eq.) and tetrakis(triphenylphosphine)palladium (18 mg, 0.016 mmol, 0.1 eq.) were charged in a microwave vial and were suspended in DME (10 mL). The suspension was degassed with argon under sonication. The vial was heated in a microwave oven to 80 °C for 3 h. The crude mixture was then filtrated over Celite and diluted with EtOAc. The organic phase was washed with $NaHCO_3$-solution (3x50 mL), Brine (2x50 mL), dried over $MgSO_4$ and the solvent was removed under reduced pressure. The residue was purified by flash chromatography (100 % Heptane) to afford the title compound was afford as white solid (255 mg, 68 %).^{1}H NMR (300 MHz, DMSO-d_6) δ = 10.03 (s, 1H, H-8), 8.05 (d, J = 1.6 Hz, 1H, H-4), 7.92 (dd, J = 7.8, 1.6 Hz, 1H, H-2), 7.61 (d, J = 7.8 Hz, 1H, H, H-5), 7.53–7.40 (m, 5H, H-10, 11, 12, 13, 14). ^{13}C NMR (126 MHz, DMSO-d_6) δ 191.87, 145.29, 137.73, 136.63, 132.40, 132.29, 130.81, 129.07, 128.50, 128.40, 127.93. MS-ESI *m/z* $[M+H]^+$: calcd 216.66, found 217.05.

Note: Older batches of tetrakis(triphenylphosphine)palladium (orange colour) performed with better overall conversion and yields than fresh ones.

The product does not always readily crystallize-it may take at least overnight.

4.11. General procedure A for reductive amination

(18) (1 eq.) and $MgSO_4$ were charged in a flask and suspended in dry DCM. After addition of the corresponding amino linker (1.3 eq.) the mixture was stirred over 1 h under argon atmosphere at room temperature. Sodium triacetoxyborhydride (STAB) (2.5 eq.) was added and the suspension was stirred overnight. Solvents were evaporated, diluted with EtOAc and washed 2x with sat. $NaHCO_3$, 2x with water and 1x with brine. The organic phase was dried over $MgSO_4$ and purified using flash chromatography using DCM/MeOH (91:9) as an eluent.

4.12. General procedure B for N-boc deprotection

N-Boc protected amines were solved in dry DCM. The flask was cooled in an ice bath and trifluoroacetic acid (TFA) in an excess was added dropwise. The solution stirred for 2h at room temperature. Solvents were evaporated until complete dryness and used without further purification in the next step.

4.13. General procedure C for sulfonamide coupling

Deprotected amines were solved in dry THF (≈0.01 M) and triethylamine (3 eq.) was added to the solution. The corresponding sulfonyl chloride was added and stirred under argon atmosphere overnight. Solvents were evaporated, diluted with EtOAc and washed 2x with water and 1x with brine. The organic phase was dried over $MgSO_4$ and purified using flash chromatography using DCM/MeOH (30:1) as an eluent.

Note: In most cases, after ≈ 1h, the solution became slightly blurry indicating the formation of product as it is scarcely soluble in THF. This in addition to the high dilution rendered the reaction chemoselective for the terminal amine.

4.14. General procedure D for the synthesis of sulfinate salts [47]

Brominated fused heterocycles (1 eq.), DABSO (DABCO-Bis(sulfur dioxide)) (1 eq.), dicyclohexylmethylamine (3 eq.), $Pd(amphos)_2Cl_2$ (0.05 eq.) were charged into a microwave vial and suspended in dry isopropanol. The reaction was heated at 110 °C for 1h. The *in situ* formed sulfinate salt was treated with the corresponding electrophile.

Synthesis of *tert*-butyl (5-(((2-chloro-[1,1′-biphenyl]-4yl) methyl)amino)pentyl)carbamate (19). (**19**) was synthesized according to **General Procedure A** using (**18**) (154 mg, 0.7 mmol, 1 eq.) and *tert*-butyl (5-aminopentyl)carbamate (210 mg, 1.04 mmol, 1.5 eq.) in dry DCM (3 mL). (200 mg, 72 %) ^{1}H NMR (500 MHz, DMSO-d_6) δ 7.52–7.31 (m, 8H), 6.75 (t, J = 5.8 Hz, 1H), 3.71 (s, 2H), 2.89 (q, J = 6.6 Hz, 2H), 2.47 (t, J = 7.0 Hz, 2H), 1.49–1.38 (m, 3H), 1.36 (s, 9H), 1.35–1.22 (m, 3H). ^{13}C NMR (126 MHz, DMSO-d_6) δ 155.57, 142.87, 138.73, 137.77, 131.12, 130.95, 129.23, 128.90, 128.18, 127.57, 126.92, 77.27, 52.00, 48.62, 29.44, 29.21, 28.27, 24.13. MS-ESI *m/z* [M+H]+: calcd 403.20, found 403.19.

Synthesis of *tert*-butyl(2-(2-(((2-chloro-[1,1′-biphenyl]-4yl) methyl)amino)etoxy)ethyl)car-bamate (20). (**20**) was synthesized according to **General Procedure A** using (**18**) (250 mg, 1.15 mmol, 1 eq.) and *tert*-butyl (2-(2-aminoethoxy)ethyl)carbamate (236 mg, 1.5 mmol, 1 eq.) in dry DCM (10 mL). (225 mg, 48 %) ^{1}H NMR (400 MHz, DMSO-d_6) δ 7.52 (d, J = 1.5 Hz, 1H), 7.49–7.32 (m, 7H), 6.85–6.80 (m, 1H), 3.75 (s, 2H), 3.47 (t, J = 5.6 Hz, 2H), 3.37 (t, J = 5.9 Hz, 2H), 3.08 (q, J = 5.9 Hz, 2H), 2.64 (t, J = 5.6 Hz, 2H), 1.36 (s, 9H). ^{13}C NMR (101 MHz, DMSO-d_6) δ 156.11, 143.10, 139.20, 138.36, 131.64, 131.47, 129.70, 129.44, 128.67, 128.07, 127.45, 78.03, 70.31, 69.63, 52.32, 48.50, 40.64, 28.70. MS-ESI *m/z* [M+H]+: calcd 405.94, found 405.21.

Synthesis of *tert*-butyl (6-(((2-chloro-[1,1′-biphenyl]-4-yl) methyl)amino)hexyl)carbamate (21). (**21**) was synthesized according to **General Procedure A** using (**18**) (200 mg, 0.92 mmol, 1 eq.) and *tert*-butyl (5-aminohexyl)carbamate (302 mg, 1.11 mmol, 1 eq.) in dry DCM (10 mL). (234 mg, 61 %) ^{1}H NMR (250 MHz, DMSO-d_6) δ 7.54 (d, J = 1.4 Hz, 1H), 7.48–7.39 (m, 5H), 7.37–7.31 (m, 2H), 6.74 (t, J = 5.3 Hz, 1H), 3.76 (s, 2H), 2.89 (q, J = 6.5 Hz, 2H), 1.43 (q, J = 7.3 Hz, 3H), 1.36

(d, J = 0.9 Hz, 8H), 1.35–1.14 (m, 7H). MS-ESI m/z [M+H]+: calcd 417.99, found 417.20.

Synthesis of *tert*-butyl 4-(2-(((2-chloro-[1,1′-biphenyl]-4-yl) methyl)amino)ethyl)piperi-dine-1-carboxylate (22). (**22**) was synthesized according to **General Procedure A** using (**18**) (430 mg, 1.98 mmol, 1 eq.) and 4-(aminoethyl)-1-N-boc-piperidine (570 mg, 2.5 mmol, 1.3 eq.) in dry DCM (13 mL) (406 mg, 57 %). ^{1}H NMR (500 MHz, Methylene Chloride-d$_2$) δ 7.47 (dt, J = 1.4, 0.7 Hz, 1H), 7.46–7.42 (m, 4H), 7.41–7.35 (m, 1H), 7.30 (dd, J = 1.5, 1.0 Hz, 2H), 4.04 (d, J = 12.2 Hz, 2H), 3.83–3.75 (m, 2H), 2.66 (d, J = 7.2 Hz, 2H), 1.65 (s, 2H), 1.53 (dddd, J = 12.5, 11.2, 4.7, 2.3 Hz, 3H), 1.46 (s, 2H), 1.43 (s, 10H), 1.16–1.01 (m, 2H). ^{13}C NMR (126 MHz, Methylene Chloride-d$_2$) δ 155.21, 142.62, 139.92, 139.36, 132.62, 131.79, 130.03, 129.87, 128.60, 128.08, 127.20, 79.35, 47.18, 37.43, 34.52, 30.62, 28.73. MS-ESI m/z [M+H]+: calcd 429.00, found 429.58.

Synthesis of *tert*-butyl 2-(((2-chloro-[1,1′-biphenyl]-4-yl) methyl)amino)-7-azaspiro[3.5]-nonane-7-carboxylate (23). (**23**) was synthesized according to **General Procedure A** using (**18**) (150 mg, 0.69 mmol, 1 eq.) and *tert*-butyl 2-amino-7-azaspiro[3.5]nonane-7-carboxylate (200 mg, 0.83 mmol, 1.2 eq.) in dry DCM (10 mL). (210 mg, 69 %) ^{1}H NMR (400 MHz, DMSO-d_6) δ 7.54 (d, J = 1.5 Hz, 1H), 7.47–7.33 (m, 7H), 3.69 (s, 2H), 3.29 (s, 1H), 3.24 (dd, J = 7.0, 3.5 Hz, 2H), 3.19 (t, J = 5.7 Hz, 2H), 2.06 (ddd, J = 10.1, 7.7, 2.6 Hz, 2H), 1.59–1.52 (m, 2H), 1.46–1.41 (m, 4H), 1.38 (s, 9H). ^{13}C NMR (101 MHz, DMSO-d_6) δ 153.96, 138.61, 138.16, 131.18, 130.96, 129.27, 129.20, 128.20, 127.64, 127.29, 78.40, 48.86, 47.32, 38.76, 31.49, 28.08. MS-ESI m/z [M+H]+: calcd 442.01, found 441.06.

Synthesis of *tert*-butyl 2-(((2-chloro-[1,1′-biphenyl]-4-yl) methyl)amino)-6-azaspiro[3.4]-octane-6-carboxylate (24). (**24**) was synthesized according to **General Procedure A** using (**18**) (230 mg, 1.06 mmol, 1 eq.) and *tert*-butyl 2-amino-6-azaspiro[3.4]octane-6-carboxylate (264 mg, 1.17 mmol, 1.1 eq.) in dry DCM (10 mL). (170 mg, %) ^{1}H NMR (400 MHz, DMSO-d_6) δ 7.53–7.32 (m, 8H), 3.65 (s, 2H), 3.21–3.12 (m, 5H), 2.10 (tdd, J = 9.9, 7.4, 2.7 Hz, 2H), 1.74 (dt, J = 19.0, 9.8 Hz, 4H), 1.38 (s, 9H). ^{13}C NMR (101 MHz, DMSO-d_6) δ 153.68, 142.47, 138.69, 137.89, 131.12, 130.93, 129.22, 129.05, 129.02, 128.19, 127.59, 127.07, 127.05, 78.06, 57.81, 57.40, 49.16, 47.92, 47.65, 47.58, 44.59, 44.36, 44.31, 44.10, 38.97, 28.18. MS-ESI m/z [M+H]+: calcd 427.99, found 427.15.

Synthesis of 3-methyl-3*H*-imidazo[4,5-*b*] pyridine-6-sulfonyl fluoride (60). (**60**) was synthesized according to **General Procedure D** using 6-bromo-3-methyl-3*H*-imidazo[4,5-*b*]pyridine (**59**) (83 mg, 0.4 mmol, 1 eq.), DABSO (96 mg, 0.4 mmol, 1 eq.), dicyclohexylmethylamine (270 μL, 1.2 mmol, 3 eq.), Pd(amphos)$_2$Cl$_2$ (14.2 mg, 0.02 mmol, 0.05 eq.). After heating in the microwave, the reaction was cooled to 0 °C using an ice bath and NFSI (*N*-Fluorosuccinimide, 189 mg, 0.6 mmol, 1.5 eq.) was added to the mixture and stirred 3h at ambient temperature. The solvent was evaporated, the crude was washed 3x with water, 1x with brine and dried over Na_2SO_4. The organic phase was evaporated and purified using flash chromatography (Heptane/EtOAc 2:1 as eluent) yielding the title compound as a white solid (61 mg, 71 %). ^{1}H NMR (400 MHz, DMSO-d_6) δ 9.07 (dd, J = 2.2, 1.1 Hz, 1H), 8.92–8.87 (d, 1H), 8.82 (s, 1H), 3.93 (s, 3H). ^{13}C NMR (101 MHz, DMSO-d_6) δ 151.34, 150.62, 143.42, 133.95, 128.14, 122.37, 122.13, 30.07. ^{19}F NMR (377 MHz, DMSO-d_6) δ −73.41. MS-ESI m/z [M+H]+: calcd 216.20, found 216.00.

Note: Addition of the NFSI resulted in an exothermic reaction (microwave vial became warm) transitioning from a grey suspension to a grey-purple colour after ~15 min.

Synthesis of *tert*-butyl (6-((3-methyl-3*H*-imidazo[4,5-*b*] pyridin-6-yl)sulfonyl)hexyl)car-bamate (62). (**62**) was synthesized according to **General Procedure D** using 6-bromo-3-methyl-3*H*-imidazo[4,5-*b*] pyridine (200 mg, 0.94 mmol, 1 eq.), DABSO (227 mg, 0.94 mmol, 1 eq.), dicyclohexylmethylamine (912 μL, 2.83 mmol, 3 eq.), Pd(amphos)$_2$Cl$_2$ (34 mg, 0.05 mmol, 0.05 eq.). After heating in the microwave *tert*-butyl (6-bromohexyl)carbamate (502 mg, 1.9 mmol, 2 eq.) solved in 1 mL of dry DMF was added to the mixture and heated in the microwave for 1h at 120 °C. The solvent was evaporated, the crude was washed 3x with water, 1x with brine and dried over Na_2SO_4. The organic phase was evaporated and purified using flash chromatography (Heptane/EtOAc 2:1 as eluent) yielding the title compound as a white solid (75 mg, 21 %). ^{1}H NMR (400 MHz, DMSO-d_6) δ 8.83 (t, J = 1.9 Hz, 1H), 8.70–8.66 (m, 1H), 8.53 (t, J = 1.8 Hz, 1H), 6.70 (t, J = 5.5 Hz, 1H), 3.91 (d, J = 1.6 Hz, 3H), 3.46–3.28 (m, 4H), 2.84 (q, J = 6.5 Hz, 2H), 1.53 (h, J = 6.8, 6.0 Hz, 2H), 1.35–1.32 (m, 9H), 1.27 (d, J = 7.2 Hz, 2H), 1.17 (td, J = 8.7, 4.2 Hz, 2H). ^{13}C NMR (101 MHz, DMSO-d_6) δ 155.56, 149.95, 149.27, 143.14, 133.88, 129.65, 127.26, 77.28, 55.33, 55.31, 39.60, 29.86, 29.07, 28.25, 28.21, 27.08, 25.63, 22.35. MS-ESI m/z [M+H]+: calcd 397.50, found 297.10 (*N*-Boc group fragmentation).

Synthesis of *tert*-butyl (4-(imidazo[1,2-*a*] pyridin-6-ylsulfonyl) butyl)carbamate (65). (**65**) was synthesized according to **General Procedure D** using 6-bromoimidazo[1,2-*a*]pyridine (79 mg, 0.4 mmol, 1 eq.), DABSO (96 mg, 0.4 mmol, 1 eq.), dicyclohexylmethylamine (270 μL, 1.2 mmol, 3 eq.), Pd(amphos)$_2$Cl$_2$ (14.2 mg, 0.02 mmol, 0.05 eq.). After heating in the microwave *tert*-butyl (4-bromobutyl)carbamate (202 mg, 0.8 mmol, 2 eq.) solved in 500 μL of dry DMF was added to the mixture and heated in the microwave for 1h at 120 °C. The solvent was evaporated, the crude was washed 3x with water, 1x with brine and dried over Na_2SO_4. The organic phase was evaporated and purified using flash chromatography (Heptane/EtOAc 2:1 as eluent) yielding the title compound as a white solid (20 mg, 14 %). ^{1}H NMR (400 MHz, DMSO-d_6) δ 9.26 (dd, J = 2.0, 1.0 Hz, 1H), 8.19 (s, 1H), 7.76 (dd, J = 5.4, 4.2 Hz, 2H), 7.53 (dd, J = 9.5, 1.9 Hz, 1H), 6.79 (t, J = 5.9 Hz, 1H), 3.44–3.37 (m, 2H), 2.88 (q, J = 6.3 Hz, 2H), 1.62–1.52 (m, 2H), 1.44 (p, J = 6.8 Hz, 2H), 1.30 (s, 9H). ^{13}C NMR (101 MHz, DMSO-d_6) δ 155.62, 144.31, 135.34, 130.66, 124.74, 121.32, 117.38, 115.43, 77.42, 54.46, 38.93, 28.17, 27.98, 19.78.MS-ESI m/z [M+H]+: calcd 354.44, found 354.15.

Synthesis of *tert*-butyl (4-(isoquinoline-5-sulfonamido)butyl) carbamate (68). 5-Isoquinoli-nesulfonylchloride (44 mg, 0.19 mmol, 1 eq) and *N*-Boc-1,4-butanediamine (54 mg, 0.29 mmol, 1.5 eq) were dissolved in dry DCM (1 mL). Triethylamine (133 μL, 0.96 mmol, 5 eq.) was added to the solution and stirred for 3 h at room temperature under argon atmosphere. The reaction mixture was concentrated and the residue diluted in DCM. The organic phase was washed with water (2x100 mL) and brine (2x100 mL). The organic phase was dried over $MgSO_4$ and the solvent was removed under reduced pressure. The residue was purified by flash chromatography (DCM/MeOH. 30:1) affording the title compound as yellow oil (42 mg, 1.49 mmol, 58 %). ^{1}H NMR (500 MHz, Methylene Chloride-d$_2$) δ 9.37–9.33 (m, 1H), 8.65 (dd, J = 6.2, 1.5 Hz, 1H), 8.44–8.38 (m, 2H), 8.25–8.20 (m, 1H), 7.71 (ddd, J = 8.7, 7.4, 1.5 Hz, 1H), 5.67 (s, 1H), 4.62 (s, 1H), 2.95 (dt, J = 28.3, 6.8 Hz, 4H), 1.41 (s, 2H), 1.40 (s, 9H), 1.37 (s, 3H), 1.29–1.21 (m, 1H). ^{13}C NMR (126 MHz, Methylene Chloride-d$_2$) δ 153.92, 145.64, 134.03, 133.77, 126.51, 117.69, 79.56, 54.43, 54.22, 54.00, 53.78, 53.57, 43.46, 40.17, 28.65, 27.90, 26.87. MS-ESI m/z [M+Na]+: calcd 402.48, found 402.08.

Synthesis of *tert*-butyl (5-(benzo[*d*] thiazole-6-sulfonamido) pentyl)carbamate (70). Benzo[*d*]thiazole-6-sulfonyl chloride (**69**) (500 mg, 2.14 mmol, 1 eq) and *N*-Boc-1,5-pentanediamine (476 mg, 2.35 mmol, 1.1 eq) were dissolved in dry THF (40 mL). Triethylamine (895 μL, 6.42 mmol, 3 eq.) was added to the solution and stirred for 3 h at room temperature under argon atmosphere. The reaction mixture was concentrated and the residue diluted in DCM. The organic phase was washed with water (2x100 mL) and brine (2x100 mL). The organic phase was dried over $MgSO_4$ and the solvent was removed under reduced pressure. The residue was purified by flash chromatography (DCM/MeOH. 30:1) affording the title compound as yellow oil (597 mg, 1.49 mmol, 70 %). ^{1}H NMR (400 MHz, DMSO-d_6) δ = 9.61 (s, 1H, H-8), 8.68 (d, J = 1.8 Hz, 1H, H-3), 8.27 (d, J = 8.6 Hz, 1H, H-1), 7.91 (dd, J = 8.6, 1.9 Hz, 1H, H-6), 7.67 (t, J = 5.7 Hz, 1H,N H-23), 6.71 (t, J = 5.7 Hz, 1H, NH-17), 2.78 (dq, J = 29.1, 6.6 Hz, 4H, H-22,18), 1.35 (s, 12H, H-13,21,24,26), 1.30–1.12 (m, 4H, H-19,20), 2.29 (s, 1H). ^{13}C NMR (126 MHz, DMSO-d_6) δ = 160.48 (C-18), 155.53 (C-16), 154.94 (C-5), 137.45

(C-2), 134.09 (C-4), 128.90 (C-1), 128.20, 124.29, 124.17, 123.67 (C-6), 122.12 (C-3), 77.31 (C-14), 42.55 (C-22), 28.92 (C-12), 28.66 (C-19), 28.26 (C-13,25,26), 23.31 (C-20). MS-ESI *m/z* [M+H]+: calcd 399.54, found 400.05.

Synthesis of Methyl *N*-(benzo[*d*]thiazol-6-ylsulfonyl)-*N*-(5-((*tert*-butoxycarbonyl)amino)-pentyl)glycinate (71). (**70**) (461 mg, 1.15 mmol, 1 eq.) was dissolved in dry ACN (15 mL) and cooled to 0 °C. Methyl bromoacetate (397 mg, 2.6 mmol, 2.25 eq.) and potassium carbonate (175 mg, 1.27 mmol, 1.1 eq.) were added to the reaction mixture. The reaction mixture was allowed to warm to room temperature and then heated to 60 °C for 16 h. TLC control showed not complete conversion of starting material and additional methylbromacetate (176 mg, 1.15 mmol, 1.2 eq.) was added to the solution and stirred for 3h. The suspension was diluted in EtOAc, washed with water (2x 100 mL) and brine (2x100 mL). The organic phase was dried over $MgSO_4$ and the solvent was removed under reduced pressure. The title compound crystalized as a yellow solid (542 mg, quant.). ^{1}H NMR (400 MHz, DMSO-d_6) δ = 9.63 (s, 1H, H-8), 8.77 (d, J = 1.9 Hz, 1H, H-3), 8.25 (d, J = 8.6 Hz, 1H, H-1), 7.93 (dd, J = 8.6, 1.9 Hz, 1H, H-6), 6.73 (s, 1H, NH-17), 4.11 (s, 2H, H-27), 3.54 (s, 3H, H-31), 3.17 (t, J = 7.4 Hz, 2H, H-22), 2.83 (q, J = 6.6 Hz, 2H, H-18), 1.43 (p, J = 7.5 Hz, 2H, H-21), 1.36 (s, 9H, H-13,25,26), 1.34–1.23 (m, 2H, H-19), 1.22–1.11 (m, 2H, H-20). ^{13}C NMR (101 MHz, DMSO-d_6) δ = 169.43 (C-28), 160.89 (C-8), 155.56 (C-16), 155.23 (C-5), 136.14 (C-2), 134.25 (C-4), 124.62 (C-1), 124.57 (C-3), 123.56 C-6), 122.73, 77.32 (C-14), 51.88 (C-31), 51.83 (C-27), 48.5 (C-22)1, 48.17 (C-18), 28.98 (C-29), 28.26 (C-13,25,26), 27.11, 23.14 (C-20). MS-ESI *m/z* [M+Na]+: calcd 494.95, found 494.15.

Synthesis of *N*-(4-(((2-chloro-[1,1′-biphenyl]-4-yl)methyl)amino)butyl)isoquinoline-5-sul-fonamide (25). (**68**) (51 mg, 0.13 mmol, 1eq.) was deprotected using **General Procedure B**. The crude product was reacted with (**18**) (20 mg, 0.09 mmol, 1 eq.) according to **General Procedure A** (20 mg, 46 %). ^{1}H NMR (500 MHz, Methylene Chloride-d$_2$) δ 10.14 (d, J = 0.9 Hz, 1H), 8.67 (d, J = 5.7 Hz, 1H), 8.27 (dd, J = 7.3, 1.2 Hz, 1H), 8.05 (dt, J = 8.4, 1.1 Hz, 1H), 7.80 (dd, J = 5.7, 1.0 Hz, 1H), 7.76 (dd, J = 8.3, 7.3 Hz, 1H), 7.48–7.26 (m, 8H), 3.79 (s, 2H), 2.94 (t, J = 6.1 Hz, 2H), 2.54 (t, J = 6.2 Hz, 2H), 1.54–1.42 (m, 4H). ^{13}C NMR (126 MHz, Methylene Chloride-d$_2$) δ 149.86, 144.18, 132.74, 131.97, 130.86, 130.22, 130.00, 129.50, 128.59, 128.12, 127.57, 121.72, 54.43, 54.22, 54.00, 53.78, 53.57, 53.12, 48.87, 43.65, 28.54, 27.94. MS-ESI *m/z* [M + H]+: calcd 480.23, found 480.02. HRMS *m/z* [M + H]+: calcd 479.14343, found 480.14920.

Synthesis of *N*-(5-(((2-chloro-[1,1′-biphenyl]-4-yl)methyl)amino)pentyl)isoquinoline-5-sulfonamide (26). (**19**) (38 mg, 0.09 mmol, 1eq.) was deprotected using **General Procedure B**. The crude product was reacted with 5-Isoquinolinsulfonylchloride (22 mg, 0.09 mmol, 1 eq.) according to **General Procedure A** (38 mg, 86 %). ^{1}H NMR (500 MHz, Methylene Chloride-d$_2$) δ 9.35 (s, 1H), 8.66 (d, J = 6.0 Hz, 1H), 8.45–8.35 (m, 2H), 8.22 (d, J = 8.2 Hz, 1H), 7.71 (t, J = 7.8 Hz, 1H), 7.47–7.40 (m, 5H), 7.38 (ddd, J = 8.9, 5.6, 3.3 Hz, 1H), 7.31–7.25 (m, 2H), 3.76 (s, 2H), 2.92 (t, J = 6.9 Hz, 2H), 2.51 (t, J = 7.0 Hz, 2H), 1.46–1.31 (m, 6H). ^{13}C NMR (126 MHz, Methylene Chloride-d$_2$) δ 153.96, 145.69, 134.04, 133.78, 131.86, 130.04, 129.99, 128.60, 128.12, 127.37, 126.51, 117.63, 54.43, 54.22, 54.00, 49.13, 43.68, 30.25, 29.50, 24.49. MS-ESI *m/z* [M + H]+: calcd 494.16, found 494.24. HRMS *m/z* [M + H]+: calcd 494.15908, found 494.16558.

Synthesis of *N*-(5-(((2-chloro-[1,1′-biphenyl]-4-yl)methyl)amino)pentyl)isoquinoline-5-sulfonamide (27). (**19**) (518 mg, 1.28 mmol, 1 eq.) was deprotected using **General Procedure B**. The crude product was reacted with naphthalene-1-sulfonylchloride (233 mg, 1.03 mmol, 0.8 eq.) according to **General Procedure A** (138 mg, 27 %). ^{1}H NMR (600 MHz, DMSO-d_6) δ 8.67 (dd, J = 8.5, 1.1 Hz, 1H), 8.22–8.18 (m, 1H), 8.12 (dd, J = 7.3, 1.3 Hz, 1H), 8.09–8.05 (m, 1H), 7.90 (s, 1H), 7.70 (ddd, J = 8.5, 6.8, 1.5 Hz, 1H), 7.67–7.60 (m, 2H), 7.48–7.44 (m, 3H), 7.43–7.38 (m, 3H), 7.35–7.30 (m, 2H), 3.65 (s, 2H), 2.78 (t, J = 7.0 Hz, 2H), 2.29 (t, J = 7.1 Hz, 2H), 1.24 (dq, J = 25.3, 7.4 Hz, 4H), 1.15–1.07 (m, 2H). ^{13}C NMR (151 MHz, DMSO-d_6) δ 142.47, 138.67, 137.81, 135.85, 133.82, 133.50, 131.05, 130.91, 129.14, 128.88, 128.81, 128.28, 128.11, 127.64, 127.57, 127.51, 126.87, 126.70, 124.71, 124.42, 51.80, 48.26, 42.28, 40.06, 28.87, 28.69, 23.62. MS-ESI *m/z* [M + H]+: calcd 493.16, found 493.13. HRMS *m/z* [M + H]+: calcd 493.1638 found 493.1693.

Synthesis of *N*-(5-(((2-chloro-[1,1′-biphenyl]-4-yl)methyl)amino)pentyl)benzo[*d*]thiazole-6-sulfonamide TFA salt (72). (**19**) (50 mg, 0.12 mmol, 1 eq.) was deprotected using **General Procedure B**. The crude product was reacted with benzo[*d*]thiazole-6-sulfonyl chloride (25 mg, 0.11 mmol, 1 eq.) according to **General Procedure A** (48 mg, 87 %). ^{1}H NMR (400 MHz, DMSO-d_6) δ = 9.61 (s, 1H, H-29), 8.69 (d, J = 1.9 Hz, 1H, H-24), 8.27 (d, J = 8.6 Hz, 1H, H-22), 7.92 (dd, J = 8.6, 1.9 Hz, 1H, H-27), 7.69 (bs, 1H, NH-15), 7.51–7.35 (m, 9H, H-3,4,7,9,10,11,12,13, NH-21), 7.32 (s, 2H, H-1), 2.77 (t, J = 6.9 Hz, 2H, H-16), 2.39 (t, J = 6.9 Hz, 2H, H-20), 2.07 (s, 2H), 1.44–1.15 (m, 6H, H-17,18,19). ^{13}C NMR (101 MHz, DMSO-d_6) δ = 160.47, 154.94, 142.67, 138.71, 137.80, 137.54, 134.09, 131.12, 130.95, 129.22, 128.90, 128.17, 127.57, 126.92, 124.18, 123.67, 122.11, 51.94, 48.43, 42.60, 28.93, 23.85. ^{19}F (282 MHz, DMSO-d_6) δ −73.56. MS-ESI *m/z* [M + H]+: calcd 500.07, found 500.10. HRMS *m/z* [M + H]+: calcd 500.1155 found 500.1210.

Synthesis of *N*-(5-(((2-chloro-[1,1′-biphenyl]-4-yl)methyl)amino)pentyl)-3-methyl-3*H*-imi-dazo[4,5-*b*]pyridine-6-sulfonamide TFA salt (61). (**61**) was synthesized based on [47]. (**19**) (75 mg, 0.19 mmol, 1 eq.) was deprotected using **General Procedure B**. The crude was solved in dry DMSO (3 mL) and transferred into a microwave vial. (**60**) (40 mg, 0.19, 1 eq.) and Triethylamine (77 μL, 0.58 mmol, 3 eq.) were added and the reaction was heated to 100 °C for 10h in a microwave oven. DMSO was evaporated using a SpeedVac. The crude was solved in DCM and washed 2x with water and 2x with brine. Solvents were evaporated and purified using reverse phase flash chromatography (H_2O/ACN as eluents). The product was not completely pure after the first round of chromatography and product was further subjected to reverse phase flash chromatography (H_2O/ACN as eluents with addition of 0.2 % of TFA) yielding the title compound as a TFA salt (17 mg, 18 %). MS-ESI *m/z* [M + H]+: calcd 499.04, found 498.20. HRMS *m/z* [M + H]+: calcd 498.1652 found 498.1709. ^{1}H NMR (500 MHz, DMSO-d_6) δ 8.89 (s, 2H), 8.79 (d, J = 1.5 Hz, 1H), 8.68 (s, 1H), 8.42 (s, 1H), 7.75 (s, 1H), 7.72 (s, 1H), 7.56–7.45 (m, 4H), 7.45–7.39 (m, 3H), 4.18 (d, J = 5.6 Hz, 2H), 3.89 (s, 3H), 2.95–2.83 (m, 2H), 2.76 (q, J = 6.6 Hz, 2H), 1.58 (q, J = 7.7 Hz, 2H), 1.48–1.38 (m, 3H), 1.30 (q, J = 7.9 Hz, 3H). ^{13}C NMR (126 MHz, DMSO-d_6) δ 150.53–147.67 (m), 142.52, 140.76, 138.54, 134.56–134.07 (m), 133.75, 132.17, 131.81, 131.69, 131.60, 129.61, 129.54, 128.81, 128.51, 126.22, 49.50, 47.11, 42.74, 30.32, 28.86, 25.36, 23.48. ^{19}F (282 MHz, DMSO-d_6) δ −73.46.

Synthesis of *N*-(5-(((2-chloro-[1,1′-biphenyl]-4-yl)methyl)amino)pentyl)-2-oxo-2,3-dihy-drobenzo[*d*]oxazole-6-sulfonamide (28). (**19**) (50 mg, 0.12 mmol, 1 eq.) was deprotected using **General Procedure B**. The crude product was reacted with 2-oxo-2,3-dihydrobenzo[*d*]oxazole-6-sulfonyl chloride (28 mg, 0.12 mmol, 1 eq.) according to **General Procedure A** (20 mg, 34 %). ^{1}H NMR (400 MHz, DMSO-d_6) δ = 9.61 (s, 1H, H-29), 8.69 (d, J = 1.9 Hz, 1H, H-24), 8.27 (d, J = 8.6 Hz, 1H, H-22), 7.92 (dd, J = 8.6, 1.9 Hz, 1H, H-27), 7.69 (bs, 1H, NH-15), 7.51–7.35 (m, 9H, H-3,4,7,9,10,11,12,13, NH-21), 7.32 (s, 2H, H-1), 2.77 (t, J = 6.9 Hz, 2H, H-16), 2.39 (t, J = 6.9 Hz, 2H, H-20), 2.07 (s, 2H), 1.44–1.15 (m, 6H, H-17,18,19). ^{13}C NMR (101 MHz, DMSO-d_6) δ = 160.47 (C-29), 154.94 (C-26), 142.67 (C-2), 138.71 (C-8), 137.80 (C-5), 137.54 (C-23), 134.09 (C-6), 131.12 (C-25), 130.95 (C-7), 129.22 (C-10,12), 128.90 (C-22), 128.17 (C-9,11,13), 127.57 (C-4), 126.92 (C-3), 124.18 (C-27), 123.67 (C-24), 122.11, 51.94 (C-1), 48.43 (C-20), 42.60 (C-16), 28.93 (C-17,19), 23.85 (C-18). MS-ESI *m/z* [M + H]+: calcd 500.07, found 500.10. HRMS *m/z* [M + H]+: calcd 500.1155, found 500.1210.

Synthesis of N-(2-(2-(((2-chloro-[1,1′-biphenyl]-4-yl)methyl)amino)ethoxy)ethyl)isoqui-noline-5-sulfonamide (29). (**20**) (31 mg, 0.08 mmol, 1 eq.) was deprotected using **General Procedure B**. The

crude product was reacted with 5-isoquinolinesulfonylchloride (18 mg, 0.08 mmol, 1 eq.) according to **General Procedure A** (32 mg, 82 %). ^{1}H NMR (400 MHz, DMSO-d_6) δ 9.46 (s, 1H), 8.68 (d, J = 6.1 Hz, 1H), 8.48–8.31 (m, 3H), 7.80 (t, J = 7.8 Hz, 1H), 7.51–7.38 (m, 6H), 7.32 (d, J = 1.6 Hz, 2H), 3.67 (s, 2H), 3.26 (t, J = 5.5 Hz, 2H), 3.22 (t, J = 5.6 Hz, 2H), 3.01 (t, J = 5.5 Hz, 2H), 2.42 (t, J = 5.6 Hz, 2H). ^{13}C NMR (101 MHz, DMSO-d_6) δ 153.31, 144.50, 142.45, 138.70, 137.89, 135.27, 133.24, 132.17, 131.17, 130.99, 130.42, 129.22, 128.95, 128.67, 128.19, 127.60, 126.95, 126.35, 117.32, 69.70, 68.70, 51.71, 47.70, 42.33. MS-ESI *m/z* [M + H]+: calcd 497.02, found 496.20. HRMS *m/z* [M + H]+: calcd 496.1383, found 494.1454.

Synthesis of *N*-(2-(2-(((2-chloro-[1,1′-biphenyl]-4-yl)methyl)amino)ethoxy)ethyl)benzo-[*d*]thiazole-6-sulfonamide (30). (**20**) (31 mg, 0.08 mmol, 1 eq.) was deprotected using **General Procedure B**. The crude product was reacted with benzo[*d*]thiazole-6-sulfonyl chloride (17 mg, 0.07 mmol, 0.95 eq.) according to **General Procedure A** (25 mg, 71 %). ^{1}H NMR (500 MHz, DMSO-d_6) δ 9.61 (s, 1H), 8.70 (d, J = 1.9 Hz, 1H), 8.26 (d, J = 8.5 Hz, 1H), 7.94 (dd, J = 8.6, 1.9 Hz, 1H), 7.50–7.38 (m, 6H), 7.33 (d, J = 1.5 Hz, 2H), 3.71 (s, 2H), 3.36 (q, J = 3.2 Hz, 4H), 2.99 (t, J = 5.6 Hz, 2H), 2.56 (t, J = 5.6 Hz, 2H). ^{13}C NMR (126 MHz, DMSO-d_6) δ 160.48, 154.96, 142.38, 138.69, 137.92, 137.72, 134.06, 131.17, 131.00, 129.22, 128.98, 128.19, 127.59, 126.99, 124.20, 123.64, 122.06, 69.75, 68.78, 51.72, 47.82, 42.56. MS-ESI *m/z* [M + H]+: calcd 503.04, found 502.05. HRMS *m/z* [M + H]+: calcd 502.0947, found 502.1009.

Synthesis of *N*-(2-(2-(((2-chloro-[1,1′-biphenyl]-4-yl)methyl)amino)ethoxy)ethyl)-2-me-thylbenzo[*d*]thiazole-6-sulfonamide (31). (**20**) (31 mg, 0.08 mmol, 1 eq.) was deprotected using **General Procedure B**. The crude product was reacted with 2-methylbenzo[*d*]thiazole-6-sulfonyl chloride (17 mg, 0.07 mmol, 0.95 eq.) according to **General Procedure A** (29 mg, 81 %). ^{1}H NMR (400 MHz, DMSO-d_6) δ 8.55 (d, J = 1.9 Hz, 1H), 8.07 (d, J = 8.6 Hz, 1H), 7.88 (dd, J = 8.6, 1.8 Hz, 1H), 7.50 (s, 1H), 7.49–7.37 (m, 5H), 7.33 (d, J = 1.4 Hz, 2H), 3.35 (t, J = 5.2 Hz, 4H), 2.98 (t, J = 5.6 Hz, 2H), 2.84 (d, J = 1.3 Hz, 3H), 2.56 (t, J = 5.6 Hz, 2H). ^{13}C NMR (101 MHz, DMSO-d_6) δ 171.63, 154.99, 142.42, 138.69, 137.90, 136.93, 135.56, 131.17, 130.99, 129.22, 128.97, 128.18, 127.59, 126.97, 124.14, 122.40, 121.42, 69.76, 68.76, 51.73, 47.84, 42.55, 20.01. MS-ESI *m/z* [M + H]+: calcd 517.07, found 516.05. HRMS *m/z* [M + H]+: calcd 516,1104 found 516.1168.

Synthesis of 2-chloro-*N*-(2-(2-(((2-chloro-[1,1′-biphenyl]-4-yl)methyl)amino)ethoxy)e-thyl)benzo[*d*]thiazole-6-sulfonamide (32). (**20**) (31 mg, 0.08 mmol, 1 eq.) was deprotected using **General Procedure B**. The crude product was reacted with 2-chlorobenzo[*d*]thiazole-6-sulfonyl chloride (20 mg, 0.07 mmol, 1 eq.) according to **General Procedure A**. The product was not completely pure after the first round of chromatography and product was further subjected to reverse phase flash chromatography (H_2O/ACN as eluents with addition of 0.2 % of TFA) yielding the title compound as a TFA salt. (30 mg, 81 %). ^{1}H NMR (400 MHz, DMSO-d_6) δ 8.93 (s, 2H), 8.67 (d, J = 1.9 Hz, 1H), 8.17 (d, J = 8.6 Hz, 1H), 7.94 (dd, J = 8.6, 1.9 Hz, 1H), 7.85 (t, J = 5.8 Hz, 1H), 7.73 (d, J = 1.6 Hz, 1H), 7.47 (dtd, J = 25.1, 7.4, 1.6 Hz, 8H), 4.25–4.18 (m, 2H), 3.61 (t, J = 5.1 Hz, 2H), 3.47 (s, 2H), 3.11 (d, J = 5.8 Hz, 2H), 3.02 (q, J = 5.8 Hz, 2H). ^{13}C NMR (101 MHz, DMSO-d_6) δ 157.71, 153.04, 140.84, 138.52, 138.27, 136.70, 133.51, 132.19, 131.87, 131.83, 129.72, 129.61, 128.84, 128.55, 125.41, 123.64, 122.53, 69.41, 65.77, 49.57, 46.49, 42.65. ^{19}F (282 MHz, DMSO-d_6) δ −73.45. MS-ESI *m/z* [M + H]+: calcd 537.49, found 536.05 HRMS *m/z* [M + H]+: calcd 536.0558, found 536.0628.

Synthesis of *N*-(2-(2-(((2-chloro-[1,1′-biphenyl]-4-yl)methyl)amino)ethoxy)ethyl)-2-oxo-2,3-dihydro-1*H*-benzo[*d*]imidazole-5-sulfonamide TFA salt (33). (**20**) (31 mg, 0.08 mmol, 1 eq.) was deprotected using **General Procedure B**. The crude product was reacted with 2-oxo-2,3-dihydro-1H-benzo[*d*]imidazole-5-sulfonyl chloride (16 mg, 0.07 mmol, 0.95 eq.) according to **General Procedure A**. The product was not completely pure after the first round of chromatography and product was further subjected to reverse phase flash chromatography (H_2O/ACN as eluents with addition of 0.2 % of TFA) yielding the title compound as a TFA salt (20 mg, 57 %). ^{1}H NMR (400 MHz, DMSO-d_6) δ 11.14 (s, 1H), 11.07 (s, 1H), 9.72 (s, 1H), 9.24 (s, 2H), 7.78 (d, J = 1.7 Hz, 1H), 7.56–7.40 (m, 8H), 7.34 (d, J = 1.8 Hz, 1H), 7.09 (d, J = 8.2 Hz, 1H), 4.23 (s, 2H), 3.63 (t, J = 5.1 Hz, 2H), 3.06 (dd, J = 7.4, 4.0 Hz, 4H), 2.91 (q, J = 5.8 Hz, 2H). ^{13}C NMR (101 MHz, DMSO-d_6) δ 155.39, 140.30, 138.12, 133.11, 132.15, 131.66, 131.49, 131.34, 129.73, 129.33, 129.17, 128.36, 128.05, 119.99, 108.30, 106.72, 68.93, 65.27, 49.01, 45.59, 45.57, 42.18. ^{19}F (282 MHz, DMSO-d_6) δ −73.45. MS-ESI *m/z* [M + H]+: calcd 501.99, found 501.05. HRMS *m/z* [M + H]+: calcd 501.1285, found 501.1353.

Synthesis of *N*-(2-(2-(((2-chloro-[1,1′-biphenyl]-4-yl)methyl)amino)ethoxy)ethyl)-1,3-dimethyl-2-oxo-2,3-dihydro-1*H*-benzo[*d*]imidazole-5-sulfonamide TFA salt (34). (**20**) (31 mg, 0.08 mmol, 1 eq.) was deprotected using **General Procedure B**. The crude product was reacted with 1,3-dimethyl-2-oxo-2,3-dihydro-1H-benzo[*d*]imidazole-5-sulfonyl chloride (18 mg, 0.07 mmol, 0.95 eq.) according to **General Procedure A**. The product was not completely pure after the first round of chromatography and product was further subjected to reverse phase flash chromatography (H_2O/ACN as eluents with addition of 0.2 % of TFA) yielding the title compound as a TFA salt (33 mg, 89 %). ^{1}H NMR (400 MHz, DMSO-d_6) δ 9.08 (s, 2H), 7.74 (d, J = 1.7 Hz, 1H), 7.57–7.40 (m, 10H), 7.34–7.28 (m, 1H), 4.22 (d, J = 5.6 Hz, 2H), 3.63 (t, J = 5.0 Hz, 2H), 3.45 (d, J = 11.5 Hz, 2H), 3.37 (s, 3H), 3.36 (s, 3H), 3.12 (p, J = 5.1 Hz, 2H), 2.95 (q, J = 5.8 Hz, 2H), 2.07 (s, 2H). ^{13}C NMR (101 MHz, DMSO-d_6) δ 140.35, 138.09, 133.08, 132.73, 131.69, 131.42, 131.36, 129.70, 129.25, 129.15, 128.35, 128.06, 120.16, 107.54, 105.93, 69.00, 65.33, 49.09, 46.00, 42.18, 27.24, 27.18, 1.15. ^{19}F (282 MHz, DMSO-d_6) δ −73.96. MS-ESI *m/z* [M + H]+: calcd 530.05, found 529.15. HRMS *m/z* [M + H]+: calcd 529.1598, found 529.1654.

Synthesis of *N*-(2-(2-(((2-chloro-[1,1′-biphenyl]-4-yl)methyl)amino)ethoxy)ethyl)-3-cya-nobenzenesulfonamide (35). (**20**) (31 mg, 0.08 mmol, 1 eq.) was deprotected using **General Procedure B**. The crude product was reacted with 3-cyanobenzenesulfonyl chloride (14 mg, 0.07 mmol, 0.95 eq.) according to **General Procedure A** (30 mg, 91 %). ^{1}H NMR (400 MHz, DMSO-d_6) δ 8.22 (t, J = 1.7 Hz, 1H), 8.11 (dd, J = 8.0, 1.7 Hz, 2H), 7.81 (t, J = 7.9 Hz, 1H), 7.58 (d, J = 1.5 Hz, 1H), 7.51–7.36 (m, 7H), 3.87 (s, 2H), 3.44 (t, J = 5.5 Hz, 2H), 3.38 (t, J = 5.5 Hz, 2H), 3.01 (t, J = 5.5 Hz, 2H), 2.72 (t, J = 5.5 Hz, 2H). ^{13}C NMR (101 MHz, DMSO-d_6) δ 142.15, 138.56, 138.53, 135.94, 131.32, 131.10, 130.91, 130.71, 130.02, 129.62, 129.20, 128.23, 127.72, 127.59, 117.63, 112.40, 68.81, 68.61, 51.06, 47.34, 42.45.MS-ESI *m/z* [M + H]+: calcd 470.98, found 470.10. HRMS *m/z* [M + H]+: calcd 470.1227, found 494.1292.

Synthesis of *N*-(6-(((2-chloro-[1,1′-biphenyl]-4-yl)methyl)amino)hexyl)isoquinoline-5-sulfonamide (36). (21) (36 mg, 0.09 mmol, 1 eq.) was deprotected using **General Procedure B**. The crude product was reacted with 5-Isoquinolinsulfonylchloride (23 mg, 0.09 mmol, 1 eq.) according to **General Procedure A** (41 mg, 90 %). ^{1}H NMR (400 MHz, DMSO-d_6) δ 9.47 (s, 1H), 8.69 (d, J = 6.1 Hz, 1H), 8.43 (dd, J = 12.1, 7.2 Hz, 2H), 8.33 (d, J = 7.3 Hz, 1H), 8.06 (s, 1H), 7.82 (t, J = 7.7 Hz, 1H), 7.53 (s, 1H), 7.51–7.40 (m, 5H), 7.36 (s, 2H), 3.76 (s, 2H), 2.78 (t, J = 7.0 Hz, 2H), 2.42 (d, J = 7.3 Hz, 2H), 1.24 (d, J = 7.1 Hz, 4H), 1.06 (q, J = 3.5 Hz, 4H). ^{13}C NMR (101 MHz, DMSO-d_6) δ 153.38, 144.51, 138.60, 138.24, 135.05, 133.29, 132.36, 131.24, 131.02, 130.39, 129.31, 129.21, 128.22, 127.68, 127.32, 126.41, 117.25, 51.42, 48.11, 42.20, 28.93, 28.54, 26.03, 25.73. MS-ESI *m/z* [M + H]+: calcd 509.078, found 508.15. HRMS *m/z* [M + H]+: calcd 508.1747, found 508.1808.

Synthesis of *N*-(6-(((2-chloro-[1,1′-biphenyl]-4-yl)methyl)amino)hexyl)-3-methylquino-line-8-sulfonamide (37). (**21**) (36 mg, 0.09 mmol, 1 eq.) was deprotected using **General Procedure B**. The crude product was reacted with 3-methylquinoline-8-sulfonyl chloride (22 mg, 0.09 mmol, 1 eq.) according to **General Procedure A** (39 mg, 83 %). ^{1}H NMR (400 MHz, DMSO-d_6) δ 8.94 (d, J = 2.3 Hz, 1H), 8.31 (dd, J = 2.3, 1.2 Hz, 1H), 8.21 (ddd, J = 12.6, 7.8, 1.5 Hz, 2H), 7.71 (dd,

J = 8.2, 7.3 Hz, 1H), 7.56 (d, J = 1.3 Hz, 1H), 7.49–7.37 (m, 7H), 7.13 (s, 1H), 3.81 (s, 2H), 2.78 (q, J = 6.5 Hz, 2H), 2.54 (s, 3H), 1.32–1.26 (m, 4H), 1.24 (s, 3H), 1.10 (h, J = 4.3, 3.3 Hz, 4H). ^{13}C NMR (101 MHz, DMSO-d_6) δ 153.50, 141.43, 139.02, 138.90, 136.80, 135.85, 133.34, 132.48, 131.75, 130.08, 129.96, 129.68, 128.82, 128.71, 128.19, 127.96, 126.26, 51.68, 48.48, 43.26, 29.38, 28.74, 26.50, 26.30, 22.57, 18.66. MS-ESI m/z [M + H]+: calcd 523.10, found 522.15. HRMS m/z [M + H]+: calcd 522.1903, found 522.1969.

Synthesis of *N*-(6-(((2-chloro-[1,1′-biphenyl]-4-yl)methyl) amino)hexyl)benzo[*d*]thiazole-6-sulfonamide (38). (**21**) (36 mg, 0.09 mmol, 1 eq.) was deprotected using **General Procedure B**. The crude product was reacted with benzo[*d*]thiazole-6-sulfonyl chloride (19 mg, 0.09 mmol, 1 eq.) according to **General Procedure A** (40 mg, 87 %). ^{1}H NMR (400 MHz, DMSO-d_6) δ 9.61 (s, 1H), 8.69 (d, J = 1.8 Hz, 1H), 8.27 (d, J = 8.6 Hz, 1H), 7.92 (dd, J = 8.6, 1.9 Hz, 1H), 7.71 (s, 1H), 7.60 (d, J = 1.5 Hz, 1H), 7.49–7.42 (m, 4H), 7.41–7.37 (m, 3H), 3.92 (s, 2H), 2.77 (t, J = 7.1 Hz, 2H), 2.64 (t, J = 7.4 Hz, 2H), 1.43 (td, J = 14.2, 7.1 Hz, 3H), 1.36 (d, J = 6.8 Hz, 3H), 1.21 (q, J = 3.4 Hz, 4H). ^{13}C NMR (101 MHz, DMSO-d_6) δ 160.50, 154.95, 138.93, 138.42, 137.53, 134.10, 131.38, 131.13, 129.98, 129.18, 129.18, 128.25, 127.92, 127.78, 124.18, 123.68, 122.11, 50.61, 47.67, 42.50, 28.92, 27.48, 25.92, 25.78. MS-ESI m/z [M + H]+: calcd 515.09, found 514.10. HRMS m/z [M + H]+: calcd 514.1311, found 514.1379.

Synthesis of *N*-(6-(((2-chloro-[1,1′-biphenyl]-4-yl)methyl) amino)hexyl)-2-methylbenzo-[*d*]thiazole-6-sulfonamide (39). (**21**) (36 mg, 0.09 mmol, 1 eq.) was deprotected using **General Procedure B**. The crude product was reacted with 2-methylbenzo[*d*]thiazole-6-sulfonyl chloride (20 mg, 0.09 mmol, 1 eq.) according to **General Procedure A** (42 mg, 88 %). ^{1}H NMR (400 MHz, DMSO-d_6) δ 8.54 (d, J = 1.8 Hz, 1H), 8.08 (d, J = 8.6 Hz, 1H), 7.85 (dd, J = 8.6, 1.9 Hz, 1H), 7.63 (s, 1H), 7.51 (d, J = 1.3 Hz, 1H), 7.47–7.39 (m, 5H), 7.34 (s, 2H), 3.72 (s, 2H), 2.84 (s, 3H), 2.75 (t, J = 7.1 Hz, 2H), 2.45 (t, J = 7.1 Hz, 2H), 1.34 (q, J = 6.9 Hz, 4H), 1.19 (d, J = 3.9 Hz, 4H). ^{13}C NMR (101 MHz, DMSO-d_6) δ 171.61, 154.97, 142.02, 138.66, 137.98, 136.78, 135.58, 131.16, 130.99, 129.21, 129.07, 128.19, 127.61, 127.08, 124.13, 122.43, 121.46, 51.73, 48.36, 42.53, 29.01, 28.96, 26.24, 25.95, 20.00. MS-ESI m/z [M + H]+: calcd 529.12, found 528.10. HRMS m/z [M + H]+: calcd 528.1468, found 528.1539.

Synthesis of 2-chloro-*N*-(6-(((2-chloro-[1,1′-biphenyl]-4-yl) methyl)amino)hexyl)benzo-[*d*]thiazole-6-sulfonamide (40). (**21**) (36 mg, 0.09 mmol, 1 eq.) was deprotected using **General Procedure B**. The crude product was reacted with 2-chlorobenzo[*d*]thiazole-6-sulfonyl chloride (24 mg, 0.09 mmol, 1 eq.) according to **General Procedure A** (5 mg, 10 %). ^{1}H NMR (400 MHz, DMSO-d_6) δ 8.66 (d, J = 1.8 Hz, 1H), 8.16 (d, J = 8.6 Hz, 1H), 7.93 (dd, J = 8.6, 1.9 Hz, 1H), 7.78 (d, J = 5.9 Hz, 1H), 7.72 (s, 1H), 7.58–7.32 (m, 8H), 4.10 (s, 2H), 2.79 (dt, J = 19.7, 6.9 Hz, 4H), 1.54 (s, 2H), 1.43–1.31 (m, 2H), 1.23 (p, J = 4.4, 3.8 Hz, 4H). ^{13}C NMR (101 MHz, DMSO-d_6) δ 152.95, 140.70, 138.57, 138.42, 136.67, 133.89, 132.15, 131.79, 131.75, 129.62, 128.82, 128.73, 128.51, 125.44, 123.59, 122.51, 49.53, 47.20, 42.93, 29.30, 26.02, 25.96, 25.82. MS-ESI m/z [M + H]+: calcd 549.54, found 548.10. HRMS m/z [M + H]+: calcd 548.0921, found 548.1002.

Synthesis of *N*-(6-(((2-chloro-[1,1′-biphenyl]-4-yl)methyl) amino)hexyl)-2-oxo-2,3-dihy-drobenzo[*d*]oxazole-6-sulfonamide (41). (**21**) (36 mg, 0.09 mmol, 1 eq.) was deprotected using **General Procedure B**. The crude product was reacted with 2-oxo-2,3-dihydrobenzo[*d*]oxazole-6-sulfonyl chloride (21 mg, 0.09 mmol, 1 eq.) according to **General Procedure A** (38 mg, 86 %). ^{1}H NMR (400 MHz, DMSO-d_6) δ 7.68 (d, J = 1.6 Hz, 1H), 7.60–7.53 (m, 2H), 7.52–7.39 (m, 8H), 7.25 (d, J = 8.1 Hz, 1H), 4.05 (s, 2H), 2.73 (dt, J = 26.5, 7.1 Hz, 4H), 1.51 (p, J = 7.3 Hz, 2H), 1.34 (q, J = 6.8 Hz, 2H), 1.21 (p, J = 3.8 Hz, 4H). ^{13}C NMR (101 MHz, DMSO-d_6) δ 155.41, 143.35, 139.52, 138.28, 136.14, 135.83, 133.21, 131.52, 131.21, 130.59, 129.17, 128.51, 128.30, 127.90, 122.87, 109.91, 107.33, 49.93, 47.26, 42.41, 28.75, 26.52, 25.73, 25.69. MS-ESI m/z [M + H]+: calcd 515.04, found 514.20. HRMS m/z [M + H]+: calcd 514.1489, found 514.1554.

Synthesis of *N*-((2-chloro-[1,1′-biphenyl]-4-yl)methyl)-4-(imidazo[1,2-*a*]pyridin-6-ylsulfo-nyl)butan-1-amine FA salt (66). (**66**) was synthesized based on [47]. (65) (20 mg, 0.08 mmol, 1 eq.) was solved in 1.5 mL of dry DCM and deprotected using 5 mL 4 M HCl in Dioxane. After 1h 300 μL of triethylamine were added to the solution and stirred 5 min. All solvents were evaporated, the crude was solved in dry DCM (5 mL) and transferred into a 50 mL round bottom flask. (**18**) (17 mg, 0.08, 1 eq.) and sodium triacetoxyborohydride (42 mg, 0.2 mmol, 2.5 eq.) were added and the reaction was stirred over night at room temperature. Sat. $NaHCO_3$ was added and stirred rigorously for 5 min. The mixture was transferred into a separatory funnel and washed 2x with water and 2x with brine and dried over $MgSO_4$. Solvents were evaporated and the crude purified using reverse phase flash chromatography (H_2O/ACN as eluents). The product was not completely pure after the first round of chromatography and product was further subjected to reverse phase flash chromatography (H_2O/ACN as eluents with addition of 0.1 % of formic acid) yielding the title compound as a FA salt (4 mg, 23 %). ^{1}H NMR (400 MHz, DMSO-d_6) δ 9.28 (s, 1H), 8.26 (s, 1H), 8.19 (s, 1H), 7.77 (d, J = 8.9 Hz, 2H), 7.59–7.37 (m, 7H), 7.32 (s, 2H), 3.73 (d, J = 2.9 Hz, 2H), 3.42 (t, J = 7.8 Hz, 3H), 2.55 (d, J = 6.9 Hz, 2H), 1.68 (t, J = 7.9 Hz, 2H), 1.54 (p, J = 7.1 Hz, 2H). ^{13}C NMR (101 MHz, DMSO-d_6) δ 138.61, 138.19, 135.36, 131.21, 131.01, 130.69, 129.27, 129.21, 128.22, 127.66, 127.25, 124.77, 121.34, 117.40, 115.44, 54.67, 51.32, 47.42, 27.12, 20.25. MS-ESI m/z [M + H]+: calcd 454.98, found 454.15. HRMS m/z [M + H]+: calcd 454.1278, found 454.1336.

Synthesis of *N*-((2-chloro-[1,1′-biphenyl]-4-yl)methyl)-6-((3-methyl-3H-imidazo[4,5-*b*]py-ridin-6-yl)sulfonyl)hexan-1-amine TFA salt (63). (**62**) (35 mg, 0.09 mmol, 1 eq.) was deprotected using **General Procedure B**. All solvents were evaporated, solved in DCM and 0.5 mL of triethylamine were added and stirred for 5 min. All solvents were evaporated again $MgSO_4$ (21 mg, 0.176 mmol, 2 eq.), sodium triacetoxyborohydride (37 mg, 0.176 mmol, 2 eq.) and (**18**) (19 mg, 0.08 mmol, 1 eq.) were added to the flask. Dry DCM (5 mL) was added and the reaction was stirred for 16 h at ambient temperature. Solvents were evaporated and the crude purified using reverse phase flash chromatography (H_2O/ACN as eluents). The product was not completely pure after the first round of chromatography and product was further subjected to reverse phase flash chromatography (H_2O/ACN as eluents with addition of 0.2 % of TFA) yielding the title compound as a TFA salt (11 mg, 25 %). ^{1}H NMR (400 MHz, DMSO-d_6) δ 8.98 (s, 2H), 8.85 (d, J = 2.0 Hz, 1H), 8.72 (s, 1H), 8.55 (d, J = 2.0 Hz, 1H), 7.73 (d, J = 1.6 Hz, 1H), 7.53–7.40 (m, 7H), 4.19 (t, J = 5.8 Hz, 2H), 3.91 (s, 3H), 3.48–3.39 (m, 2H), 2.91 (dq, J = 11.7, 6.4 Hz, 2H), 1.57 (qd, J = 7.5, 3.9 Hz, 4H), 1.37–1.25 (m, 4H). ^{13}C NMR (101 MHz, DMSO-d_6) δ 150.00, 149.38, 143.16, 140.27, 138.09, 133.86, 133.31, 131.69, 131.35, 131.24, 129.68, 129.14, 129.08, 128.33, 128.03, 127.27, 55.19, 49.04, 46.64, 29.90, 26.86, 25.29, 25.07, 22.16. ^{19}F (282 MHz, DMSO-d_6) δ −74.03. MS-ESI m/z [M + H]+: calcd 498.05, found 497.15. HRMS m/z [M + H]+: calcd 497.1699, found 497.1764.

Synthesis of *N*-((2-chloro-[1,1′-biphenyl]-4-yl)methyl)-2-(1-(isoquinolin-5-ylsulfonyl)pi-peridin-4-yl)ethan-1-amine TFA salt (48). (**22**) (29 mg, 0.07 mmol, 1 eq.) was deprotected using **General Procedure B**. The crude product was reacted with 5-isoquinolinesulfonyl-chloride (18 mg, 0.07 mmol, 1 eq.) according to **General Procedure A**. The product was not completely pure after the first round of chromatog-raphy and product was further subjected to reverse phase flash chromatography (H_2O/ACN as eluents with addition of 0.2 % of TFA) yielding the title compound as a TFA salt (23 mg, 63 %). ^{1}H NMR (400 MHz, DMSO-d_6) δ 9.50 (s, 1H), 8.98 (s, 2H), 8.70 (d, J = 6.1 Hz, 1H), 8.50 (dt, J = 8.2, 1.1 Hz, 1H), 8.46 (d, J = 6.1 Hz, 1H), 8.36 (dd, J = 7.4, 1.2 Hz, 1H), 7.88 (dd, J = 8.2, 7.4 Hz, 1H), 7.70 (d, J = 1.6 Hz, 1H), 7.52–7.38 (m, 7H), 4.17 (s, 2H), 3.75 (dt, J = 12.9, 3.6 Hz, 2H), 2.93 (t, J = 7.8 Hz, 2H), 2.44 (td, J = 12.1, 2.5 Hz, 2H), 1.73–1.62 (m, 2H), 1.51 (q, J = 7.1 Hz, 2H), 1.39–1.29 (m, 1H), 1.10 (qd, J = 12.3, 4.0 Hz, 2H). ^{13}C NMR (101 MHz, DMSO-d_6) δ 153.57, 144.87, 140.22,

138.06, 134.22, 134.07, 133.28, 131.65, 131.53, 131.31, 131.19, 131.04, 129.12, 129.03, 128.31, 128.01, 126.56, 117.18, 48.99, 45.43, 44.42, 31.59, 31.34, 30.75. ^{19}F (282 MHz, DMSO-d_6) δ −73.45. MS-ESI *m/z* [M + H]+: calcd 521.09, found 519.94. HRMS *m/z* [M + H]+: calcd 520.1747, found 520.1797.

Synthesis of 2-(1-(benzo[*d*] thiazol-6-ylsulfonyl)piperidin-4-yl)-*N*-((2-chloro-[1,1′-biphe-nyl] -4-yl)methyl)ethan-1-amine (50). (**22**) (378 mg, 0.9 mmol, 2 eq.) was deprotected using **General Procedure B**. The crude product was reacted with Then benzo[*d*]thiazole-6-sulfonyl chloride (105 mg, 0.45 mmol, 1 eq.) according to **General Procedure A**. The product was recrystallized from EtOH (169 mg, 71 %). ^{1}H NMR (500 MHz, DMSO-d_6) δ 9.66 (s, 2H), 8.71 (d, J = 1.8 Hz, 1H), 8.29 (d, J = 8.6 Hz, 1H), 7.84 (dd, J = 8.6, 1.8 Hz, 2H), 7.63 (dq, J = 7.9, 1.3 Hz, 1H), 7.47 (tt, J = 6.9, 1.2 Hz, 2H), 7.45–7.37 (m, 4H), 4.11 (s, 2H), 3.67 (dt, J = 12.1, 3.4 Hz, 2H), 2.85 (t, J = 7.8 Hz, 2H), 2.22 (td, J = 11.9, 2.5 Hz, 2H), 1.74–1.68 (m, 2H), 1.61 (q, J = 7.3 Hz, 2H), 1.32 (tq, J = 10.7, 3.7 Hz, 1H), 1.23–1.12 (m, 2H). ^{13}C NMR (101 MHz, DMSO-d_6): δ 161.17, 155.40, 140.00, 138.16, 134.49, 133.45, 132.27, 131.43, 131.14, 129.30, 129.13, 128.29, 127.94, 124.99, 123.61, 123.26, 48.73, 45.99, 44.17, 31.59, 31.21, 30.62 MS-ESI *m/z* [M + H]+: calcd 527.11, found 525.97. HRMS *m/z* [M + H]+: calcd 526.1311, found 526.1374.

Synthesis of *N*-((2-chloro-[1,1′-biphenyl] -4-yl)methyl)-2-(1-((3-methylquinolin-8-yl)sulfo-nyl)piperidin-4-yl)ethan-1-amine (49). (**22**) (29 mg, 0.07 mmol, 1 eq.) was deprotected using **General Procedure B**. The crude product was reacted with 3-methylquinoline-8-sulfonyl chloride (17 mg, 0.07 mmol, 1 eq.) according to **General Procedure A** (19 mg, 54 %). ^{1}H NMR (400 MHz, DMSO-d_6) δ 8.92 (d, J = 2.3 Hz, 1H), 8.31–8.26 (m, 1H), 8.20 (dd, J = 8.3, 1.4 Hz, 1H), 7.74–7.68 (m, 2H), 7.53–7.38 (m, 7H), 4.18 (s, 2H), 3.88 (dt, J = 13.0, 3.6 Hz, 2H), 2.95 (t, J = 7.8 Hz, 2H), 2.66 (td, J = 12.4, 2.5 Hz, 2H), 2.52 (d, J = 1.0 Hz, 3H), 1.71–1.60 (m, 2H), 1.53 (q, J = 7.2 Hz, 2H), 1.41–1.30 (m, 1H), 1.12 (tt, J = 11.9, 6.0 Hz, 2H). ^{13}C NMR (101 MHz, DMSO-d_6) δ 153.00, 141.60, 140.24, 138.05, 135.97, 135.11, 133.28, 133.25, 131.85, 131.67, 131.55, 131.31, 131.20, 129.12, 129.05, 128.61, 128.32, 128.02, 125.77, 49.03, 45.93, 44.53, 32.04, 31.59, 31.39, 18.08. MS-ESI *m/z* [M + H]+: calcd 535.12, found 534.02. HRMS *m/z* [M + H]+: calcd 534.1904, found 534.1952.

Synthesis of *N*-((2-chloro-[1,1′-biphenyl] -4-yl)methyl)-2-(1-((2-methylbenzo[*d*] thiazol-6-yl)sulfonyl)piperidin-4-yl)ethan-1-amine (51). (**22**) (29 mg, 0.07 mmol, 1 eq.) was deprotected using **General Procedure B**. The crude product was reacted with with 2-methyl-benzo[*d*]thiazole-6-sulfonyl chloride (17 mg, 0.07 mmol, 1 eq.) according to **General Procedure A** (23 mg, 61 %). ^{1}H NMR (400 MHz, DMSO-d_6) δ 8.56 (d, J = 1.8 Hz, 1H), 8.11 (d, J = 8.5 Hz, 1H), 7.79 (dd, J = 8.6, 1.9 Hz, 1H), 7.67 (d, J = 1.5 Hz, 1H), 7.51–7.38 (m, 7H), 4.10 (s, 2H), 3.66 (dt, J = 12.0, 3.6 Hz, 2H), 2.86 (s, 3H), 2.21 (td, J = 12.0, 11.5, 2.5 Hz, 2H), 1.76–1.61 (m, 2H), 1.49 (q, J = 7.3 Hz, 2H), 1.36–1.26 (m, 1H), 1.18 (qd, J = 11.8, 3.8 Hz, 3H). ^{13}C NMR (101 MHz, DMSO-d_6) δ 172.32, 155.46, 139.88, 138.14, 135.98, 131.58, 131.36, 131.25, 130.86, 129.12, 128.73, 128.30, 127.95, 124.99, 122.59, 122.35, 49.46, 46.02, 44.68, 31.96, 31.61, 30.57, 20.05. MS-ESI *m/z* [M + H]+: calcd 541.14, found 540.10. HRMS *m/z* [M + H]+: calcd 540.1468, found 540.1535.

Synthesis of *N*-((2-chloro-[1,1′-biphenyl] -4-yl)methyl)-2-(1-((2-chlorobenzo[*d*] thiazol-6-yl)sulfonyl)piperidin-4-yl)ethan-1-amine TFA salt (52). (**22**) (68 mg, 0.16 mmol, 1 eq.) was deprotected using **General Procedure B**. The crude product was reacted with 2-chlorobenzo-[*d*]thiazole-6-sulfonyl chloride (43 mg, 0.16 mmol, 1 eq.) according to **General Procedure A**. The product was not completely pure after the first round of chromatography and product was further subjected to reverse phase flash chromatography (H_2O/ACN as eluents with addition of 0.1 % of TFA) yielding the title compound as a TFA salt (52 mg, 89 %). ^{1}H NMR (400 MHz, DMSO-d_6) δ 9.33 (s, 2H), 8.67 (d, J = 1.9 Hz, 1H), 8.18 (d, J = 8.6 Hz, 1H), 7.86 (dd, J = 8.6, 1.9 Hz, 1H), 7.80 (d, J = 1.7 Hz, 1H), 7.58 (dd, J = 8.0, 1.7 Hz, 1H), 7.50–7.38 (m, 6H), 4.14 (s, 2H), 3.72–3.60 (m, 2H), 2.89 (s, 2H), 2.24 (td, J = 11.8, 2.5 Hz, 2H), 1.76–1.67 (m, 2H), 1.58 (q, J = 7.4 Hz, 2H), 1.32 (d, J = 10.8 Hz, 1H), 1.18 (qd, J = 11.8, 3.7 Hz, 2H). ^{13}C NMR (101 MHz, DMSO-d_6) δ 157.67, 152.93, 140.13, 138.10, 136.55, 133.35, 132.73, 131.55, 131.35, 131.22, 129.21, 129.12, 128.31, 127.99, 125.82, 123.06, 123.02, 48.84, 45.96, 44.29, 31.55, 31.26, 30.56. ^{19}F (282 MHz, DMSO-d_6) δ −73.47. MS-ESI *m/z* [M + H]+: calcd 561.55, found 560.10. HRMS *m/z* [M + H]+: calcd 560.0922, found 560.0980.

Synthesis of *N*-((2-chloro-[1,1′-biphenyl] -4-yl)methyl)-7-(isoquinolin-5-ylsulfonyl)-7-aza-spiro[3.5] nonan-2-amine TFA salt (53). (**23**) (30 mg, 0.07 mmol, 1 eq.) was deprotected using **General Procedure B**. The crude product was reacted with 5-Isoquinolinsulfonylchloride (18 mg, 0.07 mmol, 1 eq.) according to **General Procedure A**. The product was not completely pure after the first round of chromatography and product was further subjected to reverse phase flash chromatography (H_2O/ACN as eluents with addition of 0.2 % of TFA) yielding the title compound as a TFA salt (18 mg, 49 %). ^{1}H NMR (400 MHz, DMSO-d_6) δ 9.52 (s, 1H), 9.24 (s, 2H), 8.71 (d, J = 6.1 Hz, 1H), 8.51 (d, J = 8.2 Hz, 1H), 8.43 (d, J = 6.1 Hz, 1H), 8.37 (dd, J = 7.4, 1.2 Hz, 1H), 7.91–7.86 (m, 1H), 7.70 (d, J = 1.8 Hz, 1H), 7.51–7.38 (m, 7H), 4.02 (t, J = 5.6 Hz, 2H), 3.10 (t, J = 5.3 Hz, 2H), 3.04 (t, J = 5.4 Hz, 2H), 2.04 (dd, J = 11.6, 8.9 Hz, 2H), 1.88 (t, J = 10.1 Hz, 2H), 1.59 (dt, J = 11.6, 5.5 Hz, 4H), 1.27–1.22 (m, 1H). ^{13}C NMR (101 MHz, DMSO-d_6) δ 153.55, 144.79, 140.28, 138.05, 134.28, 134.06, 133.16, 131.85, 131.34, 131.13, 129.13, 129.00, 128.35, 128.06, 126.65, 117.23, 46.70, 42.46, 37.54, 34.50, 31.44. ^{19}F (282 MHz, DMSO-d_6) δ −73.39. MS-ESI *m/z* [M + H]+: calcd 533.09, found 532.15. HRMS *m/z* [M + H]+: calcd 532.1747, found 532.1804.

Synthesis of 7-(benzo[*d*] thiazol-6-ylsulfonyl)-*N*-((2-chloro-[1,1′-biphenyl] -4-yl)methyl)-7-azaspiro[3.5] nonan-2-amine TFA salt (54). (**23**) (38 mg, 0.09 mmol, 1 eq.) was deprotected using **General Procedure B**. The crude product was reacted with benzo[*d*]thiazole-6-sulfonyl chloride (20 mg, 0.09 mmol, 1 eq.) according to **General Procedure A**. The product was not completely pure after the first round of chromatog-raphy and product was further subjected to reverse phase flash chromatography (H_2O/ACN as eluents with addition of 0.2 % of TFA) yielding the title compound as a TFA salt (4 mg, 8 %). ^{1}H NMR (400 MHz, DMSO-d_6) δ 9.66 (s, 1H), 9.23 (s, 2H), 8.72 (dd, J = 1.9, 0.6 Hz, 1H), 8.31 (dd, J = 8.6, 0.6 Hz, 1H), 7.86 (dd, J = 8.6, 1.9 Hz, 1H), 7.68 (t, J = 1.0 Hz, 1H), 7.51–7.38 (m, 8H), 7.28–7.11 (m, 1H), 4.01 (s, 2H), 3.67 (h, J = 7.9 Hz, 1H), 2.95 (t, J = 5.4 Hz, 2H), 2.88 (t, J = 5.6 Hz, 2H), 2.09–1.96 (m, 2H), 1.91–1.81 (m, 2H), 1.64 (dt, J = 11.1, 5.5 Hz, 4H). ^{13}C NMR (101 MHz, DMSO-d_6) δ 161.14, 155.41, 140.25, 138.02, 134.50, 133.15, 132.49, 131.69, 131.32, 131.11, 129.10, 128.97, 128.90, 128.32, 128.20, 128.02, 124.93, 123.66, 123.26, 46.65, 46.25, 43.05, 42.81, 37.31, 34.73, 34.30, 31.27. ^{19}F (282 MHz, DMSO-d_6) δ −73.54. MS-ESI *m/z* [M + H]+: calcd 539.12, found 538.00. HRMS *m/z* [M + H]+: calcd 538.1312, found 538.1382.

Synthesis of *N*-((2-chloro-[1,1′-biphenyl] -4-yl)methyl)-7-((2-methylbenzo[*d*] thiazol-6-yl)sulfonyl)-7-azaspiro[3.5] nonan-2-amine TFA salt (55). (**23**) (40 mg, 0.09 mmol, 1 eq.) was deprotected using **General Procedure B**. The crude product was reacted with 2-methylbenzo-[*d*]thiazole-6-sulfonyl chloride (23 mg, 0.09 mmol, 1 eq.) according to **General Procedure A**. The product was not completely pure after the first round of chromatography and product was further subjected to reverse phase flash chromatography (H_2O/ACN as eluents with addition of 0.2 % of TFA) yielding the title compound as a TFA salt (23 mg, 45 %). ^{1}H NMR (400 MHz, DMSO-d_6) δ 9.33 (s, 2H), 8.57 (d, J = 1.8 Hz, 1H), 8.11 (d, J = 8.6 Hz, 1H), 7.80 (dd, J = 8.6, 1.9 Hz, 1H), 7.69 (d, J = 1.5 Hz, 1H), 7.51–7.37 (m, 7H), 4.02 (s, 2H), 3.67 (t, J = 8.1 Hz, 1H), 2.92 (t, J = 5.4 Hz, 2H), 2.07–1.96 (m, 2H), 1.92–1.83 (m, 2H), 1.64 (dt, J = 10.8, 5.4 Hz, 4H). ^{13}C NMR (101 MHz, DMSO-d_6) δ 172.35, 140.23, 138.04, 135.98, 133.16, 131.67, 131.61, 131.32, 131.12, 129.11, 128.98, 128.31, 128.01, 124.93, 122.57, 122.41, 46.64, 46.24, 43.05, 42.81, 37.26, 34.69, 34.27, 31.27, 20.05. ^{19}F (282 MHz, DMSO-d_6) δ −73.42. MS-ESI *m/z* [M + H]+: calcd 553.15, found

551.92. HRMS *m/z* [M + H]+: calcd 552.14680, found 552.1534.

Synthesis of *N*-((2-chloro-[1,1′-biphenyl]-4-yl)methyl)-7-((2-chlorobenzo[*d*]thiazol-6-yl)-sulfonyl)-7-azaspiro[3.5]nonan-2-amine TFA salt (56). (**23**) (30 mg, 0.07 mmol, 1 eq.) was deprotected using **General Procedure B**. The crude product was reacted with 2-chlorobenzo-[*d*]thiazole-6-sulfonyl chloride (18 mg, 0.07 mmol, 1 eq.) according to **General Procedure A**. The product was not completely pure after the first round of chromatography and product was further subjected to reverse phase flash chromatography (H_2O/ACN as eluents with addition of 0.2 % of TFA) yielding the title compound as a TFA salt (36 mg, 95 %). ^{1}H NMR (400 MHz, DMSO-d_6) δ 9.35 (s, 2H), 8.67 (d, J = 1.9 Hz, 1H), 8.18 (d, J = 8.6 Hz, 1H), 7.90–7.84 (m, 1H), 7.70 (d, J = 1.5 Hz, 1H), 7.49–7.38 (m, 7H), 4.01 (s, 2H), 3.67 (p, J = 8.2 Hz, 1H), 2.94 (t, J = 5.4 Hz, 2H), 2.87 (d, J = 6.2 Hz, 2H), 1.64 (q, J = 5.9 Hz, 4H). ^{13}C NMR (101 MHz, DMSO-d_6) δ 140.20, 138.05, 136.55, 133.26, 132.98, 131.65, 131.31, 131.12, 129.11, 128.99, 128.31, 128.01, 125.74, 123.06, 123.02, 46.66, 46.26, 43.03, 42.80, 37.25, 34.72, 34.30, 31.28. ^{19}F (282 MHz, DMSO-d_6) δ −73.40. MS-ESI *m/z* [M + H]+: calcd 573.56, found 571.95. HRMS *m/z* [M + H]+: calcd 572.0922, found 572.1077.

Synthesis of 5-((2-(((2-chloro-[1,1′-biphenyl]-4-yl)methyl)amino)-7-azaspiro[3.5]nonan-7-yl)sulfonyl)-1,3-dimethyl-1,3-dihydro-2*H*-benzo[*d*]imidazole-2-one TFA salt (57). (**23**) (30 mg, 0.07 mmol, 1 eq.) was deprotected using **General Procedure B**. The crude product was reacted with 1,3-dimethyl-2-oxo-2,3-dihydro-1H-benzo[*d*]imidazole-5-sulfonyl chloride (17 mg, 0.07 mmol, 1 eq.) according to **General Procedure A**. The product was not completely pure after the first round of chromatography and product was further subjected to reverse phase flash chromatography (H_2O/ACN as eluents with addition of 0.2 % of TFA) yielding the title compound as a TFA salt (34 mg, 90 %). ^{1}H NMR (400 MHz, DMSO-d_6) δ 9.17 (s, 2H), 7.68 (d, J = 1.5 Hz, 1H), 7.52–7.41 (m, 6H), 7.45–7.36 (m, 3H), 7.37 (d, J = 8.2 Hz, 1H), 4.00 (s, 2H), 3.64 (p, J = 8.0 Hz, 1H), 3.41 (s, 3H), 2.88 (t, J = 5.5 Hz, 2H), 2.81 (t, J = 5.6 Hz, 2H), 2.00 (td, J = 9.3, 8.2, 5.3 Hz, 2H), 1.90–1.81 (m, 2H), 1.63 (dt, J = 10.6, 5.0 Hz, 4H). ^{13}C NMR (101 MHz, DMSO-d_6) δ 154.07, 140.07, 138.09, 133.81, 133.18, 131.63, 131.30, 130.98, 129.79, 129.12, 128.85, 128.30, 127.98, 127.64, 121.13, 107.62, 106.76, 46.82, 46.34, 43.07, 42.82, 37.37, 35.02, 34.40, 31.27, 27.29, 27.26. ^{19}F (282 MHz, DMSO-d_6) δ −73.64. MS-ESI *m/z* [M + H]+: calcd 566.13, found 565.02. HRMS *m/z* [M + H]+: calcd 565.1962, found 565.2015.

Synthesis of 5-(5-((2-(((2-chloro-[1,1′-biphenyl]-4-yl)methyl)amino)-7-azaspiro[3.5]no-nan-7-yl)sulfonyl)-2-ethoxyphenyl)-1-methyl-3-propyl-1,6-dihydro-7*H*-pyrazolo[4,3-*d*]pyrimidin-7-one TFA salt (58). (**23**) (30 mg, 0.07 mmol, 1 eq.) was deprotected using **General Procedure B**. The crude product was reacted with 4-ethoxy-3-(1-methyl-7-oxo-3-propyl-6,7-dihydro-1H-pyrazolo[4,3-*d*]pyrimidine-5-yl)benzenesulfonyl chloride (28 mg, 0.07 mmol, 1 eq.) according to **General Procedure A**. The product was not completely pure after the first round of chromatography and product was further subjected to reverse phase flash chromatography (H_2O/ACN as eluents with addition of 0.2 % of TFA) yielding the title compound as a TFA salt (39 mg, 81 %). ^{1}H NMR (400 MHz, DMSO-d_6) δ 12.21 (s, 1H), 9.47 (s, 1H), 7.90 (d, J = 2.6 Hz, 1H), 7.84 (dd, J = 8.8, 2.5 Hz, 1H), 7.72 (d, J = 1.6 Hz, 1H), 7.55–7.33 (m, 8H), 7.30–7.08 (m, 1H), 4.21 (q, J = 6.9 Hz, 2H), 4.16 (s, 3H), 4.05 (s, 2H), 3.73 (q, J = 8.2 Hz, 1H), 2.97–2.92 (m, 2H), 2.87 (d, J = 5.8 Hz, 2H), 2.78 (t, J = 7.4 Hz, 2H), 2.11–1.99 (m, 2H), 1.94 (dd, J = 12.5, 8.2 Hz, 2H), 1.84–1.73 (m, 2H), 1.65 (dt, J = 10.8, 5.4 Hz, 4H), 1.34 (t, J = 6.9 Hz, 3H), 0.94 (t, J = 7.4 Hz, 3H). ^{13}C NMR (101 MHz, DMSO-d_6) δ 159.77, 148.16, 144.96, 140.26, 138.06, 137.80, 133.15, 131.67, 131.36, 131.27, 131.16, 129.84, 129.12, 129.00, 128.89, 128.31, 128.19, 128.00, 127.29, 124.41, 113.26, 64.86, 46.26, 42.96, 42.69, 37.86, 37.25, 34.72, 34.33, 31.34, 27.17, 21.66, 14.27, 13.83. ^{19}F (282 MHz, DMSO-d_6) δ −73.71. MS-ESI *m/z* [M + H]+: calcd 716.33, found 715.20. HRMS *m/z* [M + H]+: calcd 715.2755, found 715.2828.

Synthesis of *N*-((2-chloro-[1,1′-biphenyl]-4-yl)methyl)-6-(isoquinolin-8-ylsulfonyl)-6-aza-spiro[3.4]octan-2-amine (42). (**24**) (30 mg, 0.07 mmol, 1 eq.) was deprotected using **General Procedure B**. The crude product was reacted with 5-Isoquinolinsulfonylchloride (19 mg, 0.07 mmol, 1 eq.) according to **General Procedure A** (30 mg, 83 %). ^{1}H NMR (500 MHz, DMSO-d_6) δ 9.48 (s, 1H), 8.71 (d, J = 6.1 Hz, 1H), 8.44 (t, J = 6.1 Hz, 2H), 8.33 (d, J = 7.3 Hz, 1H), 7.83 (t, J = 7.7 Hz, 1H), 7.60 (s, 1H), 7.45 (t, J = 7.4 Hz, 2H), 7.39 (d, J = 8.0 Hz, 4H), 7.27–7.08 (m, 1H), 3.53 (p, J = 6.7, 6.0 Hz, 1H), 2.29 (s, 1H), 2.20–2.12 (m, 1H), 1.98 (p, J = 5.8 Hz, 2H), 1.93–1.86 (m, 2H), 1.82 (p, J = 6.0 Hz, 1H), 1.68 (dt, J = 15.5, 9.8 Hz, 2H), 1.29–1.17 (m, 1H). ^{13}C NMR (126 MHz, DMSO-d_6) δ 153.41, 144.56, 139.31, 135.47, 133.48, 132.49, 131.41, 131.12, 130.35, 129.15, 128.61, 128.26, 127.84, 126.53, 117.20, 47.62, 47.34, 43.21, 42.26, 42.03, 30.34. MS-ESI *m/z* [M + H]+: calcd 519.07, found 518.10. HRMS *m/z* [M + H]+: calcd 518.1591, found 518.1650.

Synthesis of 6-(benzo[*d*]thiazol-6-ylsulfonyl)-*N*-((2-chloro-[1,1′-biphenyl]-4-yl)methyl)-6-azaspiro[3.4]octan-2-amine TFA salt (43). (**24**) (30 mg, 0.07 mmol, 1 eq.) was deprotected using **General Procedure B**. The crude product was reacted with benzo[*d*]thiazole-6-sulfonyl chloride (16 mg, 0.07 mmol, 1 eq.) according to **General Procedure A**. The product was not completely pure after the first round of chromatography and product was further subjected to reverse phase flash chromatography (H_2O/ACN as eluents with addition of 0.2 % of TFA) yielding the title compound as a TFA salt (29 mg, 83 %). ^{1}H NMR (400 MHz, DMSO-d_6) δ 9.62 (s, 1H), 8.69 (d, J = 1.8 Hz, 1H), 8.27 (d, J = 8.6 Hz, 1H), 8.06 (d, J = 8.5 Hz, 1H), 7.92 (dd, J = 8.6, 1.9 Hz, 1H), 7.64 (d, J = 1.5 Hz, 1H), 7.48–7.38 (m, 8H), 3.94 (s, 2H), 3.60 (h, J = 8.2 Hz, 2H), 3.45 (p, J = 8.0 Hz, 2H), 3.24–2.99 (m, 1H), 2.26 (ddd, J = 11.6, 7.6, 3.9 Hz, 1H), 2.09 (ddt, J = 24.7, 12.3, 4.6 Hz, 4H), 1.96 (ddd, J = 16.6, 8.3, 4.6 Hz, 2H), 1.76 (dt, J = 11.4, 7.8 Hz, 3H). ^{13}C NMR (101 MHz, DMSO-d_6) δ 160.59, 155.04, 139.86, 138.34, 138.16, 134.57, 134.08, 131.58, 131.26, 130.79, 129.15, 128.67, 128.30, 127.96, 124.26, 123.65, 122.16, 47.12, 47.08, 43.32, 42.19, 42.03, 38.31, 37.74, 30.55. ^{19}F (282 MHz, DMSO-d_6) δ −73.64. MS-ESI *m/z* [M + H]+: calcd 525.09, found 524.10. HRMS *m/z* [M + H]+: calcd 524.1155, found 524.1290.

Synthesis of *N*-((2-chloro-[1,1′-biphenyl]-4-yl)methyl)-6-((2-methylbenzo[*d*]thiazol-6-yl)-sulfonyl)-6-azaspiro[3.4]octan-2-amine TFA salt (44). (**24**) (30 mg, 0.07 mmol, 1 eq.) was deprotected using **General Procedure B**. The crude product was reacted with 2-methylbenzo[*d*]thiazole-6-sulfonyl chloride (17 mg, 0.07 mmol, 1 eq.) according to **General Procedure A**. The product was not completely pure after the first round of chromatography and product was further subjected to reverse phase flash chromatography (H_2O/ACN as eluents with addition of 0.2 % of TFA) yielding the title compound as a TFA salt (20 mg, 53 %). ^{1}H NMR (400 MHz, DMSO-d_6) δ 9.19 (s, 1H), 8.54 (d, J = 1.9 Hz, 1H), 8.08 (d, J = 8.6 Hz, 1H), 8.00 (d, J = 8.6 Hz, 1H), 7.85 (dd, J = 8.6, 1.9 Hz, 1H), 7.68 (d, J = 1.5 Hz, 1H), 7.51–7.37 (m, 7H), 3.99 (s, 2H), 3.67–3.57 (m, 1H), 3.57–3.51 (m, 1H), 3.09 (q, J = 7.3 Hz, 1H), 2.85 (s, 3H), 2.32–2.23 (m, 1H), 2.16–2.04 (m, 4H), 1.96 (ddd, J = 12.1, 7.4, 5.2 Hz, 1H), 1.76 (ddd, J = 11.6, 8.6, 6.2 Hz, 2H). ^{13}C NMR (101 MHz, DMSO-d_6) δ 171.77, 171.77, 140.16, 138.09, 137.52, 135.56, 133.44, 131.65, 131.32, 131.05, 129.15, 128.91, 128.32, 128.01, 124.21, 122.42, 121.53, 46.90, 46.83, 43.26, 42.10, 41.99, 37.79, 37.19, 30.58, 20.03. ^{19}F (282 MHz, DMSO-d_6) δ −73.66. MS-ESI *m/z* [M + H]+: calcd 539.12, found 538.10. HRMS *m/z* [M + H]+: calcd 538.1312, found 538.1372.

Synthesis of *N*-((2-chloro-[1,1′-biphenyl]-4-yl)methyl)-6-((2-chlorobenzo[*d*]thiazol-6-yl)-sulfonyl)-6-azaspiro[3.4]octan-2-amine TFA salt (45). (**24**) (30 mg, 0.07 mmol, 1 eq.) was deprotected using **General Procedure B**. The crude product was reacted with 2-chlorobenzo[*d*]thiazole-6-sulfonyl chloride (19 mg, 0.07 mmol, 1 eq.) according to **General Procedure A**. The product was not completely pure after the first round of chromatography and product was further subjected to reverse phase flash chromatography (H_2O/ACN as eluents

with addition of 0.2 % of TFA) yielding the title compound as a TFA salt (38 mg, 86 %). ^{1}H NMR (400 MHz, DMSO-d_6) δ 8.65 (d, J = 1.9 Hz, 1H), 8.15 (d, J = 8.6 Hz, 1H), 8.09 (d, J = 8.5 Hz, 1H), 7.92 (dd, J = 8.6, 1.9 Hz, 1H), 7.66 (d, J = 1.4 Hz, 1H), 7.50–7.37 (m, 7H), 3.96 (s, 2H), 3.60 (p, J = 8.1 Hz, 1H), 3.49–3.44 (m, 1H), 3.09 (q, J = 7.3 Hz, 1H), 2.27 (ddd, J = 11.3, 7.6, 3.4 Hz, 1H), 2.13–2.04 (m, 3H), 1.99 (dt, J = 11.5, 4.7 Hz, 1H), 1.77 (ddd, J = 11.5, 8.7, 5.4 Hz, 2H). ^{13}C NMR (101 MHz, DMSO-d_6) δ 157.16, 152.54, 139.96, 138.75, 138.12, 136.13, 134.20, 131.61, 131.28, 130.88, 129.15, 128.75, 128.31, 127.98, 125.04, 123.06, 122.05, 47.02, 43.30, 42.14, 41.98, 38.14, 37.56, 30.56. ^{19}F (282 MHz, DMSO-d_6) δ −73.67. MS-ESI m/z [M + H]+: calcd 559.54, found 558.05. HRMS m/z [M + H]+: calcd 558.0765, found 558.0847.

Synthesis of 5-((2-(((2-chloro-[1,1′-biphenyl]-4-yl)methyl)amino)-6-azaspiro[3.4]octan-6-yl)sulfonyl)-1,3-dimethyl-1,3-dihydro-2*H*-benzo[*d*]imidazole-2-one (46). (**24**) (30 mg, 0.07 mmol, 1 eq.) was deprotected using **General Procedure B**. The crude product was reacted with 1,3-dimethyl-2-oxo-2,3-dihydro-1H-benzo[*d*]imidazole-5-sulfonyl chloride (18 mg, 0.07 mmol, 1 eq.) according to **General Procedure A** (38 mg, 86 %). ^{1}H NMR (400 MHz, DMSO-d_6) δ 8.89 (s, 1H), 7.75 (d, J = 8.6 Hz, 1H), 7.66 (d, J = 1.1 Hz, 1H), 7.54–7.50 (m, 2H), 7.49–7.44 (m, 4H), 7.42–7.39 (m, 2H), 7.32 (d, J = 8.7 Hz, 1H), 3.98 (s, 2H), 3.51 (dq, J = 19.7, 7.9 Hz, 3H), 3.39 (s, 3H), 3.37 (s, 3H), 2.28 (ddd, J = 11.5, 7.6, 3.7 Hz, 1H), 2.09 (tdd, J = 12.1, 7.5, 4.7 Hz, 4H), 1.96 (ddd, J = 12.0, 7.3, 5.1 Hz, 1H), 1.76 (ddd, J = 11.3, 8.6, 2.0 Hz, 2H). ^{13}C NMR (101 MHz, DMSO-d_6) δ 140.06, 138.08, 133.84, 132.65, 131.65, 131.29, 130.93, 129.55, 129.14, 128.80, 128.32, 128.01, 120.16, 107.48, 105.93, 47.00, 43.25, 42.16, 42.05, 38.05, 37.43, 30.58, 27.25, 27.19. MS-ESI m/z [M + H]+: calcd 552.10, found 551.15. HRMS m/z [M + H]+: calcd 551.1805, found 551.1865.

Synthesis of 6-((2-(((2-chloro-[1,1′-biphenyl]-4-yl)methyl)amino)-6-azaspiro[3.4]octan-6-yl)sulfonyl)benzo[*d*]oxazol-2(3*H*)-one (47). (**24**) (30 mg, 0.07 mmol, 1 eq.) was deprotected using **General Procedure B**. The crude product was reacted with 2-oxo-2,3-dihydrobenzo[*d*]oxazole-6-sulfonyl chloride (16 mg, 0.07 mmol, 1 eq.) according to General Procedure A (38 mg, 86 %). ^{1}H NMR (500 MHz, DMSO-d_6) δ 7.82 (d, J = 8.5 Hz, 1H), 7.59 (t, J = 9.1 Hz, 3H), 7.50–7.45 (m, 2H), 7.40 (d, J = 7.4 Hz, 4H), 7.24 (d, J = 7.9 Hz, 1H), 7.19–7.09 (m, 1H), 3.82 (s, 2H), 3.53 (d, J = 8.1 Hz, 1H), 3.27 (s, 2H), 2.28–2.19 (m, 1H), 2.07 (ddt, J = 18.2, 11.9, 6.3 Hz, 2H), 1.97–1.84 (m, 3H), 1.77–1.68 (m, 2H). ^{13}C NMR (126 MHz, DMSO-d_6) δ 154.59, 143.00, 139.24, 138.29, 134.63, 134.59, 131.44, 131.13, 130.18, 129.15, 128.90, 128.27, 128.12, 127.85, 123.04, 109.78, 107.65, 47.80, 47.50, 43.33, 42.34, 42.09, 30.48. MS-ESI m/z [M + H]+: calcd 525.03, found 524.10. HRMS m/z [M + H]+: calcd 524.1333, found 524.1394.

Synthesis of Methyl *N*-(benzo[*d*]thiazol-6-ylsulfonyl)-*N*-(5-(((2-chloro-[1,1′-biphenyl]-4-yl)methyl)amino)pentyl)glycinate TFA salt (73). To a solution of (68) (50 mg, 0.09 mmol, 1 eq.) in DCM (1 mL) was added TFA (1 mL) at 0 °C. The reaction mixture was allowed to warm to room temperature and stirred for 1 h. The reaction mixture was concentrated, co-evaporate two times with Toluol, quenching with triethylamine (0.5 mL) and again co-evaporated two times with toluol. The residue was dried under vacuum for 16 h. The crude amine was solved in DCM (3 mL), (**18**) (21 mg, 0.09 mmol, 1 eq.) and $MgSO_4$ was added and stirred for 10 min. Sodium triacetoxyborohydride (42 mg, 0.2 mmol, 2 eq.) was added and stirred overnight. The mixture was concentrated and the residue was solved DCM. The organic phase was washed with water 2x, brine 2x, dried over $MgSO_4$ and the solvent was removed under reduced pressure. The residue was purified by rp-flash chromatography (H_2O/ACN). The product was not completely pure after the first round of chromatography and product was further subjected to reverse phase flash chromatography (H_2O/ACN as eluents with addition of 0.2 % of TFA) yielding the title compound as a TFA salt (24 mg, 42 %). ^{1}H NMR (400 MHz, DMSO-d_6) δ = 9.63 (s, 1H), 8.78 (d, J = 1.9 Hz, 1H), 8.25 (d, J = 8.6 Hz, 1H), 7.93 (dd, J = 8.7, 1.9 Hz, 1H), 7.54 (d, J = 1.3 Hz, 1H), 7.50–7.38 (m, 8H), 7.36 (d, J = 1.4 Hz, 2H), 4.12 (s, 2H), 3.76 (s, 2H), 3.54 (s, 3H), 3.19 (t, J = 7.3 Hz, 2H), 1.43 (dp, J = 23.3, 7.4 Hz, 6H), 1.30–1.14 (m, 4H). ^{13}C NMR (101 MHz, DMSO-d_6) δ = 169.46, 160.91, 155.23, 138.60, 136.15, 134.25, 131.21, 131.00, 129.20, 128.20 C-29), 127.64, 127.25, 124.56, 123.56, 122.73, 51.83, 48.55, 48.52, 48.26, 48.17, 27.34, 23.57. ^{19}F (282 MHz, DMSO-d_6) δ −73.40. MS-ESI m/z [M + H]+: calcd 573.14, found 572.20. HRMS m/z [M + H]+: calcd 572.1366, found 572.1439.

Synthesis of Methyl 3-(3-(3-(((2-chloro-[1,1′-biphenyl]-4-yl)methyl)amino)propanamido)-propanamido)benzoate TFA salt (14). (**14**) was synthesized according to [45]. Additionally, purification was performed using reverse phase flash chromatography (H_2O/ACN as eluents with addition of 0.2 % of TFA) yielding the title compound as a TFA salt (32 mg, 30 % over 5 steps). ^{1}H NMR (400 MHz, DMSO-d_6) δ 10.22 (s, 1H), 8.96 (s, 2H), 8.34–8.20 (m, 2H), 7.81 (ddd, J = 8.2, 2.3, 1.1 Hz, 1H), 7.74 (d, J = 1.6 Hz, 1H), 7.63 (dt, J = 7.8, 1.3 Hz, 1H), 7.53–7.42 (m, 8H), 4.23 (t, J = 5.5 Hz, 2H), 3.84 (s, 3H), 3.39 (q, J = 6.4 Hz, 2H), 3.16 (p, J = 6.9 Hz, 2H), 2.58–2.51 (m, 4H). ^{13}C NMR (101 MHz, DMSO-d_6) δ 170.22, 169.56, 166.59, 140.80, 140.01, 138.53, 133.56, 132.21, 131.84, 131.75, 130.54, 129.66, 129.62, 129.60, 128.81, 128.52, 124.20, 123.97, 120.06, 52.66, 49.50, 43.32, 36.60, 35.50, 31.40. ^{19}F (282 MHz, DMSO-d_6) δ −74.20. MS-ESI m/z [M + H]+: calcd 494.99, found 494.10.

Synthesis of 3-(3-(3-(((2-chloro-[1,1′-biphenyl]-4-yl)methyl)amino)propanamido)propan-amido)benzoic acid HCl salt (15). (**15**) was synthesized according to Ref. [45]. Additionally, purification was performed by precipitating the product as HCl salt with 4 N HCl in dioxane and rinsing the product with DCM and diethyl ether (20 mg, 43 % over 6 steps). ^{1}H NMR (400 MHz, DMSO-d_6) δ 10.30 (q, J = 3.3 Hz, 1H), 8.34 (d, J = 6.8 Hz, 1H), 8.28 (q, J = 1.8 Hz, 1H), 7.85–7.80 (m, 2H), 7.60 (ddd, J = 8.0, 3.7, 2.2 Hz, 2H), 7.49–7.39 (m, 7H), 4.17 (s, 2H), 3.37 (q, J = 6.4 Hz, 2H), 3.09 (t, J = 7.3 Hz, 2H), 2.61 (td, J = 6.8, 3.7 Hz, 2H), 2.54 (t, J = 6.7 Hz, 2H). ^{13}C NMR (101 MHz, DMSO-d_6) δ 169.74, 169.19, 167.23, 140.07, 139.44, 138.16, 133.72, 131.60, 131.27, 129.17, 129.12, 128.87, 128.31, 127.98, 123.89, 123.16, 119.91, 49.01, 42.85, 36.21, 35.13, 31.21. MS-ESI m/z [M + H]+: calcd 480.96, found 480.10.

5. Author information

Manuscript was drafted by FAG and edited by all authors. FAG designed compounds which were synthesized by FAG, JG and JM. AK performed ITC measurement, provided the proteins for the DSF assay and performed the X-ray crystallography and structural analyses; LE did the kinome wide DSF measurements and ADP glo assay; TALE performed NanoBRET measurements with the help of our student Fabian Göllner; Scientific supervision by SM, TH and SK.

CRediT authorship contribution statement

Francesco A. Greco: Writing – original draft, Formal analysis, Data curation, Conceptualization. **Andreas Krämer:** Writing – review & editing, Investigation, Formal analysis, Data curation. **Laurenz Wahl:** Methodology, Investigation, Data curation. **Lewis Elson:** Methodology, Investigation, Data curation. **Theresa A.L. Ehret:** Methodology, Investigation, Data curation. **Joshua Gerninghaus:** Methodology, Investigation, Data curation. **Janina Möckel:** Methodology, Investigation, Data curation. **Susanne Müller:** Writing – review & editing, Validation, Supervision. **Thomas Hanke:** Writing – review & editing, Supervision, Formal analysis, Data curation, Conceptualization. **Stefan Knapp:** Writing – review & editing, Supervision, Project administration, Funding acquisition, Conceptualization.

Declaration of competing interest

The authors declare that they have no known competing financial interests or personal relationships that could have appeared to influence the work reported in this paper.

Data availability

Data will be made available on request.

Acknowledgement

FAG, AK, JG, TE, LW, TH, SK are grateful for support by the Structural Genomics Consortium (SGC), a registered charity (no: 1097737) that receives funds from Bayer AG, Boehringer Ingelheim, Bristol Myers Squibb, Genentech, Genome Canada through Ontario Genomics Institute, EU/EFPIA/OICR/McGill/KTH/Diamond Innovative Medicines Initiative 2 Joint Undertaking [EUbOPEN grant 875510], Janssen, Pfizer and Takeda. We would like to thank Takeda for helping with the kinome-wide tracer displacement assay. AK and SK are grateful for support by the German Cancer Research Center DKTK and AK, SM and SK by the Frankfurt Cancer Institute (FCI). FAG would like to acknowledge support by the LOEWE project TRABITA and TH by the program ENABLE. We thank the staff at the Swiss Light Source (CH) and Diamond Light Source (UK) for assistance during X-ray data collection.

Appendix A. Supplementary data

Supplementary data to this article can be found online at https://doi.org/10.1016/j.ejmech.2024.116672.

Abbreviations

ATP	adenosine triphosphate
CDK	Cyclin-dependent kinase
CK2	casein kinase-2
CLK	Cdc2-like kinase
Cy_2NME	*N,N*-dicyclohexylmethylamine;
DABSO	DABCO (1,4-diazabicyclo[2.2. 2]octane)-Bis(sulfur dioxide)
DAPK	Death associated protein kinase
DCM	dichloromethane
DMAP	4-dimethylaminopyridine;
DME	1,2-dimethoxyethane
DMF	*N,N*-dimethylformamide;
DMSO	dimethyl sulfoxide;
DSF	differential scanning fluorimetry
DYRK	dual-specificity tyrosine-regulated kinase
FLT	fms related receptor tyrosine kinase
GTP	guanosine triphosphate
HIPK	Homeodomain-interacting protein kinase
i-PrOH	isopropanol
ITC	isothermal titration calorimetry
MAPK	mitogen-activated protein kinase
$N(Et)_3$	triethylamine;
N-Boc	*N-tert*-butyloxycarbonyl
NFSI	*N*-Fluorobenzenesulfonimide;
on	overnight
PDB	Protein Data Base
PEG	polyethylene glycol
PIM	Pim-1 Proto-Oncogene Serine/Threonine Kinase
PK	protein kinase; rt, room temperature
SAR	structure activity relationship;
SGC	Structural Genomic Consortium
S_N2	bimolecular nucleophilic substitution
TBK	TANK-binding kinase
THF	tetrahydrofuran
Tm shift	thermal shift
μW	microwave

References

[1] S. Röhm, A. Krämer, S. Knapp, Function, structure and Topology of protein kinases, in: S. Laufer (Ed.), Proteinkinase Inhibitors, Springer, Cham, 2021, pp. 1–24.
[2] A.M. Fry, L. O'Regan, S.R. Sabir, R. Bayliss, Cell cycle regulation by the NEK family of protein kinases, J. Cell Sci. 125 (2012) 4423–4433, https://doi.org/10.1242/jcs.111195.
[3] A. Fortner, A. Chera, A. Tanca, O. Bucur, Apoptosis regulation by the tyrosine-protein kinase CSK, Front. Cell Dev. Biol. 10 (2022) 1078180, https://doi.org/10.3389/fcell.2022.1078180.
[4] P. Singh, P. Ravanan, P. Talwar, Death associated protein kinase 1 (DAPK1): a regulator of apoptosis and Autophagy, Front. Mol. Neurosci. 9 (2016) 46, https://doi.org/10.3389/fnmol.2016.00046.
[5] M. Hluchý, P. Gajdušková, I. Ruiz de Los Mozos, M. Rájecký, M. Kluge, B.-T. Berger, Z. Slabá, D. Potěšil, E. Weiß, J. Ule, Z. Zdráhal, S. Knapp, K. Paruch, C. C. Friedel, D. Blazek, CDK11 regulates pre-mRNA splicing by phosphorylation of SF3B1, Nature 609 (2022) 829–834, https://doi.org/10.1038/s41586-022-05204-z.
[6] S. Laufer (Ed.), Proteinkinase Inhibitors, Springer, Cham, 2021.
[7] H. Patterson, R. Nibbs, I. McInnes, S. Siebert, Protein kinase inhibitors in the treatment of inflammatory and autoimmune diseases, Clin. Exp. Immunol. 176 (2014) 1–10, https://doi.org/10.1111/cei.12248.
[8] I. Lonskaya, M.L. Hebron, N.M. Desforges, A. Franjie, C.E.-H. Moussa, Tyrosine kinase inhibition increases functional parkin-Beclin-1 interaction and enhances amyloid clearance and cognitive performance, EMBO Mol. Med. 5 (2013) 1247–1262, https://doi.org/10.1002/emmm.201302771.
[9] M. Montenarh, C. Götz, The interactome of protein kinase CK2, in: L.A. Pinna (Ed.), Protein Kinase CK2, Wiley-Blackwell, Ames, Iowa, USA, 2013, pp. 76–116.
[10] L.A. Pinna (Ed.), Protein Kinase CK2, Wiley-Blackwell, Ames, Iowa, USA, 2013.
[11] M. Buljan, R. Ciuffa, A. van Drogen, A. Vichalkovski, M. Mehnert, G. Rosenberger, S. Lee, M. Varjosalo, L.E. Pernas, V. Spegg, B. Snijder, R. Aebersold, M. Gstaiger, Kinase interaction Network expands functional and disease roles of human kinases, Mol. Cell 79 (2020) 504–520.e9, https://doi.org/10.1016/j.molcel.2020.07.001.
[12] D.C. Seldin, P. Leder, Casein kinase II alpha transgene-induced murine lymphoma: relation to theileriosis in cattle, Science 267 (1995) 894–897, https://doi.org/10.1126/science.7846532.
[13] H.A. Lashuel, C.R. Overk, A. Oueslati, E. Masliah, The many faces of α-synuclein: from structure and toxicity to therapeutic target, Nat. Rev. Neurosci. 14 (2013) 38–48, https://doi.org/10.1038/nrn3406.
[14] C.A. Marshall, J.D. McBride, L. Changolkar, D.M. Riddle, J.Q. Trojanowski, V.M.-Y. Lee, Inhibition of CK2 mitigates Alzheimer's tau pathology by preventing NR2B synaptic mislocalization, Acta Neuropathol. Commun 10 (2022) 30, https://doi.org/10.1186/s40478-022-01331-w.
[15] V. Pastori, E. Sangalli, P. Coccetti, C. Pozzi, S. Nonnis, G. Tedeschi, P. Fusi, CK2 and GSK3 phosphorylation on S29 controls wild-type ATXN3 nuclear uptake, Biochim. Biophys. Acta 1802 (2010) 583–592, https://doi.org/10.1016/j.bbadis.2010.03.007.
[16] I.-Y. Chen, S.C. Chang, H.-Y. Wu, T.-C. Yu, W.-C. Wei, S. Lin, C.-L. Chien, M.-F. Chang, Upregulation of the chemokine (C-C motif) ligand 2 via a severe acute respiratory syndrome coronavirus spike-ACE2 signaling pathway, J. Virol. 84 (2010) 7703–7712, https://doi.org/10.1128/JVI.02560-09.
[17] J.M. Firzlaff, D.A. Galloway, R.N. Eisenman, B. Lüscher, The E7 protein of human papillomavirus type 16 is phosphorylated by casein kinase II, New Biol. 1 (1989) 44–53.
[18] C.P. Quezada Meza, M. Ruzzene, Protein kinase CK2 and SARS-CoV-2: an expected Interplay story, Kinases and Phosphatases 1 (2023) 141–150, https://doi.org/10.3390/kinasesphosphatases1020009.
[19] X. Yang, R.J. Dickmander, A. Bayati, S.A. Taft-Benz, J.L. Smith, C.I. Wells, E. A. Madden, J.W. Brown, E.M. Lenarcic, B.L. Yount, E. Chang, A.D. Axtman, R. S. Baric, M.T. Heise, P.S. McPherson, N.J. Moorman, T.M. Willson, Host kinase CSNK2 is a target for inhibition of Pathogenic SARS-like β-Coronaviruses, ACS Chem. Biol. 17 (2022) 1937–1950, https://doi.org/10.1021/acschembio.2c00378.
[20] S.A.J. Augustine, Y.Y. Kleshchenko, P.N. Nde, S. Pratap, E.A. Ager, J.M. Burns, M. F. Lima, F. Villalta, Molecular cloning of a Trypanosoma cruzi cell surface casein kinase II substrate, Tc-1, involved in cellular infection, Infect. Immun. 74 (2006) 3922–3929, https://doi.org/10.1128/IAI.00045-06.
[21] O.K. ole-MoiYoi, Casein kinase II in theileriosis, Science 267 (1995) 834–836, https://doi.org/10.1126/science.7846527.
[22] H.W. Ong, D.H. Drewry, A.D. Axtman, CK2 chemical probes: Past, present, and future, Kinases and Phosphatases 1 (2023) 288–305, https://doi.org/10.3390/kinasesphosphatases1040017.
[23] Y. Chen, Y. Wang, J. Wang, Z. Zhou, S. Cao, J. Zhang, Strategies of targeting CK2 in drug discovery: Challenges, Opportunities, and Emerging Prospects, J. Med. Chem. 66 (2023) 2257–2281, https://doi.org/10.1021/acs.jmedchem.2c01523.
[24] S. Day-Riley, R.M. West, P.D. Brear, M. Hyvönen, D.R. Spring, CK2 inhibitors targeting inside and outside the catalytic box, Kinases and Phosphatases 2 (2024) 110–135, https://doi.org/10.3390/kinasesphosphatases2020007.
[25] A. Krämer, C.G. Kurz, B.-T. Berger, I.E. Celik, A. Tjaden, F.A. Greco, S. Knapp, T. Hanke, Optimization of pyrazolo1,5-apyrimidines lead to the identification of a highly selective casein kinase 2 inhibitor, Eur. J. Med. Chem. 208 (2020) 112770, https://doi.org/10.1016/j.ejmech.2020.112770.
[26] D. Lindenblatt, V. Applegate, A. Nickelsen, M. Klußmann, I. Neundorf, C. Götz, J. Jose, K. Niefind, Molecular Plasticity of crystalline CK2α' leads to KN2, a bivalent inhibitor of protein kinase CK2 with Extraordinary selectivity, J. Med. Chem. 65 (2022) 1302–1312, https://doi.org/10.1021/acs.jmedchem.1c00063.

[27] J. Iegre, E.L. Atkinson, P.D. Brear, B.M. Cooper, M. Hyvönen, D.R. Spring, Chemical probes targeting the kinase CK2: a journey outside the catalytic box, Org. Biomol. Chem. 19 (2021) 4380–4396, https://doi.org/10.1039/d1ob00257k.
[28] I. Kufareva, B. Bestgen, P. Brear, R. Prudent, B. Laudet, V. Moucadel, M. Ettaoussi, C.F. Sautel, I. Krimm, M. Engel, O. Filhol, M. Le Borgne, T. Lomberget, C. Cochet, R. Abagyan, Discovery of holoenzyme-disrupting chemicals as substrate-selective CK2 inhibitors, Sci. Rep. 9 (2019) 15893, https://doi.org/10.1038/s41598-019-52141-5.
[29] C. Borgo, C. D'Amore, S. Sarno, M. Salvi, M. Ruzzene, Protein kinase CK2: a potential therapeutic target for diverse human diseases, Signal Transduct. Target. Ther. 6 (2021) 183, https://doi.org/10.1038/s41392-021-00567-7.
[30] ClinicalTrials.gov..
[31] J. Vahter, K. Viht, A. Uri, E. Enkvist, Oligo-aspartic acid conjugates with benzoc2,6naphthyridine-8-carboxylic acid scaffold as picomolar inhibitors of CK2, Bioorg. Med. Chem. 25 (2017) 2277–2284, https://doi.org/10.1016/j.bmc.2017.02.055.
[32] F. Pierre, P.C. Chua, S.E. O'Brien, A. Siddiqui-Jain, P. Bourbon, M. Haddach, J. Michaux, J. Nagasawa, M.K. Schwaebe, E. Stefan, A. Vialettes, J.P. Whitten, T. K. Chen, L. Darjania, R. Stansfield, J. Bliesath, D. Drygin, C. Ho, M. Omori, C. Proffitt, N. Streiner, W.G. Rice, D.M. Ryckman, K. Anderes, Pre-clinical characterization of CX-4945, a potent and selective small molecule inhibitor of CK2 for the treatment of cancer, Mol. Cell. Biochem. 356 (2011) 37–43, https://doi.org/10.1007/s11010-011-0956-5.
[33] M.B. Robers, R. Friedman-Ohana, K.V.M. Huber, L. Kilpatrick, J.D. Vasta, B.-T. Berger, C. Chaudhry, S. Hill, S. Müller, S. Knapp, K.V. Wood, Quantifying target Occupancy of small molecules within living cells, Annu. Rev. Biochem. 89 (2020) 557–581, https://doi.org/10.1146/annurev-biochem-011420-092302.
[34] C.I. Wells, D.H. Drewry, J.E. Pickett, A. Tjaden, A. Krämer, S. Müller, L. Gyenis, D. Menyhart, D.W. Litchfield, S. Knapp, A.D. Axtman, Development of a potent and selective chemical probe for the pleiotropic kinase CK2, Cell Chem. Biol. 28 (2021) 546–558.e10, https://doi.org/10.1016/j.chembiol.2020.12.013.
[35] R. Hu, H. Xu, P. Jia, Z. Zhao, KinaseMD: kinase mutations and drug response database, Nucleic Acids Res. 49 (2021) D552–D561, https://doi.org/10.1093/nar/gkaa945.
[36] Y. Zhou, S. Xiang, F. Yang, X. Lu, Targeting gatekeeper mutations for kinase drug discovery, J. Med. Chem. 65 (2022) 15540–15558, https://doi.org/10.1021/acs.jmedchem.2c01361.
[37] A. Lyczek, B.-T. Berger, A.M. Rangwala, Y. Paung, J. Tom, H. Philipose, J. Guo, S. K. Albanese, M.B. Robers, S. Knapp, J.D. Chodera, M.A. Seeliger, Mutation in Abl kinase with altered drug-binding kinetics indicates a novel mechanism of imatinib resistance, Proc. Natl. Acad. Sci. U. S. A. 118 (2021), https://doi.org/10.1073/pnas.2111451118.
[38] M. Salvi, C. Borgo, L.A. Pinna, M. Ruzzene, Targeting CK2 in cancer: a valuable strategy or a waste of time? Cell Death Discov 7 (2021) 325, https://doi.org/10.1038/s41420-021-00717-4.
[39] K. Niefind, B. Guerra, I. Ermakowa, O.G. Issinger, Crystal structure of human protein kinase CK2: insights into basic properties of the CK2 holoenzyme, EMBO J. 20 (2001) 5320–5331, https://doi.org/10.1093/emboj/20.19.5320.
[40] C. de Fusco, P. Brear, J. Iegre, K.H. Georgiou, H.F. Sore, M. Hyvönen, D.R. Spring, A fragment-based approach leading to the discovery of a novel binding site and the selective CK2 inhibitor CAM4066, Bioorg. Med. Chem. 25 (2017) 3471–3482, https://doi.org/10.1016/j.bmc.2017.04.037.
[41] P. Brear, C. de Fusco, K. Hadje Georgiou, N.J. Francis-Newton, C.J. Stubbs, H. F. Sore, A.R. Venkitaraman, C. Abell, D.R. Spring, M. Hyvönen, Specific inhibition of CK2α from an anchor outside the active site, Chem. Sci. 7 (2016) 6839–6845, https://doi.org/10.1039/c6sc02335e.
[42] A. Bancet, R. Frem, F. Jeanneret, A. Mularoni, P. Bazelle, C. Roelants, J.-G. Delcros, J.-F. Guichou, C. Pillet, I. Coste, T. Renno, C. Battail, C. Cochet, T. Lomberget, O. Filhol, I. Krimm, Cancer selective cell death induction by a bivalent CK2 inhibitor targeting the ATP site and the allosteric αD pocket, iScience 27 (2024) 108903, https://doi.org/10.1016/j.isci.2024.108903.
[43] D.W. Litchfield, Protein Kinase CK2: Structure, Regulation and Role in Cellular Decisions of Life and Death.
[44] R. Battistutta, A. Ranchio, E. Papinutto, Crystal Structure of the Apo-form of Human CK2 Alpha at pH 8.5, 2011.
[45] J. Iegre, P. Brear, C. de Fusco, M. Yoshida, S.L. Mitchell, M. Rossmann, L. Carro, H. F. Sore, M. Hyvönen, D.R. Spring, Second-generation CK2α inhibitors targeting the αD pocket, Chem. Sci. 9 (2018) 3041–3049, https://doi.org/10.1039/c7sc05122k.
[46] H. Woolven, C. González-Rodríguez, I. Marco, A.L. Thompson, M.C. Willis, DABCO-bis(sulfur dioxide), DABSO, as a convenient source of sulfur dioxide for organic synthesis: utility in sulfonamide and sulfamide preparation, Org. Lett. 13 (2011) 4876–4878, https://doi.org/10.1021/ol201957n.
[47] A.T. Davies, J.M. Curto, S.W. Bagley, M.C. Willis, One-pot palladium-catalyzed synthesis of sulfonyl fluorides from aryl bromides, Chem. Sci. 8 (2017) 1233–1237, https://doi.org/10.1039/c6sc03924c.
[48] M.S. Gadd, A. Testa, X. Lucas, K.-H. Chan, W. Chen, D.J. Lamont, M. Zengerle, A. Ciulli, Structural basis of PROTAC cooperative recognition for selective protein degradation, Nat. Chem. Biol. 13 (2017) 514–521, https://doi.org/10.1038/nchembio.2329.
[49] F. Musumeci, A. Cianciusi, I. D'Agostino, G. Grossi, A. Carbone, S. Schenone, Synthetic heterocyclic derivatives as kinase inhibitors tested for the treatment of Neuroblastoma, Molecules 26 (2021), https://doi.org/10.3390/molecules26237069.
[50] K. Taruneshwar Jha, A. Shome, Chahat, P.A. Chawla, Recent advances in nitrogen-containing heterocyclic compounds as receptor tyrosine kinase inhibitors for the treatment of cancer: biological activity and structural activity relationship, Bioorg. Chem. 138 (2023) 106680, https://doi.org/10.1016/j.bioorg.2023.106680.
[51] S. Monteleone, J.E. Fuchs, K.R. Liedl, Molecular Connectivity Predefines polypharmacology: aliphatic rings, chirality, and sp3 centers enhance target selectivity, Front. Pharmacol. 8 (2017) 552, https://doi.org/10.3389/fphar.2017.00552.
[52] J. Shearer, J.L. Castro, A.D.G. Lawson, M. MacCoss, R.D. Taylor, Rings in clinical trials and drugs: present and future, J. Med. Chem. 65 (2022) 8699–8712, https://doi.org/10.1021/acs.jmedchem.2c00473.
[53] Y. Hirozane, M. Toyofuku, T. Yogo, Y. Tanaka, T. Sameshima, I. Miyahisa, M. Yoshikawa, Structure-based rational design of staurosporine-based fluorescent probe with broad-ranging kinase affinity for kinase panel application, Bioorg. Med. Chem. Lett. 29 (2019) 126641, https://doi.org/10.1016/j.bmcl.2019.126641.
[54] J.D. Vasta, C.R. Corona, J. Wilkinson, C.A. Zimprich, J.R. Hartnett, M.R. Ingold, K. Zimmerman, T. Machleidt, T.A. Kirkland, K.G. Huwiler, R.F. Ohana, M. Slater, P. Otto, M. Cong, C.I. Wells, B.-T. Berger, T. Hanke, C. Glas, K. Ding, D.H. Drewry, K.V.M. Huber, T.M. Willson, S. Knapp, S. Müller, P.L. Meisenheimer, F. Fan, K. V. Wood, M.B. Robers, Quantitative, wide-spectrum kinase profiling in live cells for assessing the effect of cellular ATP on target engagement, Cell Chem. Biol. 25 (2018) 206–214.e11, https://doi.org/10.1016/j.chembiol.2017.10.010.
[55] J. Raaf, K. Klopffleisch, O.-G. Issinger, K. Niefind, The catalytic subunit of human protein kinase CK2 structurally deviates from its maize homologue in complex with the nucleotide competitive inhibitor emodin, J. Mol. Biol. 377 (2008) 1–8, https://doi.org/10.1016/j.jmb.2008.01.008.
[56] R. Battistutta, E. de Moliner, S. Sarno, G. Zanotti, L.A. Pinna, Structural features underlying selective inhibition of protein kinase CK2 by ATP site-directed tetrabromo-2-benzotriazole, Protein Sci. 10 (2001) 2200–2206, https://doi.org/10.1110/ps.19601.
[57] T. Oshima, Y. Niwa, K. Kuwata, A. Srivastava, T. Hyoda, Y. Tsuchiya, M. Kumagai, M. Tsuyuguchi, T. Tamaru, A. Sugiyama, N. Ono, N. Zolboot, Y. Aikawa, S. Oishi, A. Nonami, F. Arai, S. Hagihara, J. Yamaguchi, F. Tama, Y. Kunisaki, K. Yagita, M. Ikeda, T. Kinoshita, S.A. Kay, K. Itami, T. Hirota, Cell-based screen identifies a new potent and highly selective CK2 inhibitor for modulation of circadian rhythms and cancer cell growth, Sci. Adv. 5 (2019) eaau9060, https://doi.org/10.1126/sciadv.aau9060.
[58] S. Sarno, P. Ghisellini, L.A. Pinna, Unique activation mechanism of protein kinase CK2. The N-terminal segment is essential for constitutive activity of the catalytic subunit but not of the holoenzyme, J. Biol. Chem. 277 (2002) 22509–22514, https://doi.org/10.1074/jbc.M200486200.
[59] B. Zhou, D.A. Ritt, D.K. Morrison, C.J. Der, A.D. Cox, Protein kinase CK2α maintains extracellular signal-regulated kinase (ERK) activity in a CK2α kinase-independent manner to promote resistance to inhibitors of RAF and MEK but not ERK in BRAF mutant melanoma, J. Biol. Chem. 291 (2016) 17804–17815, https://doi.org/10.1074/jbc.M115.712885.
[60] M.P. Schwalm, A. Krämer, A. Dölle, J. Weckesser, X. Yu, J. Jin, K. Saxena, S. Knapp, Tracking the PROTAC degradation pathway in living cells highlights the importance of ternary complex measurement for PROTAC optimization, Cell Chem. Biol. 30 (2023) 753–765.e8, https://doi.org/10.1016/j.chembiol.2023.06.002.
[61] Z.W. Davis-Gilbert, A. Krämer, J.E. Dunford, S. Howell, F. Senbabaoglu, C.I. Wells, F.M. Bashore, T.M. Havener, J.L. Smith, M.A. Hossain, U. Oppermann, D. H. Drewry, A.D. Axtman, Discovery of a potent and selective naphthyridine-based chemical probe for casein kinase 2, ACS Med. Chem. Lett. 14 (2023) 432–441, https://doi.org/10.1021/acsmedchemlett.2c00530.
[62] W. Kabsch, Xds, Acta Crystallogr. D Biol. Crystallogr. 66 (2010) 125–132, https://doi.org/10.1107/S0907444909047337.
[63] P.R. Evans, G.N. Murshudov, How good are my data and what is the resolution? Acta Crystallogr. D Biol. Crystallogr. 69 (2013) 1204–1214, https://doi.org/10.1107/S0907444913000061.
[64] A.A. Lebedev, A.A. Vagin, G.N. Murshudov, Model preparation in MOLREP and examples of model improvement using X-ray data, Acta Crystallogr. D Biol. Crystallogr. 64 (2008) 33–39, https://doi.org/10.1107/S0907444907049839.
[65] P. Emsley, K. Cowtan, Coot: model-building tools for molecular graphics, Acta Crystallogr. D Biol. Crystallogr. 60 (2004) 2126–2132, https://doi.org/10.1107/S0907444904019158.
[66] A.A. Vagin, R.A. Steiner, A.A. Lebedev, L. Potterton, S. McNicholas, F. Long, G. N. Murshudov, REFMAC5 dictionary: organization of prior chemical knowledge and guidelines for its use, Acta Crystallogr. D Biol. Crystallogr. 60 (2004) 2184–2195, https://doi.org/10.1107/S0907444904023510.